PER-ENERGY CAPACITY IN MACRO-FEMTO ENVIRONMENT UNDER FADING CONDITION AND INACCURATE POWER CONTROL

BY

MOHAMMED ABOBAKER MOHAMMED KHALIFA

A Thesis Presented to the
DEANSHIP OF GRADUATE STUDIES

KING FAHD UNIVERSITY OF PETROLEUM & MINERALS

DHAHRAN, SAUDI ARABIA

In Partial Fulfillment of the
Requirements for the Degree of

MASTER OF SCIENCE

In

TELECOMMUNICATION ENGINEERING

May, 2014

KING FAHD UNIVERSITY OF PETROLEUM & MINERALS
DHAHRAN 31261, SAUDI ARABIA

DEANSHIP OF GRADUATE STUDIES

This thesis, written by **MOHAMMED ABOBAKER MOHAMMED KHALIFA** under the direction of his thesis advisor and approved by his thesis committee, has been presented to and accepted by the Dean of Graduate Studies, in partial fulfillment of the requirements for the degree of **MASTER OF SCIENCE IN TELECOMMUNICATION ENGINEERING**

Thesis Committee

Prof. Azzedine Zerguine (Advisor)

Prof. Asrar U.H. Sheikh (Co-Advisor)

Dr. Ashraf S. H. Mahmoud (Member)

Dr. Saad Al-Ahmadi (Member)

Dr. Samir Al-Ghadhban (Member)

Dr. Ali A. Al-Shaikhi
(Department Chairman)

Prof. Salam A. Zummo
(Dean of Graduate Studies)

27/5/14

Date:

To my dear parents,

my kind brothers, and my clever sister

To my beloved wife,

my smart sons, and my lovely daughter

Acknowledgments

I am most grateful to Almighty ALLAH, the Beneficent, the Merciful, for enabling me to complete this work. Peace and blessings of ALLAH be upon his Last messenger Mohammed (Sallallah-Alaihe-Wasallam) and his family, who guided us to the right path.

First and the foremost acknowledgments are due to the King Fahd University of Petroleum and Minerals and to the Department of Electrical Engineering for supporting my research work.

I wish to express my deep appreciation and heartfelt gratitude to Professor Azzedine Zerguine, my thesis advisor for his unfailing encouragement, advice and suggestions through this work and Co - advisor Chair Professor Asrar U.H. Sheikh who guided me with his dedicated attention, expertise and knowledge throughout this research. I also wish to thank my Committee Members, Associate Professor Ashraf S. H. Mahmoud, Assistant Professor Saad Al-Ahmadi and Assistant Professor Samir Al-Ghadhban for their constructive guidance and support.

Finally, my cordial thanks and appreciations are due to my parents, my wife, children, brothers, friends and colleagues who always supported me with their help, love, patience, encouragement and prayers.

Contents

List of Tables

List of Figures

LIST OF ABBREVIATIONS

EE	Energy Efficiency
ICT	Information and Communications Technologies
OFDM	Orthogonal Frequency Division Multiplexing
MIMO	Multiple Input Multiple output
UE	User Equipment
QoS	Quality of Service
RBS	Radio Base Station
BS	Base Station
FAPs	Femtocell Access Points
3G	3^{th} Generation
4G	4^{th} Generation
EARTH	Energy Aware Radio and Networking Technologies Project
OPERA-Net	Optimizing Power Efficiency in Mobile Radio Networks Project
eWIN	Electronic Workforce Information Network Portal Project
DSP	Digital Signal Processing
SISO	Single Input Single Output
DSA	Dynamic Spectrum Access
RAT	Radio Access Technology
DAS	Distributed Antenna Systems
3GPP	3rd Generation Partnership Project
HNB	Home Node B
HeNB	Home eNode B
HSPA	High Speed Packet Access

LIST OF ABBREVIATIONS (Continued)

GSM	Global System for Mobile Communications
WiMAX	Worldwide Interoperability for Microwave Access
PAs	Power Amplifiers
ETSI	European Telecommunications Standards Institute
RRH	Remote Radio Head
WLAN	Wireless Local Area Networks
WCDMA	Wideband Code Division Multiple Access
MAC	Medium Access Control
DFS	Dynamic Frequency Selection
TPC	Transmit Power Control
ARQ	Automatic Repeat Request
UMTS	Universal Mobile Telecommunications System
FEC	Forward Error Correction
SIR	Signal to Interference Ratio
SNR	Signal to Noise Ratio
MS	Mobile Station
DL	Downlink
UL	Uplink
TND	Thermal Noise Density

THESIS ABSTRACT

Name: MOHAMMED ABOBAKER MOHAMMED KHALIFA.

Title: PER-ENERGY CAPACITY UNDER FADING CONDITIONS AND INACCURATE POWER CONTROL.

Degree: Master of Science.

Major Field: Telecommunication Engineering.

Date of Degree: May, 2014.

Energy efficiency (EE) metrics have been articulated in the literature to judge and decide whether a given wireless communication component, device/equipment, or system/network is energy efficient or not. Per-energy capacity ratio is a useful energy efficiency (EE) metric which compares the performance of two systems. This thesis comprehensively studies the per-energy capacity ratio in macro-femto environment. In addition, it investigates the per-energy capacity in macro-femto environment under fading conditions. Furthermore, the degradation in the per-energy capacity ratio due to fading is evaluated and how this degradation is compensated. Finally, the impact of the instantaneous inaccurate power control on the per-energy capacity in macro-femto environment is investigated. The result shows that the deployment of the femtocells besides the macrocells is energy efficient. In addition, it is found that the degradation in the per-energy capacity in macro-femto environment is a function of the fading ratio and hence on the channel behaviors or type.

THESIS OF SCIENCE DEGREE

KING FAHD UNIVERSITY OF PETROLEUM AND MINERALS

31261- DHAHRAN, SAUDI ARABIA

ملخص الرسالة

الاســــــــــم : محمد أبوبكر محمد خليفه.

عنـوان الرسالة : دراسة مقياس السعة لكل وحدة طاقة تحت الاضمحلال و التحكم التقريبي بالطاقة.

التخصص : هندسة اتصالات.

تاريخ التخرج : رجب 1435 هجرية.

مقاييس كفاءة الطاقة أصبحت ذات أهمية كبيرة في أنظمة الاتصالات الحديثة حيث أنها تستخدم لتحديد مستوى الكفاءة في استخدام الطاقة. يعتبر مقياس (السعة لكل وحدة طاقة) احد المعايير المستحدثة لتحديد مدى كفاءة أي نظام اتصالات في استثمار الطاقة و يستخدم للمقارنة بين منظومتي اتصالات لتحديد أيهما يمتلك كفاءة اكبر. في هذه الرسالة نقوم بدراسة مقياس (السعة لكل وحدة طاقة) بشكل عام و نستخدمه للمقارنة بين أنظمة خلايا الاتصالات الأربعة (الماكروسيل، المايكروسيل، البيكوسيل، والفيمتوسيل) بشكل عام و بين الماكروسيل والفيمتوسيل بشكل خاص. كما تمت دراسة هذا المقياس في وجود ظاهرة اضمحلال قوة الإشارة. في هذه الرسالة أيضاً تم حساب مدى الضعف الناتج عن اخذ الاضمحلال في قوة الإشارة بعين الاعتبار كم تمت عملية دراسة كيفية تعويض ذلك الضعف. أخيرا تمت دراسة كيفية التحكم التقريبي بمستوى الطاقة لغرض تحسين مستوى الأداء و رفع الكفاءة.

Chapter 1

Introduction

1.1 Introduction

A reduction in energy consumption of a wireless communication system is of great interest because to the increasingly harmful impact of new wireless communication networks technologies on the environment due to the increased energy consumption. In addition, the rapid expansion of wireless communications forces mobile operators, governments, as well as researchers to investigate more powerful energy efficient solutions in order to solve issues caused by the increased energy consumption like global warming, operating expenses, ... and so on.

According to a forecast by Gartner, by the end of this year, mobile phones will outdo the PC and it will assume the role of an essential web access device [6]. Furthermore, the data volume of networks is expected to increase by a staggering 1000 times, which could increase the energy consumption significantly. Mobile networks have a considerable share in the overall energy consumption of the Information and Communications Technologies (ICT) sector, which itself is responsible for 2 to 10 % of the world energy consumption. In near future, mobile communications will constitute

15 to 20 % of the total ICT energy footprint and 0.3 - 0.4 % of annual world carbon dioxide emissions [7].

In wireless communications networks, the essential resources are the bandwidth and the energy. However, these two resources are limited. Therefore, application of efficient resource allocation algorithms is an essential prerequisite. In this regards, energy efficient techniques are considered as important approaches that professionally manage network resources.

In the past, the performance of the communication systems has been considered as the primary concern and energy efficiency has been receiving less attention in the system design and operation. The design and implementation of wireless communications that have significantly high energy efficiency is not an easy task. In order to achieve energy efficiency, a holistic view is necessary from the system architecture level to the component level. Thus, researchers seek creative designs and development of new architectures, deployment strategies, spectrum management schemes, backhaul network options, energy efficiency metrics and models [8].

In general, after reviewing literature regarding energy efficiency problems in wireless communication networks, we have addressed two fundamental guidelines towards energy efficient wireless communications; firstly we should discover proper solutions to the energy efficiency challenges in the existing communication wireless networks. Secondly, we should include cost efficiency as well.

In addition, we have considered many network energy saving techniques that are proposed in the literature. All these techniques are designed to save energy and hence yield energy efficient wireless communication systems. One category pertains to advanced physical layer techniques. Under this category, we have orthogonal frequency division multiplexing (OFDM), network coding, multiple-input multiple-output (MIMO) cooperative communication, cognitive radio, ... and so on. Another

category is deployment of radio and network resources (energy and bandwidth) management schemes. Examples of this category are: dynamic power saving, multiple radio access technologies coordination, cross layer optimization techniques, ... etc. In addition, new network architectures such as heterogeneous networks, distributed antennas, multi-hop cellular systems have been suggested to deal with the issues related to resource management and energy [1].

One of the attractive suggestions is the layered structure approach, which is another form of the heterogeneous networks. An example of a two-layer structure is a network that deploys macrocells at one layer and femtocells at the other layer. In this case femtocells are usually installed closer to the user equipment and potentially can have large capacity while maintaining the same quality of service (QoS). As a result, offloading the traffic from the macrocell RBS to the FAPs will reduce the energy consumption significantly. Further, more energy saving can be achieved by applying energy saving techniques at the macrocell radio base station. Generally, the layered structure is used to improve capacity, coverage, and energy efficiency of the network. It dynamically allocates the traffic load among different layers of the system and reconfigures these layers to meet service requirements and energy saving goals. However, this can't be done without using efficient traffic offloading algorithms and mobility management [9].

The per-energy capacity metric is defined as the capacity achieved by the system per unit energy [5]. It is introduced in literature as an appropriate metric that determines the amount of achieved energy saving in a specific wireless communications network. Consequently, this measure can be practically used to enhance wireless communications network performance. Moreover, an improved version of this metric, the per-energy capacity ratio introduced in [4] simplifies the analysis and makes the comparisons easier by introducing the concept of ratios.

In the related literature, the per-energy capacity ratio in the macro-femto environment is studied in not many papers. Therefore, it was decided to study the per-energy capacity ratio in the macro-femto environment in order to explore parts that have not been studied and introduce some elaboration that enhances the work and provides useful conclusions that emphasize the viability of per-energy capacity metric as useful energy efficiency metric.

1.2 Thesis Organization

In this thesis the following tasks are carried out:

- Firstly, the work done in the literature regarding the per-energy capacity ratio in the macro-femto environment is reproduced. Moreover, the analysis is extended to include factors that were not included earlier.
- Secondly, the per-energy capacity ratio is studied in the macro-femto environment under fading conditions.
- Thirdly, the degradation in the per-energy capacity ratio due to fading is evaluated and a new mathematical expression, which proves that the degradation in the per-energy capacity ratio due to fading in a function of the channel type, is derived. Moreover, using that derived expression we have estimated the degradation compensation value that should be used to bring back the per-energy capacity ratio to its original value.
- Finally, the expected instantaneous per-energy capacity ratio under the inaccurate power control has been studied.

The remainder of the thesis is organized as follows. In Chapter II, the literature review is presented. In Chapter III, the per-energy capacity ratio analysis in the

macro-femto environment in the uplink is studied. In Chapter IV, the per-energy capacity ratio analysis in the macro-femto environment under fading conditions is carried out. In Chapter V, the analysis of per-energy capacity ratio degradation due to fading conditions and its compensation are presented. Finally, in Chapter VI, conclusions from the work done are drawn and recommendations are made on future works.

Chapter 2

Literature Review

2.1 Literature Review

Since the beginning of the 21^{st} century, global warming and climate changing have arisen to be one of the most important challenges for human being. In communication systems, the fast and comprehensive developments in information and communication technology (ICT) resulted in a remarkable increasing rate of energy consumption. For example in Italy, it is reported that Telecom Italy is the second biggest energy consumer [10]. Furthermore, it is noticed that mobile communications will demand additional energy according to the rate of deployment of 3G systems in developing countries (like China and India) and later 4G systems [1].

Therefore, mobile communication community has become aware of the large rate of energy consumption in mobile networks. In addition, both academia as well as industry are seeking solutions that fulfill the quality of service (QoS) constraints in the presence of energy efficiency. Consequently, energy efficiency has become among the hottest research area during the current decade and numerous worldwide research projects devoted to investigate energy-efficient wireless communications were

completed.

The recommended solutions regarding the energy efficiency problem were outlined in five international major research projects [1]; Green Radio [11], Energy Aware Radio and neTworking tecHnologies (EARTH) [12, 13], Optimizing Power Efficiency in mobile RAdio Networks (OPERA-Net) [14, 15], and electronic Workforce Information Network portal (eWIN) [16, 17]. These research projects have suggested numerous ideas to deal with this problem and solutions to it. Among the five international major research projects, the two research projects Green Radio [11] and (EARTH) [12, 13] are more related to the subject area of thesis research. Table 2-1 gives a brief information about the recommended solutions in these two major research projects.

Table 2 .1: Possible Solutions for Energy-Efficient Wireless Communications [1].

Project Name	**Solutions**
Green Radio	**1. Energy Metrics & Models:** • **Energy metrics to accurately quantify consumption.** • Communications energy consumption models. **2. Energy-Efficient Hardware:** • Hardware integration & advanced power amplifier techniques. • Maximize equipment and base station re-use. **3. Energy-Efficient Architectures:** • **Large vs. small cell deployment.** • **Overlay source (microcell, picocell, femtocell)** & multi-hop routing, relay & network coding and cooperative networking. • Bounding energy requirements by strict end-to-end QoS and efficient backhaul. **4. Energy-Efficient Resource Management:** • Differentiated QoS, exploiting delay tolerant applications and user mobility for energy reduction. • SISO vs. MIMO with packet scheduling. • Identification of energy-efficient cooperative physical layer architecture using emerging information theory ideas to mitigate interference. • Applying dynamic spectrum access (DSA) to minimize energy consumption. • Solar-powered relaying allocating resources to match combined traffic and weather patterns.
Earth	**1. Energy-Efficient Analysis, Metrics and Targets:** • **Energy-efficient metrics on system level.** • Life cycle analysis of energy consumption by telecommunications products. **2. Energy-Efficient Architectures:** • Optimization of cell size. • **Heterogeneous network deployment.** • Relay and cooperative communications. **3. Energy-Efficient Resource Management:** • Dynamic load adaptation and transmission mode adaptation. • Cooperative scheduling, interference coordination, and joint power and resource allocation. • Multi-RAT (radio access technology) coordination. **4. Radio Technologies and Components:** • MIMO, OFDM, adaptive antennas and other advanced transmission techniques. • Power scalable transceiver and power control on component, front end and system level.

Since in this thesis the per-energy capacity ratio in macro-femto environment under fading conditions and inaccurate power control is studied, therefore it is important to provide some background information about the topics related to the direction of the thesis. In this regards, the literature on the following topics is reviewed.

2.1.1 Femtocells:

- **Indoor Coverage Challenges:**

Providing a good indoor coverage is an essential aspect in modern telecommunication networks. In cellular and wireless networks, it is expected that almost 90% of data services and about 60% of calls will occur from the sources located indoors [2]. However, providing an excellent service to indoor user via outdoor cells is extremely difficult and a number of surveys demonstrate that 30% of businesses and 45% of households clients will experience poor indoor coverage [18].

Using macrocells or microcells, which is called 'outside in' approach, to provide indoor coverage has many drawbacks like; firstly, it is pricey and not energy efficient where a higher power is needed to overcome high penetration losses. Secondly, to provide a better capacity or quality of service (QoS) operators should set up more outdoor base station sites which is difficult and costly in urban and densely populated areas. Moreover, even if more outdoor base station sites were established the result will be increased interference. Furthermore, in this case the network planning and optimization will become more complicated and convolved. Another drawback is, modern communication networks like 3G, 4G ... etc. are designed for a carrier frequency around 2GHz or above. Therefore, providing a strong coverage and good service, specially for large buildings, is a big challenges due to high attenuation and penetration losses [2].

Thus, many devices were introduced and implemented to enhance the service and improve the outdoor signal, examples of these devices are repeaters, radiating cables and Distributed Antenna Systems (DAS). In addition, picocells and recently femtocells have been introduced as an excellent solution which outweighs the above mentioned traditional solutions. However, recently femtocells have proved that they provide a better performance than picocells. A comparison between the different indoor coverage techniques is given in Table 2-3 while a comparison between picocells and femtocells is presented in Table 2-4.

Table 2 .2: Comparison between the different indoor coverage techniques [2].

Parameter	Macrocell/ Microcell	Repeaters	DAS	Radiating Cable	Picocell/ Femtocell
Price	Expensive	Convenient	Convenient	Convenient	Cheap
Installation	Expensive	Difficult	Easy	Difficult	Very sasy
Power	High	Low	Low	Low	Very low
Indoor coverage	Bad	Acceptable	Good	Good	Good

Table 2 .3: Comparison between picocell and femtocell [2].

Parameter	Picocell	Femtocell
Installation	By the operator	By the user
Connection to the core network	Co-axial or fibre optic	ADSL Cable
Price	Cheap	Very cheap
Capacity	10-50 users	3-5 users
Coverage range	<100 m	<30 m

- **Femtocell Access point (FAP):**

A femtocell access point is a cellular network access point that connects standard mobile devices to a mobile operator's network via cable broadband connections,

residential DSL, optical fibres or wireless last-mile technologies. Practically it is a simple home base station. In 3rd Generation Partnership Project (3GPP) a femtocell is termed as Home Node B (HNB). Femtocells were firstly proposed in 2006 and in February 2007 several companies introduced femtocells at the 3GSM World Congress (Barcelona), with operators announcing trials.

Femto Forum [19] is the organization which deployed their experts to promote femtocell standardizations and technologies worldwide. It was established in July 2007. In 2008, Home NodeB (HNB) and Home eNodeB (HeNB) were first introduced in 3rd Generation Partnership Project (3GPP) Release 8, signaling. The large scale of femtocell deployment was started in 2010 and nowadays femtocells are used all over the world [2]. In March 2013, it is reported that the worldwide femtocell market, which includes 2G, 3G and 4G products, improved by 66 % between the third quarter and fourth quarter of 2012. In addition, in 2012 the market totaled $425 million i.e. there is an increase in the worldwide femtocell market of 21% over the year 2011 [20]. According to Informa Telecoms & Media, by 2014, there will be 49 million femtocell access points used by 114 million users [21].

- **Femtocell Classification and Deployment:**

Femtocell Access points (FAPs) are classified depending on either their capacity or the cellular technologies used [2]. According to their capacity FAPs are classified into two types: home and enterprise FAPs. Home FAPs have less capacity so they can provide service to three up to five users whereas enterprise FAPs are able to serve up to 16 users. According to the cellular technologies applied, FAPs are classified into UMTS FAP, HSPA FAP, GSM FAP, WiMAX FAP, ... etc.

FAPs are considered as consumer electronics. Therefore, they are self-deployed by users rather than operators. However, the random deployment of femtocells may cause a huge interference to outdoor macrocells. Therefore, to limit the interference,

a femtocell is designed with the ability to configure itself automatically according to the situation. Automatic configuration of FAP includes many phases and tasks like sensing phase and an auto-tuning phase. Automatic configuration of FAP is essential to the successful femtocells deployment.

- **Femtocell Access Control Strategies:**

Three access control strategies are used in femtocell deployment [22]. In the first deployment scenario no user equipments are allowed to access the femtocell except the user equipments belonging to the owners of the FAP, i.e., the users who has the key to use the FAP like password. Other users and visitors are not able to benefit from the service, this is known as closed access mode. In the second deployment scenario all user equipments are allowed to access the femtocell, the user equipments belonging to the owners as well as the visitors; i.e. a public access to the femtocell is provided and no need for password or any other key to use the FAP and benefit from the service. This is known as open access mode. In the third deployment scenario, the femtocell owners may desire to permit access to all user equipments (UEs). However, the access priority is given to guaranteed users, owners of the FAP. This is known as hybrid access mode.

2.1.2 Energy Efficiency and Energy Efficiency Metrics:

Generally speaking, energy efficiency is a comparison concept because it compares two sides or parameters to show how much one parameter (or side) outweighs the other. In electrical engineering in general and in wireless communication in particular, energy efficiency is defined according to two approaches. The first approach is by defining as the performance per unit of energy consumption. This definition is widely used in digital signal processing (DSP), computer systems, and communication sys-

tems. In communication systems, sometimes in the past decades it was called the throughput in bits per second. The Second way of defining EE is by determining the ratio of efficient output power/energy to total input power/energy. This definition is suitable for systems and components such as power supplies, power amplifiers (PAs), and antennas.

In a typical cellular communication network, RBS is the part of the network at which most of the energy is consumed. According to [23], the major source of energy consumption in the network of a mobile operator is the RBS. In the RBS, PAs are the components that drain the greatest part of the energy. For example, PA of RBS in GSM consumes 1320 watt power. Therefore, many researchers are working on the investigation of effective energy efficient solutions to improve the performance of the RBS components, especially for the PAs, from the energy efficiency point of view. However, this research area is out of the scope of this thesis. The cellular network power consumption is shown below in Fig. 2.1.

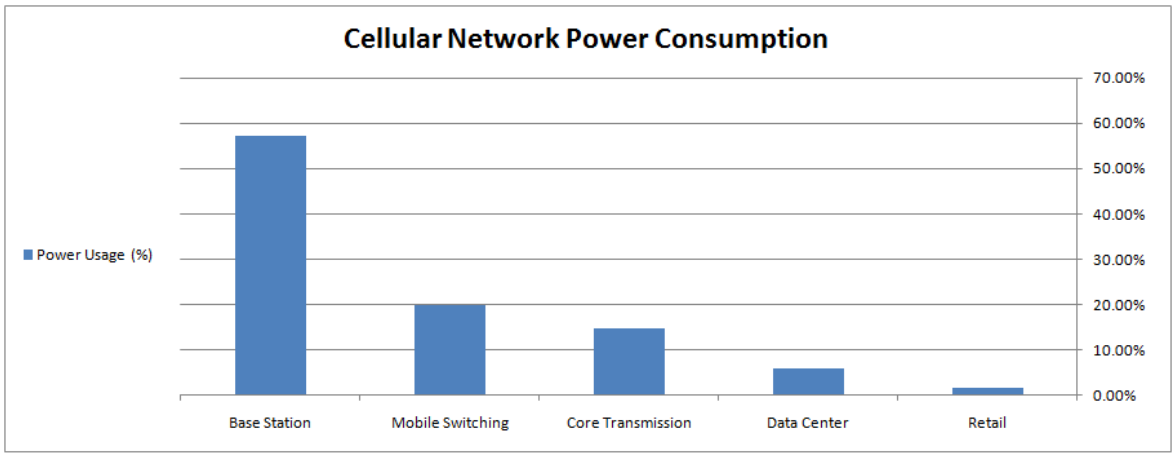

Figure 2 .1: Power consumption of a typical wireless cellular network [3]

Recently, the essential objective in wireless communication is setting of a suitable and powerful energy efficient metric which is able precisely to judge that across the en-

tire protocol layers the optimized decisions have been taken appropriately. Therefore, an energy metric is not efficient unless it is straightforward linked to the optimized decisions across all the protocol layers. In literature, EE metrics are divided into two classes: absolute metrics and relative metrics. Absolute metrics show the amount of the real energy consumed for a given performance while the relative metrics illustrate how much EE is enhanced [8, 1].

In wireless communication, energy efficiency metrics are applied at three levels. These levels are: the component level, equipment level, and system/network level. In addition it should be noted that EE metrics used at each level are significantly different and in general mostly difficult. As a comparison, EE metrics are well formulated at the component level unlike at the two other levels, equipment and system/network, in which establishing EE metrics is more convoluted because in the market numerous manufacturers use different equipment and systems with different competing technologies in energy consumption, capacity, and performance.

At the component level, energy efficiency is generally defined as the ratio of the input power to the radiated or transmitted power. For example, for the antenna, the efficiency is the ratio of the power radiated by the antenna and the input power to the antenna. At the equipment level, different equipments are available in the market. In addition, the way in which wireless equipments are categorized is not straightforward. According to [8], wireless equipment are divided into two categories, the radio base stations and wireless terminals, where by radio base station it is meant a cellular RBS or wireless access point while by wireless terminal a user terminal equipped with wireless interfaces is meant.

Few metrics and methods were defined by the standard body European Telecommunications Standards Institute (ETSI) to evaluate EE of RBSs. In addition, it has set standardized energy consumption measurements to evaluate energy consumption

for both RBS equipment and a RBS site [3]. To give a brief description consider the RBS as an example. In RBS, measurements should include the power consumption in all cases and load conditions; i.e., samples from all load conditions should be taken. Usually, in wireless communication networks three load conditions; low load, medium term load, and busy hours load. The duration in each load condition is denoted as t_{Low}, t_{Med}, and t_{BH}, respectively. In addition, let the average power consumption calculated in each load conditions to be P_{Low}, P_{Med}, and P_{BH}, respectively, then the average power consumption in watt is defined as:

$$P_{equip} = \frac{t_{BH}P_{BH} + t_{Med}P_{Med} + t_{Low}P_{Low}}{t_{BH} + t_{Med} + t_{Low}}. \quad (2\ .1)$$

Let us now consider another RBS which is the distributed RBS. Similar to concentrated RBS, the power consumption for all remote radio heads (RRH) which is denoted by P_{RRH} is calculated independently. In addition, the power consumption of the elements in the central location which is denoted by P_c is also calculated. The way in which the power consumption is evaluated is approximately the same to that used in (2 .1) . Finally, the total average power consumption of the distributed RBS is given as:

$$P_{equip} = P_{RRH} + P_c. \quad (2\ .2)$$

As shown above at the equipment level EE, it is more important to determine the average power consumption than making comparisons and by using energy saving features we should try to reduce the power consumption as much as possible. For instance, for a Flexi EDGE Base Station configured as three sectors and four carriers per sector, the average power consumption is 978 watts and by using energy saving customized solution called Flexi EDGE, it can be reduced to 562 watts in some

instances [9].

Mobile phones, mobile computers such as tablets, netbooks, notebooks .... etc., are the most common wireless terminals. On these devices many applications and programs are installed and to run these applications sometimes there is no need to establish wireless connection. As a result, we can conclude that for these devices the communication is a function which often supports these applications. Obviously, all portable devices in general and wireless terminals in specific are by default energy constrained. Therefore, EE is one of the principal objectives in wireless terminals implementation as well as in design. Actually, from the users point of view, energy-efficient wireless communication is also necessary. According to [24], the iPhone received top marks in every category except for battery life. In [25] some measurements were done on Nokia 6630 mobile phone and these measurements show that the wireless modem in Nokia 6630 consumes about 1.2 watts out off 3 watts, the total power consumption of the phone, while other applications and peripherals consumes the remaining 1.8 watts.

The de-facto standard to measure EE of a mobile phone is the talking time and stand-by time by a fully charged battery. This standard can be used to obtain an appropriate EE metrics of a mobile phone if these data are normalized by the capacity of the mobile battery [9]. For computers, where mobile or portable computers are one part of this category, US government has put an international standard called the energy star. The last version of energy star standard is Version 6 [26]. Nowadays, the important thing that is noticed by scientists, manufacturers, and users is the more and more haziness of the boundaries between mobile phones and mobile computers.

At systems/networks level too, energy efficiency is considered as a primary constraint. In literature, we have generally four categories of wireless systems/networks. The First category is the cellular networks, which depends on RBSs to maintain ac-

cess services. Wireless local area networks (WLAN) belong to the second category in which the access point does the same job of the RBS in cellular networks. The satellite links is the third category but it constitutes a small fraction of the entire wireless industry. Therefore, it is not included in the description. Finally, the last part is ad hoc networks.

In the systems/network level in addition to energy consumed by the RBS site, the features and properties linked to capacity and coverage of the network are also included in the EE metrics evaluation. For the GSM system ETSI defines two network EE levels. In rural areas, the network is usually moderately loaded. Therefore, the coverage area is used in EE metric to reflect energy to achieve coverage, where rural area EE metric is stated as the ratio of the average site power consumption in watts and RBS coverage area in km^2. However, since urban areas are usually fully loaded and traffic demands frequently exceed the RBS capacity, the urban areas EE metric is defined as the ratio of the average site power consumption and the number of subscribers based on average busy hour traffic demand by subscribers and average RBS busy hour traffic.

Unlike what is shown above regarding GSM, in 4G cellular systems, all services are carried by packets whereas in GSM and WCDMA system the major service is the voice. Therefore, the fundamental EE metric for 4G cellular systems is likely to be the Bit-per-Joule. Additionally, it probably will be the fundamental metric for next cellular systems generations.

For WLAN many studies was proposed in the literature in which EE is taken in consideration as a primary constraint. The performance of medium access control (MAC) protocol is the topic which usually gets the attention, some instances are [27, 28]. For IEEE 802.11 standards, which is the de-facto standard for WLAN, a new scheme, which is called the sleep mode has been recommended to access point

station. By applying this scheme a station, which is idle (has nothing to send or transmit), should temporarily shuts down its transceiver and wakes up periodically to transmit or receive buffered messages. Clearly, the EE metric used in this case is the ratio of saved power to the power without the use of the sleep mode. In addition to the sleep mode scheme, dynamic frequency selection (DFS) and transmit power control (TPC) schemes are also introduced to IEEE 802.11h to save more energy.

In wireless ad hoc networks, energy saving can be accomplished by the following methods: the sleep mode, radio turnaround reduction, channel and battery aware schedule, collision avoidance, automatic repeat-request (ARQ) and forward error correction (FEC), topology aware power control, EE routing, or application aware power saving. EE is a primary constraint in wireless ad hoc networks. Therefore, in wireless ad hoc networks EE studies have covered all layers [8].

In the literature, it is also investigated that in addition to EE, which is not the sole measure of the efficiency and reliability of wireless networks design, other metrics like spectral efficiency, network coverage, deployment cost, and QoS requirements are significantly essential and should be considered. In [29] tradeoffs among metrics such as deployment efficiency vs. EE, spectrum efficiency vs. EE, bandwidth vs. power, and delay vs. power are proposed and studied.

- **Bits-per-Joule Metric:**

Among the numerous EE metrics exploited, bits-per-joule metric stands out. It evaluates the numbers of bits (system throughput) for a given unit-energy consumption. In [30, 31], by taking either bits-per-joule metric or capacity per unit energy in consideration, information theoretic results for energy-efficient communications at the link level was specified and calculated. In [32], the capacity of wireless ad hoc networks has been analyzed and a new framework was developed. In that paper the supplied energy to the nodes was considered as the primary constraint and the

capacity was measured in bit-per-joule. Moreover, in game-theoretic schemes for energy saving in wireless networks, bits-per-joule metric is used extensively as a utility function [33, 34]. In [35], EE using the measure bits-per-Joule has been exploited by introducing a link-adaptive transmission scheme for MIMO-OFDM systems which utilizes dynamic power allocation based on the channel state in addition to the circuit power consumption.

- **Per-Energy Capacity Metric:**

The per-energy capacity metric is not as popular as bits-per-Joule metric. However, it shows strong signals regarding its ability to evaluate the degree to which energy efficiency is supported by a given network deployment strategy. Actually, it is recently introduced. Thus it needs time to become more common. The per-energy capacity metric is defined as the capacity achieved by the system per unit energy. From its definition, it is almost similar to the bits-per-joule metric. However, the way it is used in evaluating the energy efficiency of a given wireless system or network is different, where the concept of ratio is usually employed.

In [5] the per-energy capacity metric is studied and analyzed culminating in a proposal of an appropriate handoff strategy under the constraint of the energy consumption. In [4] the impact of cell size on energy saving and system capacity has been evaluated. In that study, it has been shown in a simple and clear way how small-cell based future mobile communication systems are very helpful in terms of energy efficiency. Furthermore, the concept of ratios has been originally proposed with the aim of making the comparisons easier and more accurate.

In both references [5] and [4], three types of ratios were introduced in order to compare between any two different cell types, by cell types here we mean macrocells, microcells, picocells, and femtocells. The first ratio is ***total system transmit power*** ratio while the second is ***system capacity ratio*** and the last ratio is ***per-energy***

capacity ratio. However, the way in which the above mentioned ratios have been defined is different. In [5] the ratio equations are more detailed whereas in [4] the ratio equation are very simple and they are only related to cell radii.

2.1.3 Per-Energy Capacity Ratio

The per-energy capacity ratio is recently introduced in [4]. In that paper the effect of cell size on energy saving and system capacity was inspected and the results have shown that small-cell based future mobile communication systems are more effective in terms of energy efficiency as well as accommodation of high data rates. In addition the authors have derived the per-energy capacity ratio equation in an elementary form. In the downlink the per-energy capacity ratio equation is given as:

$$\frac{U_k^{BS}}{U_1^{BS}} = \left(\frac{R_1}{R_k}\right)^n, \tag{2 .3}$$

while in the uplink case it is given as:

$$\frac{U_k^{MS}}{U_1^{MS}} = \left(\frac{R_1}{R_k}\right)^{n+2}, \tag{2 .4}$$

where U_k^{BS} is the per-energy capacity of the base station, U_k^{MS} is the per-energy capacity of mobile station, R_k is the radius of cell type k, and n is the path-loss exponent. The four cell types are cell type 1, cell type 2, cell type 3, and cell type 4; point to a macrocell with a radius of 1000 m, a microcell with a radius of 500 m, a picocell with a radius of 100 m, and a femtocell with a radius of 10 m, Fig. 2.2 illustrates the four different cell types model used in this thesis.

Using the two equation mentioned above two simulations were done in [4] and the resultant figure in the downlink case is shown in Fig. 2.3:

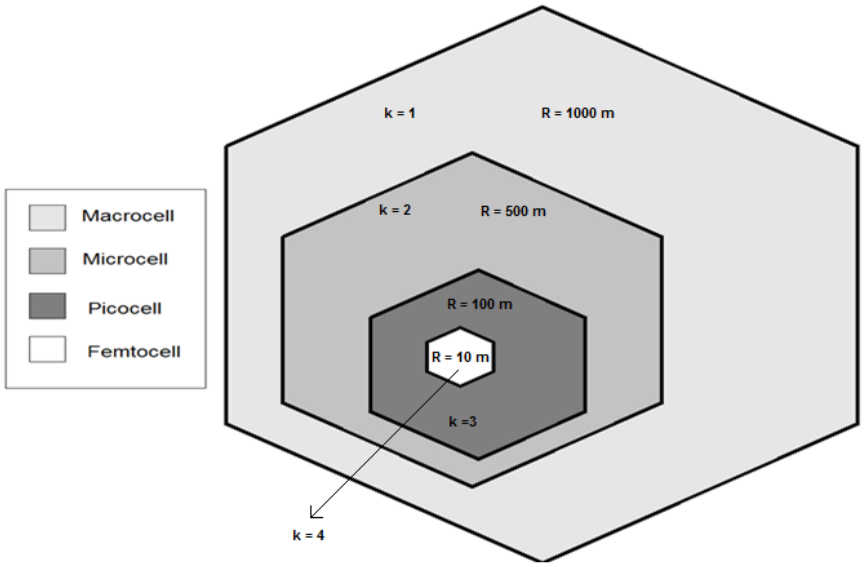

Figure 2 .2: The four different cell types model used in this thesis.

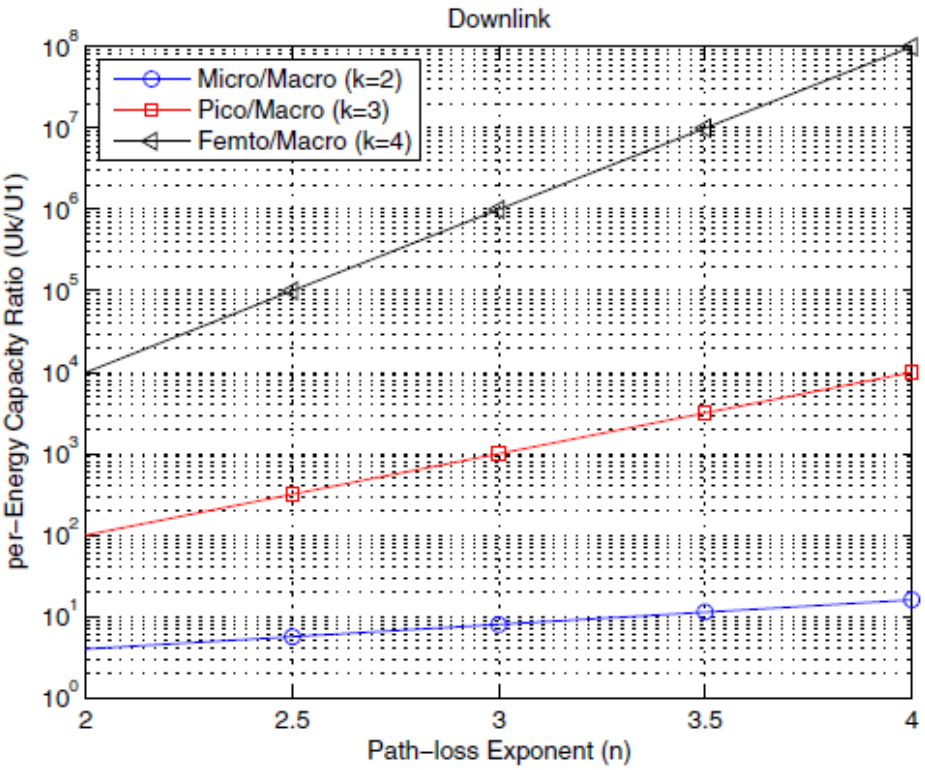

Figure 2 .3: Per-energy capacity in the downlink in [4].

in the uplink case the resultant figure is shown in Fig. 2.4:

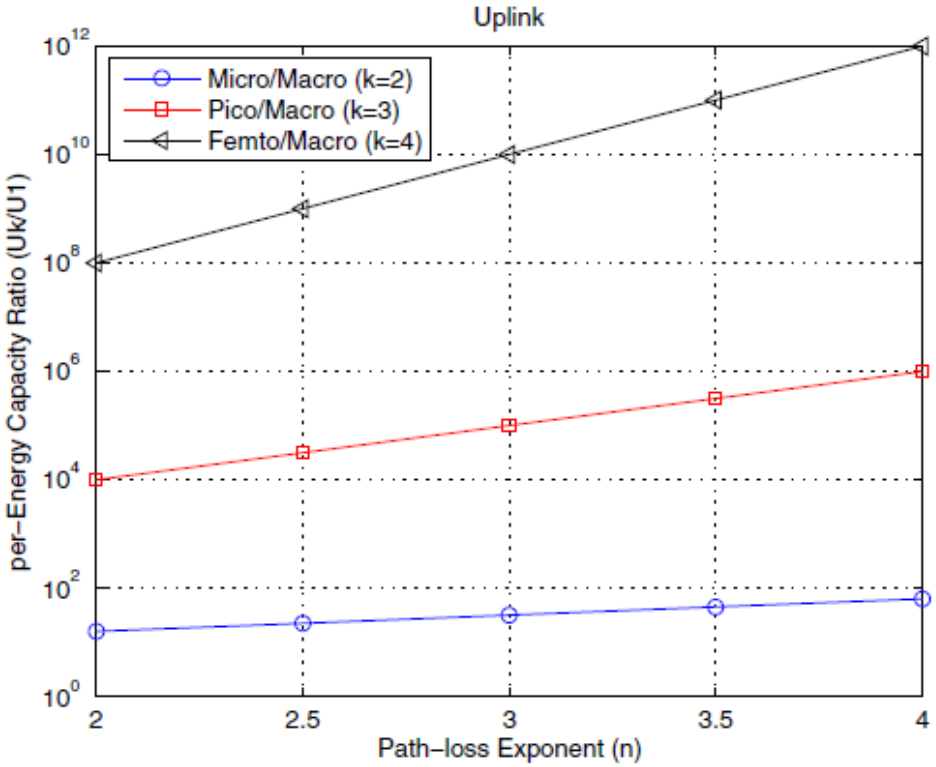

Figure 2 .4: Per-energy capacity in the uplink in [4].

As shown in Fig. 2.3 and Fig. 2.4, the results in [4] are good where it is shown that as the cell size is reduced the performance is better. For example, when the path loss exponent is 4 and the per-energy capacity of the macrocell is normalized to 1, the per-energy capacities of a microcell , picocell, and femtocell are 16, 10^4, and 10^8 in downlink and 64, 10^6, and 10^{12} in uplink, respectively.

Actually, the good results in [4] encouraged the authors of [5] to follow and work on the lines suggested in [4]. In [5] the downlink was only considered but more elaboration on the bandwidth allocation strategies was done where both the dedicated channel bandwidth allocation strategy and co-channel bandwidth allocation strategy was considered. In addition, the equations used to formulate the per-energy capacity ratios were more specific. The per-energy capacity ratio $\Gamma_u(k)$ equation in [5] is given

as:

$$\Gamma_u(k) = \frac{U_k}{U_1} = \frac{\frac{C_k}{S_k h}}{\frac{C_1}{S_1 h}} = \frac{C_k}{C_1}\left[\frac{S_K}{S_1}\right]^{-1} = \Gamma_c(k)\Gamma_s(k)^{-1}, \quad (2.5)$$

where $\Gamma_c(k)$ is the capacity ratio equation and it is given as:

$$\Gamma_c(k) = \frac{C_k}{C_1} = \frac{C(P_k, R_k)\frac{A_1}{A_k}}{C(P_1, R_1)\frac{A_1}{A_1}} = \frac{C(P_k, R_k)}{C(P_1, R_1)}\frac{R_1^2}{R_k^2}, \quad (2.6)$$

and $\Gamma_s(k)$ is the power ratio equation and it is given as:

$$\Gamma_s(k) = \frac{S_k}{S_1} = \frac{P_k\frac{A_1}{A_k}}{P_1\frac{A_1}{A_1}} = \frac{P_k}{P_1}\frac{A_1^2}{A_k^2} = \frac{P_k}{P_1}\frac{R_1^2}{R_k^2}, \quad (2.7)$$

in addition, P_k is the transmit power of the cell k , S_k is the total transmit power of the cell k, R_k is the radius of cell type k, C_k is the total capacity of cell k, A_k is the coverage area of cell type k, and h is the units of time. Using the equations mentioned above two simulations were done in [5]. The resultant figure in the dedicated channel case is shown in Fig. 2.5 while the resultant figure in the co-channel case is shown in Fig. 2.6.

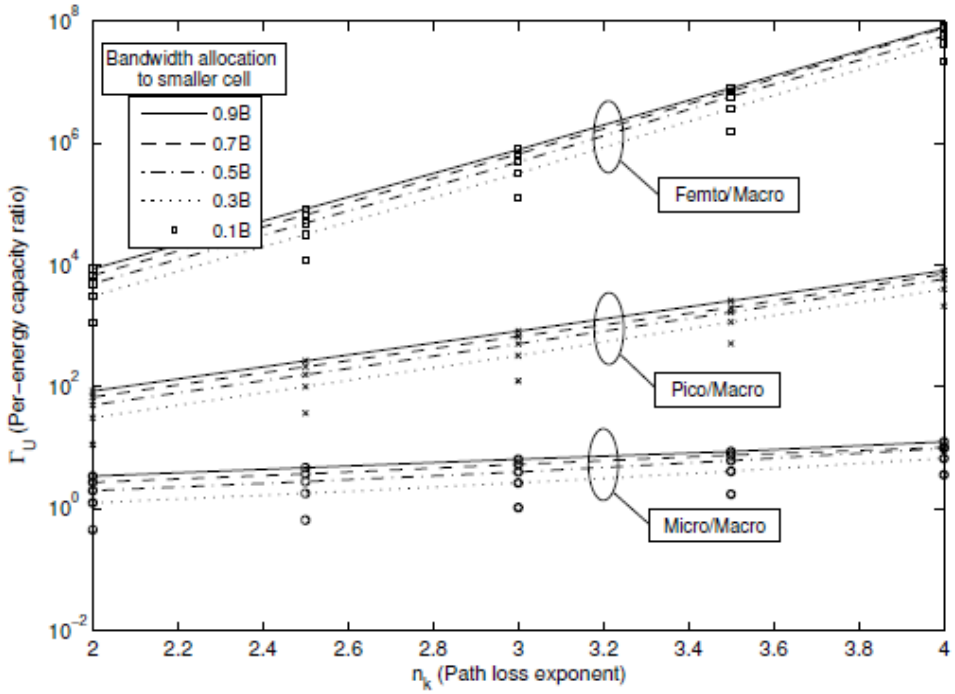

Figure 2 .5: Per-energy capacity in the downlink dedicated channel case in [5].

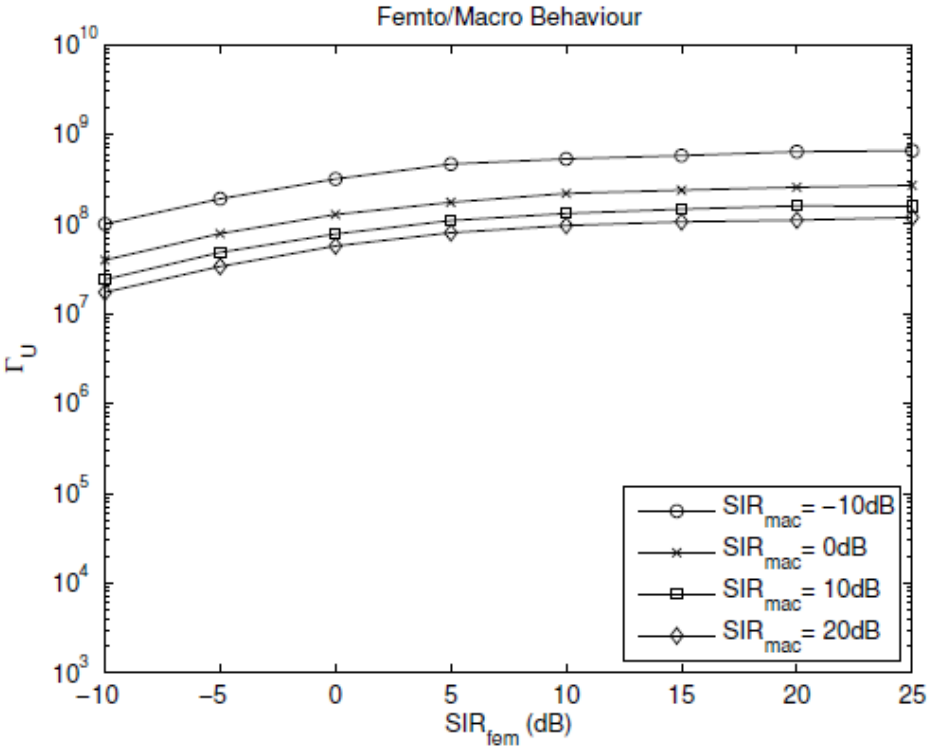

Figure 2 .6: Per-energy capacity in the downlink co-channel case in [5].

As shown above the resulting figures in [5] emphasizes the pervious results in [4]. In addition, it added more comments regarding the per-energy capacity ratio in the downlink; it is shown that in the dedicated case channel as more bandwidth fraction is given to the smaller cells in comparison to the macrocell bandwidth, the performance gets better and the per-energy capacity ratio value increases. Furthermore, in the co-channel the effect of the change of the femtocell signal to interference ratio (femtocell SIR) value and the macrocell signal to interference ratio (macrocell SIR) value is also shown where as the femtocell SIR value increases the per-energy capacity value increases too. However, when the value of the macrocell SIR increases the per-energy capacity value decreases.

2.2 Per-Energy Capacity in the Downlink

In the light of the results showed in [5] regarding per-energy capacity ratio in the downlink, the first step was to reproduce those results. In this thesis, the methodologies used to evaluate the per-energy capacity ratio in each section are different. In this part, the reproduction of the per-energy capacity ratio results in macro-femto environment in the downlink channel, the same expressions in [5] were used. Accordingly, equation (2.7) is used to determine the power ratio, equation (2.6) is used to determine the capacity ratio, and equation (2.5) is used to determine the per-energy capacity ratio.

Two simulation experiments were done for the downlink communication channel. In the first simulation the dedicated channel operation was considered while in the second the co-channel operation was considered. The parameters used in the simulations of this section are summarized below in Table 2.4.

In the dedicated channel case, the per-energy capacity ratio versus the path loss

Table 2 .4: Parameters used in the downlink.

Symbol	Description	Value
k	Cell type index	$\{1,2,3,4\} = \{Macrocell, Microcell, Picocell, Femtocell\}$
R_k	Cell radii	$\{R_1 = 1000m, R_2 = 500m, R_3 = 100m, R_4 = 10m\}$
B	Bandwidth	5 MHz
f	Carrier frequency	2100 MHz
P_1	Tx. power of macrocell	43 dBm
P_2	Tx. power of microcell	38 dBm
P_3	Tx. power of picocell	23 dBm
P_4	Tx. power of femtocell	18 dBm
N_0	Thermal noise density	-174 dBm/Hz
h_b	Macro base station height	15 m
h_m	Mobile station height	1.5 m
h_f	Femto base station height	1.5 m

was studied. In this regards, three per-energy capacity ratios were simulated and the results plotted. The first per-energy capacity ratio compares the microcell to the macrocell while the second per-energy capacity ratio compares the picocell to the macrocell and the third per-energy capacity ratio compares the femtocell to the macrocell. For each per-energy capacity ratio, the femtocell bandwidth was set differently in five cases; in the first case, the femtocell bandwidth was selected as 0.1 of the macrocell bandwidth, in the second case the femtocell bandwidth was 0.3 of the macrocell bandwidth, in the third case the femtocell bandwidth was 0.5 of the macrocell bandwidth, in the fourth case the femtocell bandwidth was set to 0.7 of the macrocell bandwidth, and in the fifth and last case the femtocell bandwidth was 0.9 of the macrocell bandwidth.

In the co-channel simulations, the per-energy capacity ratio was plotted versus the macrocell SIR. The macrocell SIR has been set to four values; in the first instance the

macrocell SIR was set to -10 dB, in the second the macrocell SIR was set to 0 dB, in the third the macrocell SIR was set to 10 dB, and in the fourth the macrocell SIR has been set to 20 dB. However, in the co-channel simulations only the femtocell-macrocell environment is considered. In the co-channel simulation, in order to select the proper value of the path loss exponent value in the simulation experiments two propagation models were considered. In the first model the break point approximation method [36] was used to estimate the path loss exponent value in the simulation while in the second model the 3GPP (2005) model [37] is used to estimate the path loss exponent value in the simulation. The 3GPP (2005) sets the path loss exponent to be a fixed value equal to 3.76 and according to [38] it is widely used over the range of frequencies around to 2 GHz.

2.2.1 Per-Energy Capacity in the Downlink (Dedicated Channel)

As shown below in Fig. 2.7 the per-energy capacity ratio is plotted versus the path loss exponent n_k. In addition, a comparison between the per-energy capacity ratio in three environments: the micro-macro environment, pico-macro environment, and femto-macro environment, is provided. The results in Fig. 2.7 are similar to those in the literature and the following observations were made:

1. The per-energy capacity ratio is the best in the femto-macro environment whereas it is the worse in the micro-macro environment.

2. For the entire three environments; macro-micro, pico-macro, and femto-macro; the higher the path loss exponent value the better is the per-energy capacity ratio value. In addition, the per-energy capacity ratio slope or rate of increase

with respect to the path loss exponent increases more as the cell size moves towards smaller cells.

3. As higher bandwidth fraction is assigned to the smaller cells, the per-energy capacity ratio value increases. However, the per-energy capacity ratio rate of increase is inversely proportional to the bandwidth fraction increment.

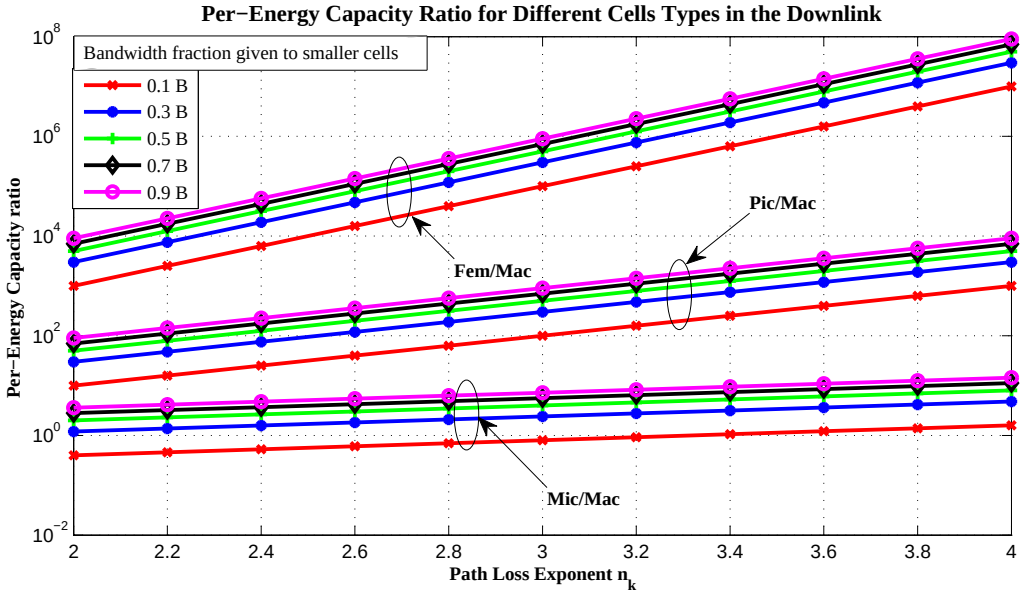

Figure 2 .7: Per-energy capacity ratios in the downlink for the dedicated channel as a function of the path loss exponent.

2.2.2 Per-Energy Capacity in the Downlink (Co-Channel)

As shown in Figs. 2.8 and 2.9 the per-energy capacity ratio versus femtocell SIR has been investigated for four different macrocell SIR values. However, unlike the dedicated channel case only the femto-macro environment was considered. The results in the two Figs. 2.8 and 2.9 are almost similar to those reported in the literature and the following observations are made:

1. For a given constant macrocell SIR, the per-energy capacity ratio increases as the femtocell SIR value increases.

2. For a given constant femtocell SIR, the per-energy capacity ratio decreases as the macrocell SIR value increases.

3. The per-energy capacity ratio performance when the value of the path loss exponent is estimated by using of the break point approach [36] is better than the per-energy capacity ratio performance resulted when the value of the path loss exponent is estimated by using the 3GPP (2005) model [37].

- **Using Breakpoint Approach:**

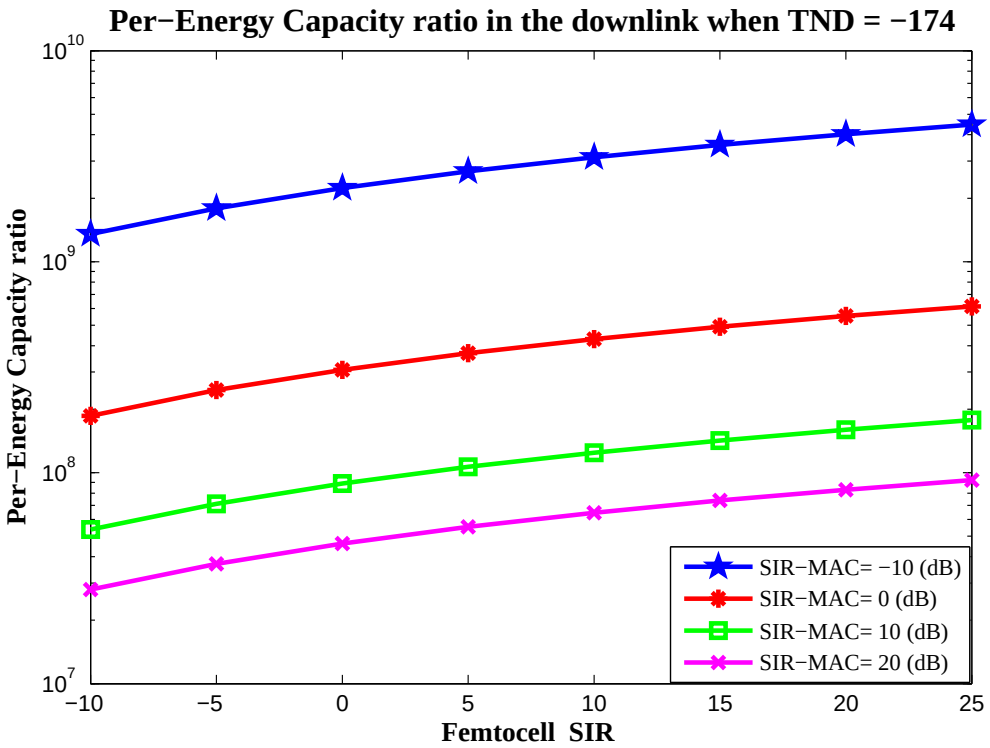

Figure 2 .8: Per-energy capacity ratios in the downlink for the co-channel using breakpoint approach.

- **Using 3GPP (2005) Model:**

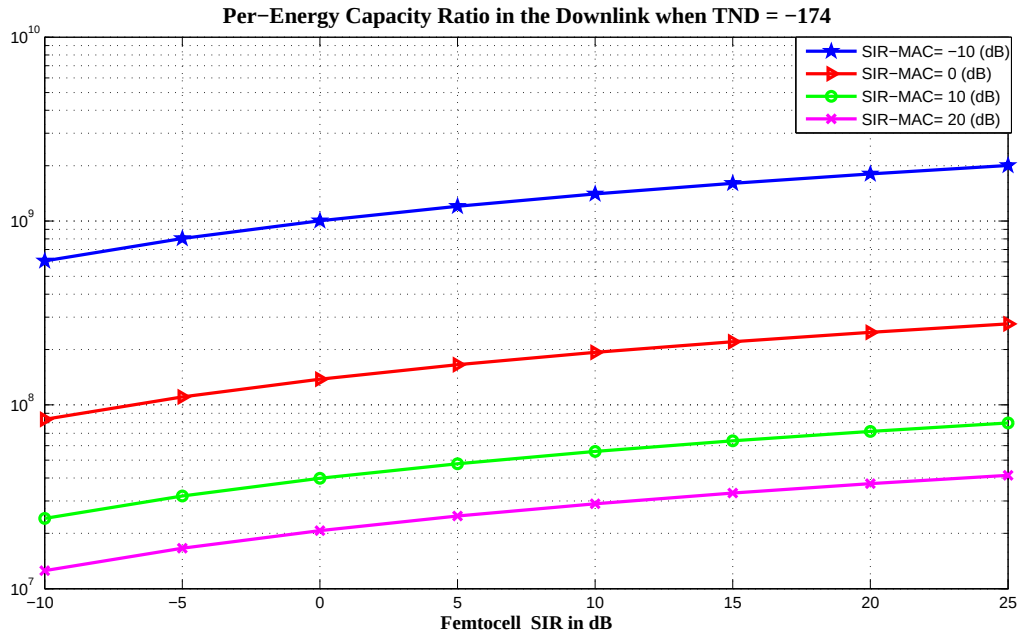

Figure 2 .9: Per-energy capacity ratios in the downlink for the co-channel using 3GPP (2005) model.

2.3 Summary

In this chapter some background information about the topics related to the thesis content was provided. The first topic was the femtocell which is a small wireless access point used to connect the UE's to the mobile operator wireless network. In addition, a comparison between the femtocell and other indoor coverage technologies was provided. The energy efficiency was also discussed in this chapter showing the ways used to define this comparison concept. Thirdly, energy efficiency metrics were investigated. In addition, the levels at which the energy efficiency metrics are applied were discussed comprehensively. Furthermore, a brief information about the most

popular energy efficiency metrics in the literature were shown. Finally, the per-energy capacity ratio metric was illustrated.

In addition, the work done in the literature regarding the per-energy capacity ratio under non-fading condition in the macro-femto environment in the downlink was reproduced for both the dedicated channel case as well as co-channel case .

Chapter 3

Per-Energy Capacity Over the Uplink Channel

3.1 Methodology

The uplink is considered to be less reliable than the downlink. Therefore, it is important and motivating to do simulations over the uplink. The methodology used to evaluate the per-energy capacity ratio in this section, the per-energy capacity ratio in macro-femto environment in the uplink, is different where the equations used in [5] are used as baseline equations. Practically, the power ratio $\Gamma_s(k)$ given in (2.7) is modified so that it can be used for the uplink channel.

In the absence of channel fading, the term $\frac{p_k}{p_1}$ is given as:

$$\frac{P_k}{P_1} = \frac{R_k^{n_k}}{R_1^{n_1}}, \tag{3 .1}$$

In (2.7), which is used to express the per-energy capacity under non-fading conditions in the downlink, and by substituting the value of the term $\frac{p_k}{p_1}$ from (3.1), the

power ratio $\Gamma_{s_{DL}}(k)$ in the downlink channel is given as:

$$\Gamma_{s_{DL}}(k) = \frac{P_k}{P_1}\frac{R_1^2}{R_k^2} = \frac{R_k^{n_k}}{R_1^{n_1}}\frac{R_1^2}{R_k^2} = \frac{R_k^{(n_k-2)}}{R_1^{(n_1-2)}}. \quad (3.2)$$

In the uplink, equation (2.7) is modified so that it can be used for the uplink simulations and the power ratio $\Gamma_{s_{UL}}(k)$ under non-fading conditions in the uplink is given as:

$$\Gamma_{s_{UL}}(k) = \frac{S_k}{S_1} = \frac{P_k}{P_1}, \quad (3.3)$$

by substituting the value of the term $\frac{p_k}{p_1}$ from (3.1), the power ratio $\Gamma_{s_{UL}}(k)$ in the uplink channel is now given as:

$$\Gamma_{s_{UL}}(k) = \frac{P_k}{P_1} = \frac{R_k^{(n_k)}}{R_1^{(n_1)}}. \quad (3.4)$$

The per-energy capacity ratio in [5] is illustrated earlier in (2.5) and by a proper substitution of the power ratio in the uplink $\Gamma_{s_{UL}}(k)$ from (3.4), the per-energy capacity ratio in the uplink is evaluated. Thus, two simulations in the uplink communication channel were done. In the first simulation, the dedicated channel transmission was considered while in the second the co-channel operation was considered. The parameters used in the simulations of this section are summarized in Table 3.1.

The effect of the deployment of smaller cells in general and femtocells in specific on the per-energy capacity ratio will now be analyzed and discussed. Accordingly, first the dedicated case is considered; this is followed by a discussion on the co-channel case.

Table 3 .1: Parameters used in uplink.

Symbol	Description	Value
$\boldsymbol{k}$	Cell type index	$\{1,2,3,4\} = \{Macrocell, Microcell, Picocell, Femtocell\}$
R_k	Cell radii	$\{R_1 = 1000m, R_2 = 500m, R_3 = 100m, R_4 = 10m\}$
$\boldsymbol{B}$	Bandwidth	5 MHz
$\boldsymbol{f}$	Carrier frequency	2100 MHz
P_1	Tx. power of macrocell	18 dBm
P_2	Tx. power of microcell	18 dBm
P_3	Tx. power of picocell	18 dBm
P_4	Tx. power of femtocell	18 dBm
N_0	Thermal noise density	-174 dBm/Hz
h_b	Macro base station height	15 m
h_m	Mobile station height	1.5 m
h_f	Femto base station height	1.5 m

3.2 Dedicated channel Analysis

In the dedicated channel case, the per-energy capacity ratio versus the path loss is studied. Three per-energy capacity ratios were simulated and obtained. The first per-energy capacity ratio compares the microcell to the macrocell while the second per-energy capacity ratio compares the picocell to the macrocell and the third per-energy capacity ratio compares the femtocell to the macrocell. For each per-energy capacity ratio, the femtocell bandwidth has been set to five cases; in the first case the femtocell bandwidth equal to one tenth (0.1) of the macrocell bandwidth, in the second case the femtocell bandwidth is taken to be 30 % of the macrocell bandwidth, in the third case the femtocell bandwidth is half of the macrocell bandwidth, in the fourth case the femtocell uses a bandwidth equal to 70 % of the macrocell bandwidth, and in the fifth case the femtocell bandwidth is 0.9 of the macrocell bandwidth.

As shown below in Fig. 3.1, the per-energy capacity ratio is plotted versus the path loss exponent (n_k). The figure provides a comparison between the per-energy capacity ratio in three environments; micro-macro environment, pico-macro environment, and femto-macro environment.

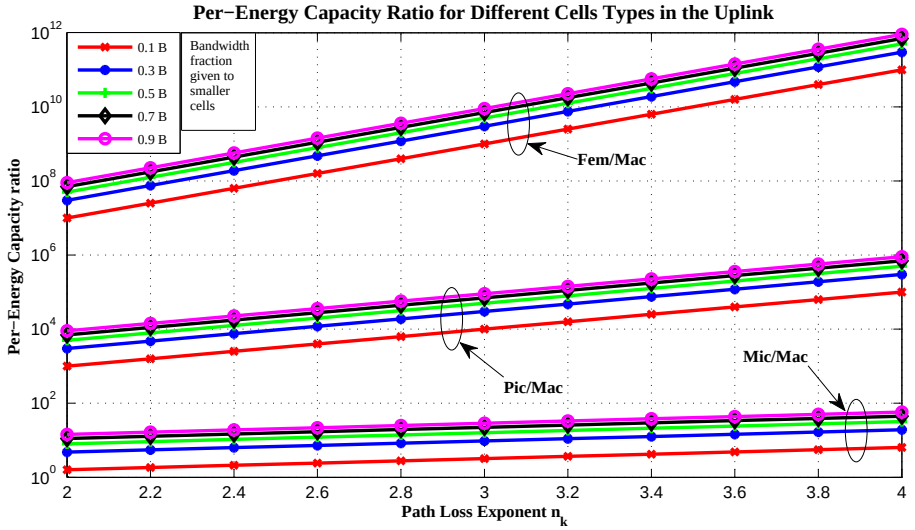

Figure 3 .1: Per-energy capacity ratios in the uplink for the dedicated channel as a function of the path loss exponent.

The per-energy capacity ratio is the best in the femto-macro environment whereas it is the worse in the micro-macro environment. In addition, for the entire three environments the more the path loss exponent value the better the performance and the larger the per-energy capacity ratio. Moreover, the per-energy capacity ratio slope increases as we move towards smaller cells. To illustrate further, we can easily notice that the slope in the femto-macro environment is greater than the slope in the pico-macro environment as well as in the micro-macro environment. Similarly, the slope in the pico-macro environment is greater than the slope in the micro-macro environment.

In addition, if more bandwidth fraction is assigned to the smaller cells the per-energy capacity ratio increases. However, the per-energy capacity ratio rate of in-

crease is inversely proportional to the bandwidth fraction increment. For example, as the bandwidth fraction, given to the femtocell in comparison to the macrocell, increases from 0.1 to 0.3 the per-energy capacity ratio increases by a value greater than the resultant increment in the per-energy capacity ratio when the bandwidth fraction given to the femtocell in comparison to the macrocell increases from 0.3 to 0.5 and the same scenario is repeated as the bandwidth fraction given to the femtocell in comparison to the macrocell increases from 0.5 to 0.7 and so on.

Finally, the comparison of the resultant figure in this part to the resultant figure in the downlink part, shows that the per-energy capacity ratio performance in the uplink is better than the per-energy capacity ratio performance in the downlink.

3.3 Co-channel Analysis

Unlike the dedicated channel simulations, in the co-channel simulations the per-energy capacity ratio has been plotted versus the macrocell SIR. Four values of macrocell SIR were used; in the first case the macrocell SIR was set to -10 dB, in the second case the macrocell SIR was set to 0 dB, in the third case the macrocell SIR of 10 dB is used, and in the fourth case the macrocell SIR of 20 dB is used. However, in the co-channel simulations, only the femtocell-macrocell environment is considered.

In the co-channel simulation two propagation models were used in simulations. In the first case, the break point approach model given in [36] is used to estimate the path loss exponent value, while in the second case the 3GPP (2005) model given in [37] is used to find applicable path loss exponent value. The 3GPP (2005) sets the path loss exponent to a fixed value equal to 3.76 and according to [38] it is widely used over the range of frequencies near to 2 GHz.

As mentioned earlier two cases of the path loss value have been used in the simu-

lation.

3.3.1 Using breakpoint approach

As shown below in Fig. 3.2, in the co-channel case only the femtocell-macrocell environment was considered. The per-energy capacity ratio performance has been investigated versus femtocell SIR for different macrocell SIR. The resultant figure gives a clear and reasonable picture on the per-energy capacity ratio in the co-channel case where for each curve, i.e. the macrocell SIR value is constant, the per-energy capacity ratio increases as the femtocell SIR value increases. However, the per-energy capacity ratio value decreases as the macrocell SIR value increases when the femtocell SIR is kept constant.

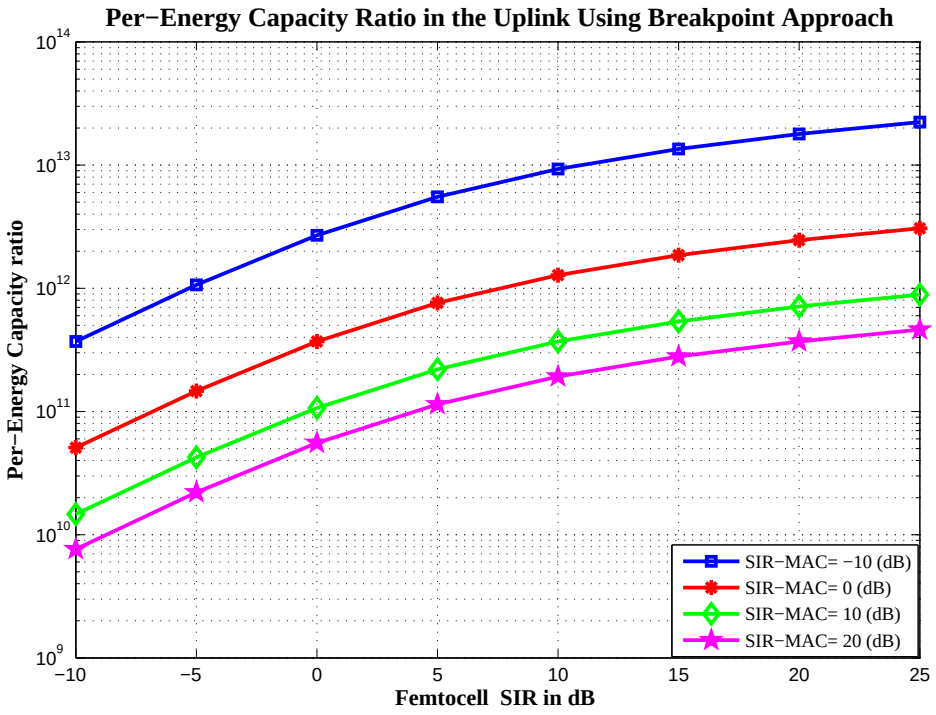

Figure 3 .2: Per-energy capacity ratios in the uplink in the co-channel case using breakpoint approach.

Another aspect is the per-energy capacity ratio rate of increase with respect to the macrocell SIR and femtocell SIR. As shown above, as the femtocell SIR value increases the per-energy capacity ratio rate of increase decreases since the slope decreases whereas the per-energy capacity ratio rate of decrease decreases as the macrocell SIR value increases.

To illustrate more, for a fixed femtocell SIR value say 5 dB, when the macrocell SIR increases from -10 dB to 0 dB the per-energy capacity ratio decreases by value greater than the value resulted when the macrocell SIR is increased from 0 dB to 10 dB and the same scenario is repeated when the macrocell SIR is increased from 10 dB to 20 dB at which the per-energy capacity ratio decrease is observed to be the smallest. Similarly, for a given fixed macrocell SIR value say 10 dB, when the femtocell SIR increases from -10 dB to -5 dB the per-energy capacity ratio increases by value greater than the value resulted when the femtocell SIR increases from 15 dB to 20 dB

3.3.2 Using 3GPP (2005) model

As shown below in Fig. 3.3, the figure has the same pattern of Fig. 3.2 where the per-energy capacity ratio is directly proportional to the femtocell SIR and inversely proportional to the macrocell SIR. In addition, as the femtocell SIR value increases the per-energy capacity ratio rate of increase decreases since the slope decreases whereas the per-energy capacity ratio rate of decrease decreases as the macrocell SIR value increases.

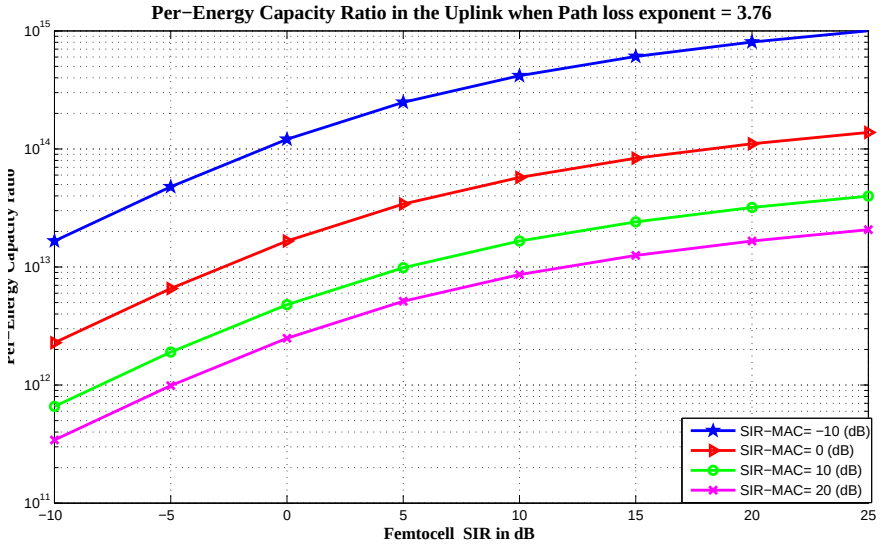

Figure 3 .3: Per-energy capacity ratio in the uplink in the co-channel case using 3GPP (2005) model.

Moreover, the per-energy capacity ratio performance, when the estimated value of the path loss exponent by using the break point approach [36], is better than the per-energy capacity ratio performance when the value of the path loss exponent is evaluated from the 3GPP (2005) model [37].

Finally, in the co-channel simulations, we found that the per-energy capacity ratio performance over the uplink is better than the per-energy capacity ratio performance over the downlink.

As a conclusion, a remarkable improvement is resulted after the femtocells are deployed. For example, in the dedicated case when the path loss exponent values are 2, 3, and 4, respectively and under the condition that the per-energy capacity ratio of the macrocell is normalized to 1, and if the bandwidth fraction given to the femtocell is 0.9 the bandwidth given to the macrocell; the per-energy capacity of the femtocell is 10^8, 10^{10}, and 10^{12}, respectively, which means that deployment of femtocells results in strikingly high per-energy capacity. Moreover in the co-channel case, the

femtocell-macrocell per-energy capacity ratio outweighs the femtocell-macrocell per-energy capacity ratio in the dedicated channel case. Hence, these results emphasize the fact that the femtocells deployment results in huge capacity increase.

3.4 Summary

In this chapter the per-energy capacity ratio under non-fading condition in the macro-femto environment in the uplink was investigated. Accordingly, two simulations in the uplink communication channel were carried out. In the first simulation, the dedicated channel transmission was investigated while in the second the co-channel operation was considered.

In the dedicated channel case, the per-energy capacity ratio versus the path loss was investigated and three per-energy capacity ratios were obtained. The first per-energy capacity ratio compared the microcell to the macrocell while the second per-energy capacity ratio compared the picocell to the macrocell and the third per-energy capacity ratio compared the femtocell to the macrocell. In the co-channel simulations the per-energy capacity ratio has been plotted versus the macrocell SIR. Four values of macrocell SIR were selected; in the first case the macrocell SIR was set to -10 dB, in the second case the macrocell SIR was set to 0 dB, in the third case the macrocell SIR of 10 dB is used, and in the fourth case the macrocell SIR of 20 dB is used. However, in the co-channel simulations, only the femtocell-macrocell environment is considered.

Chapter 4

Per-energy Energy Capacity Under Fading Conditions

4.1 Introduction

In wireless communication channel, the received signal undergoes attenuation which takes different forms. For example, we have path-loss, slow fading, fast fading and so on. Fading is defined as the random fluctuation of the signal power with time, geographical position, or radio frequency. In wireless systems, fading takes place due to multipath propagation or due to shadowing from obstacles affecting the wave propagation, sometimes referred to as shadow fading.

Evaluating per-energy capacity ratio under fading environment is important. In addition, it will enhance the work and provide conclusions that can be used to emphasize the viability of per-energy capacity ratio metric as a useful energy efficiency metric under different channel conditions. Therefore, the study of the behavior of the per-energy capacity ratio under fading environment with respect to all parameters that affect the performance in the communication system network is of considerable

importance. The important parameters are femtocell SIR, macrocell SIR, path loss exponent, and macrocell radius.

In this chapter, only the femtocell-macrocell environment is considered since it has been shown earlier that the best per-energy capacity ratio performance is resulted in this environment and it outweighs the per-energy capacity ratio performance in the picocell-macrocell environment as well as the microcell-macrocell environment.

In the femtocell-macrocell environment, the per-energy capacity ratio under fading for the dedicated channel case and the co-channel case were evaluated. In addition, in each channel assignment both the downlink and uplink transmission channels were considered. Accordingly, the following cases were studied:

- In dedicated channel case, the per-energy capacity ratio under fading environment is analyzed as a function of:

    1. Femtocell SIR and macrocell radius.
    2. Femtocell SIR and macrocell SIR.
    3. Femtocell SIR and path loss exponent.
    4. Macrocell radius and macrocell SIR.
    5. Macrocell radius and path loss exponent.
    6. Macrocell SIR and path loss exponent.

    Actually the per-energy capacity ratio under fading environment as a function of two parameters is analyzed in each simulation for two reasons; first to inspect the per-energy capacity ratio behaviors in the 3D view as well as in the 2D view and secondly to complete the picture that illustrates the per-energy capacity ratio behavior under fading environment with respect to each parameter.

In the dedicated channel, as in the previous simulations, the bandwidth fraction of the femtocell in comparison to the bandwidth of the macrocell was set to 0.1, 0.3, 0.5, 0.7, and 0.9 fractions of the macrocell bandwidth.

- In co-channel case, we have analyzed the per-energy capacity ratio under fading environment as a function of:

    1. Femtocell SIR and macrocell radius: Under this section, the values of the macrocell SIR were selected to be -10 dB, 0 dB, 10 dB, and 20 dB.
    2. Femtocell SIR and path loss exponent: Under this section, the values of the macrocell SIR were selected to be -10 dB, 0 dB, 10 dB, and 20 dB.
    3. Macrocell radius and path loss exponent: Under this section, the two simulations, the first using the values of the femtocell SIR of -10 dB, 0 dB, 10 dB, and 20 dB under the condition that the macrocell SIR equal to 3 dB while in the second the values of the macrocell SIR were selected to be -10 dB, 0 dB, 10 dB, and 20 dB while keeping SIR femtocell equal to 3 dB.

    As mentioned above, in all simulation cases, both transmission channels the downlink and the uplink were studied and simulated. In addition, all values of SIR or SNR are average values under fading conditions. Accordingly, first the dedicated case is considered; this is followed by a discussion on the co-channel case.

The degradation in the per-energy capacity ratio under fading environment:

The analysis of the per-energy capacity ratio degradation under fading conditions is one of the main objectives in this thesis. Therefore to achieve this goal, the per-

energy capacity ratio was evaluated under fading environment as well as non fading conditions so that the difference between the two situations is defined as the degradation in the per-energy capacity ratio due to fading. Thus, in all the simulation cases, the degradation in the per-energy capacity ratio due to fading is investigated and commented.

4.2 Methodology

To describe the methodology used in this chapter two, main references [5] and [4] are used. In both references, it is assumed that the received power at the cell boundary for any cell type can be expressed by:

$$P_r = \frac{\alpha_1 P_1}{R_1^{n_1}} = \frac{\alpha_k P_k}{R_k^{n_k}}, \tag{4 .1}$$

where P_k is the transmit power of cell type k, R_k is the radius of cell type k, and n_k is the path loss exponent of cell type k. In [5], α is considered to be the path loss parameter while in [4] α is considered to be the channel gain. In both references, they considered that (α_1=α_k) and thus they reduced (4.1) to a simplified form without the index α. The new simplified form was given as:

$$\frac{P_1}{R_1^{n_1}} = \frac{P_k}{R_k^{n_k}}, \tag{4 .2}$$

which leads to the following equation:

$$\frac{P_k}{P_1} = \frac{R_k^{n_k}}{R_1^{n_1}}. \tag{4 .3}$$

The total power ratio for a given cell type k, is given in [5] as:

$$\Gamma_s(k) = \frac{S_k}{S_1} = \frac{P_k \frac{A_1}{A_k}}{P_1 \frac{A_1}{A_1}} = \frac{P_k}{P_1}\frac{A_1}{A_k} = \frac{P_k}{P_1}\frac{R_1^2}{R_k^2}, \quad (4.4)$$

by substituting the value of $\frac{p_k}{p_1}$ from (4.3) in (4.4), the resultant total power ratio equation for a given cell type k, has been derived in [5] as:

$$\Gamma_s(k) = \frac{P_k}{P_1}\frac{R_1^2}{R_k^2} = \frac{R_k^{n_k}}{R_1^{n_1}}\frac{R_1^2}{R_k^2} = \frac{R_k^{(n_k-2)}}{R_1^{(n_1-2)}}. \quad (4.5)$$

However, the following points regarding the parameter α and (4.1) should be noted:

1. In [4], the parameter α is assumed to be the channel gain. However, it is difficult to justify that the channel gains in the macrocell environment and the femtocell environment are the same.

2. In [5], it was considered that α is the path loss parameter. However, the effect of path loss is reflected in the terms $R_k^{n_k}$ and $R_1^{n_1}$ in (4.1).

Therefore, in this thesis it is considered that α should neither be the path loss parameter nor the channel gain. In addition, it is concluded that α should represent the fading parameter.

In femtocell/indoor environment, fast fading is negligible because a UE is either not moving or it moves very slowly. Thus, in the macrocell environment both multi-path fading and shadowing should be considered while in the femtocell environment inclusion of only shadowing is sufficient.

The system considered in this thesis depends on fixed power strategy. In downlink transmission, MSs at the cell-boundary receive indistinguishable SNR values because

the transmit power level of BS is fixed to a definite value. Consequently, the cell coverage area is adjusted by controlling the transmit power.

In the uplink, the situation is different where all MSs in the cell transmit data with almost equal power level. Therefore, the transmitted signal power to the BS from MSs at the cell boundary should have a suitable SNR value so that it can be decoded at the receiver.

For both cell types, the femtocell (denoted by the index k) and the macrocell (denoted by the index 1) and under fading conditions, the received power level at the cell boundary is denoted by P_r and it is given by:

$$P_r = \frac{f_{mac} P_1}{R_1^{n_1}} = \frac{f_{fem} P_k}{R_k^{n_k}}, \tag{4 .6}$$

where (4.6) is a modified version of (4.1). After reconfiguration we get:

$$\frac{P_k}{P_1} = \frac{f_{mac} R_k^{n_k}}{f_{fem} R_1^{n_1}}, \tag{4 .7}$$

by substituting for the value of $\frac{p_k}{p_1}$ from (4.7) in (4.4), a new equation is obtained, which evaluates the total power ratio under fading conditions, which is denoted by $\Gamma_{s_{fad}}(k)$, and it is given as:

$$\Gamma_{s_{fad}}(k) = \frac{P_k}{P_1}\frac{A_1}{A_k} = \frac{P_k}{P_1}\frac{R_1^2}{R_k^2} = \frac{f_{mac} R_k^{n_k}}{f_{fem} R_1^{n_1}}\frac{R_1^2}{R_k^2} = \frac{f_{mac}}{f_{fem}}\Gamma_s(k). \tag{4 .8}$$

Consequently, a new equation which evaluates the per-energy capacity ratio under fading conditions, denoted by $\Gamma_{u_{fad}}(k)$, is derived as follows:

$$\Gamma_{u_{fad}}(k) = \Gamma_c(k)\Gamma^{-1}_{s_{fad}}(k) = \Gamma_c(k)\Big(\frac{f_{mac}}{f_{fem}}\Gamma_s(k)\Big)^{-1} = \Big(\frac{f_{mac}}{f_{fem}}\Big)^{-1}\Gamma_c(k)\Gamma_s(k)^{-1}, \tag{4 .9}$$

by substituting for the value of $(\Gamma_c(k)\Gamma_s(k)^{-1})$ from (2.5) in (4.9), eq. (4.10) is obtained:

$$\Gamma_{u_{fad}}(k) = \left(\frac{f_{mac}}{f_{fem}}\right)^{-1} \Gamma_c(k)\Gamma_s(k)^{-1} = \left(\frac{f_{mac}}{f_{fem}}\right)^{-1} \Gamma_u(k). \qquad (4.10)$$

In this thesis the term $\frac{f_{mac}}{f_{fem}}$ is named as the fading ratio. As shown above, the reciprocal of the fading ratio $\frac{f_{mac}}{f_{fem}}$ is introduced in equation (4.10) to scale the old the per-energy capacity ratio which is the per-energy capacity ratio without fading conditions. The modified mathematical expression given in (4.10) is used to evaluate the per-energy capacity ratio under fading conditions.

It should be noted that the parameter f_{mac} contains both the shadowing and fading contributors while the parameter f_{fem} contains only the effect due to shadowing. Consequently, two Lognormal random variables were generated and one Rayleigh variable. Moreover, the macrocell channel and femtocell channel using short time (or distance) snapshots were used. The snapshots used were short because the time resolution used in the simulation was in the microsecond range which makes monitoring of channel for long time is difficult.

4.3 Per-energy capacity ratio analysis in the dedicated fading channel

As shown in this section, the per-energy capacity ratio performance is evaluated under fading environment as a function of the femtocell SIR, the macrocell radius, the macrocell SIR, and the path loss exponent. In each case, two parameters were selected and the per-energy capacity ratio performance under fading environment as a function of that combination was investigated. For each case eight figures were plotted: four figures represent the per-energy capacity ratio under fading environment

in the downlink and the other four figures represent the per-energy capacity ratio under fading environment in the uplink. In each plot, the bandwidth fraction of the femtocell in comparison to the bandwidth of the macrocell was set to 0.1, 0.3, 0.5, 0.7, and 0.9 fractions of the macrocell bandwidth. Consequently, several cases were investigated and results in the form of graphs were obtained. In this part, some sample cases are selected to show the behavior of the per-energy capacity ratio performance under fading environment.

4.3.1 Femtocell SIR and path loss exponent

As shown in the figures below, in this sample case, the per-energy capacity ratio performance under fading environment was investigated as a function of the two parameters: femtocell SIR and path loss exponent. The relation between the per-energy capacity ratio in fading environments and each parameter, additionally the resultant degradation in the per-energy capacity ratio in fading environment are illustrated in details in the following paragraphs.

- **Downlink channel:**

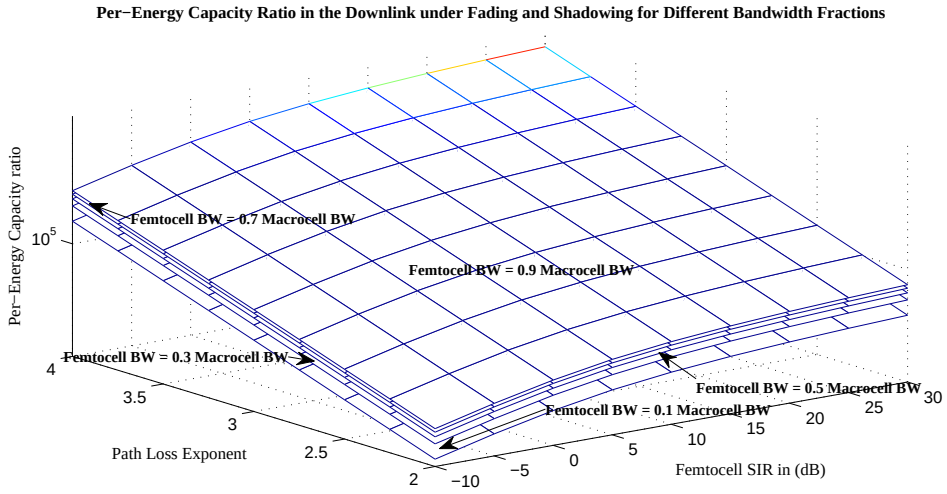

Figure 4 .1: Per-energy capacity ratios in the dedicated channel (downlink) under fading and shadowing (femtocell SIR, path loss exponent).

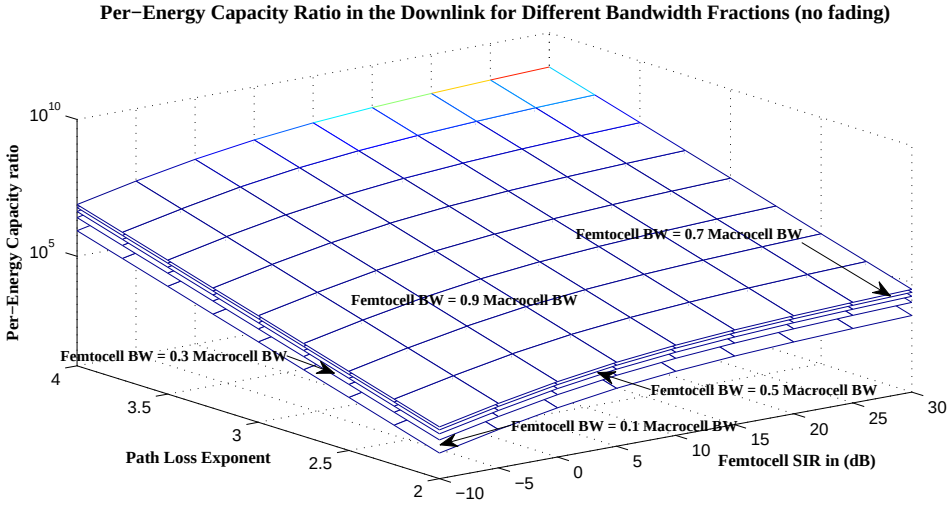

Figure 4 .2: Per-energy capacity ratios in the dedicated channel (downlink) without fading or shadowing (femtocell SIR, path loss exponent).

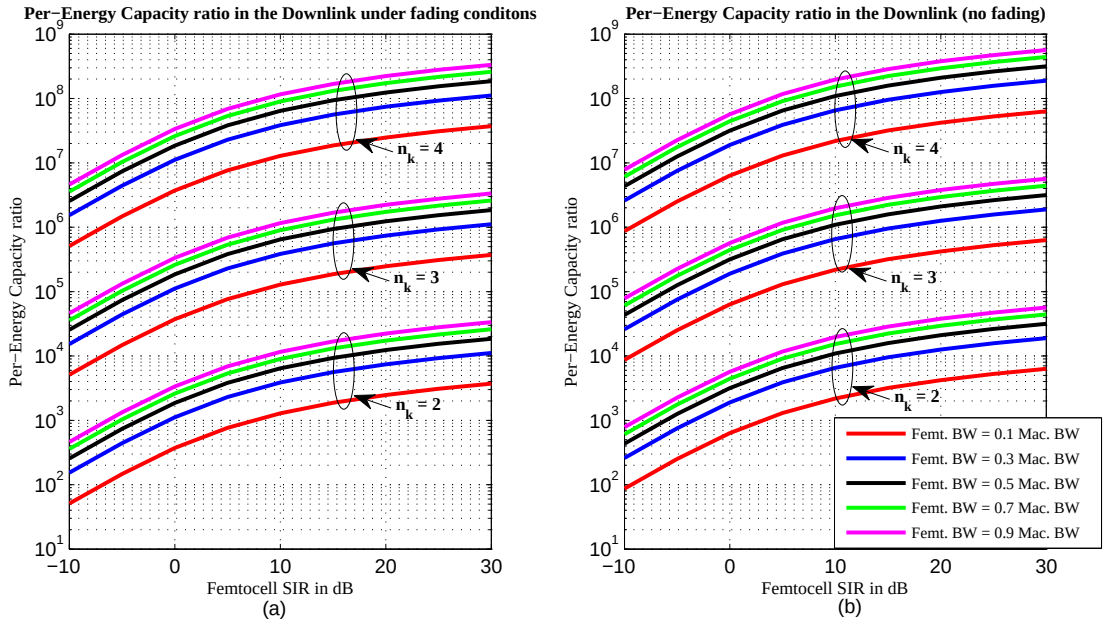

Figure 4 .3: Per-energy capacity ratios in the dedicated channel (downlink) as a function of femtocell SIR for some path loss exponent values (a) under fading condition (b) under non-fading condition.

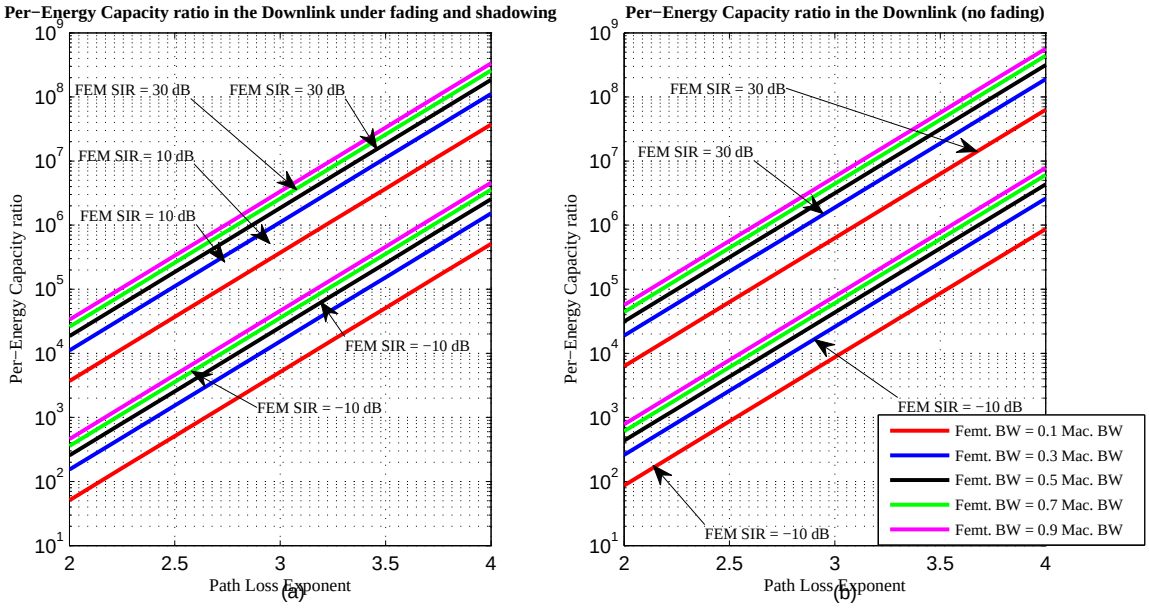

Figure 4 .4: Per-energy capacity ratios in the dedicated channel (downlink) as a function of path loss exponent for some femtocell SIR values (a) under fading condition (b) under non-fading condition.

- **Uplink channel:**

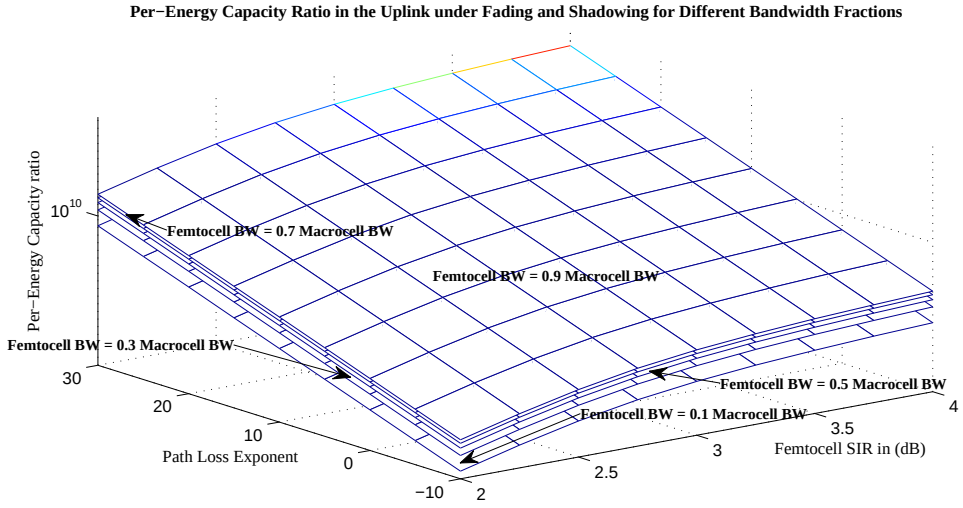

Figure 4 .5: Per-energy capacity ratios in the dedicated channel (downlink)uplink under fading and shadowing (femtocell SIR, path loss exponent).

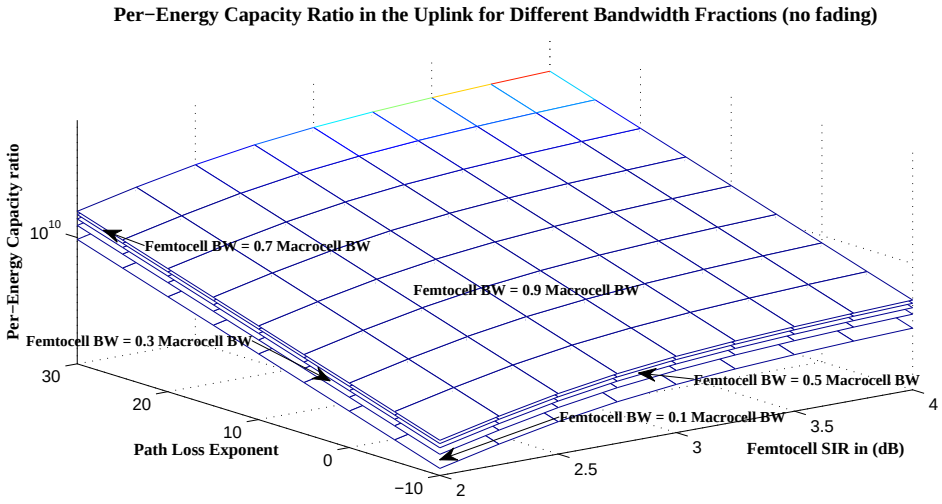

Figure 4 .6: Per-energy capacity ratios in the dedicated channel (uplink) without fading and shadowing (femtocell SIR, path loss exponent).

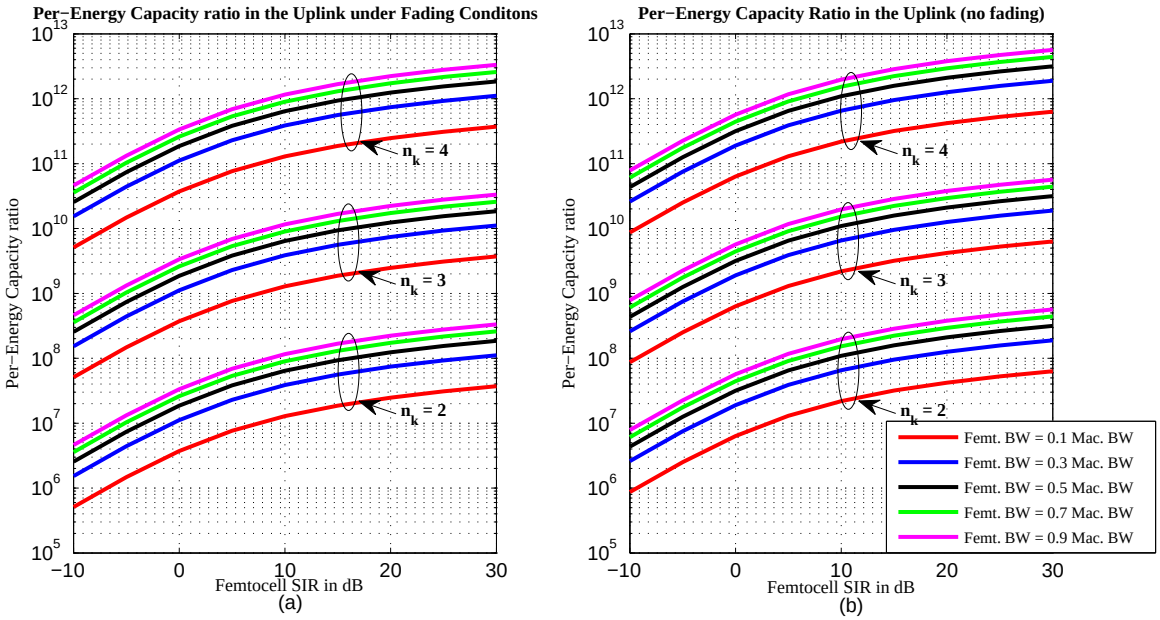

Figure 4 .7: Per-energy capacity ratios in the dedicated channel (uplink) as a function of femtocell SIR for some path loss exponent values (a) under fading condition (b) under non-fading condition.

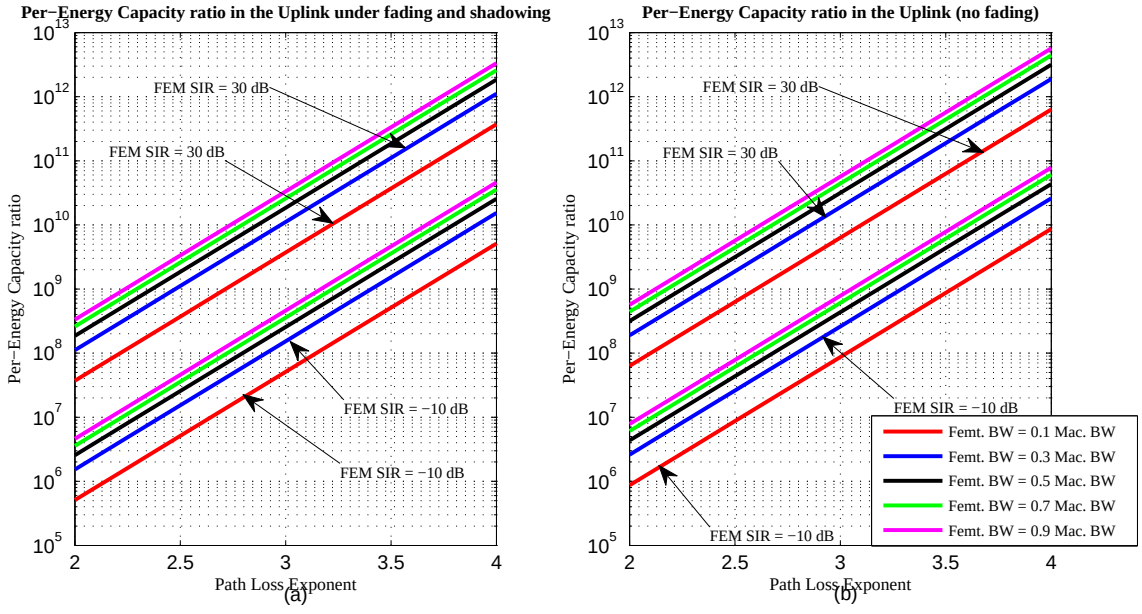

Figure 4 .8: Per-energy capacity ratios in the dedicated channel (uplink) as a function of path loss exponent for some femtocell SIR values (a) under fading condition (b) under non-fading condition.

- **The relation between the per-energy capacity ratio under fading conditions and the femtocell SIR:**

  The per-energy capacity ratio under fading conditions is directly proportional to the femtocell SIR. Further, as the femtocell SIR value increases, the per-energy capacity ratio rate of increase with respect to the femtocell SIR decreases. For an example, in Fig. 4.4 in the downlink and Fig. 4.8 in the uplink, when the femtocell bandwidth = 0.5 the macrocell bandwidth (black color lines) and when the path loss exponent = 3, as the femtocell SIR value increases from -10 dB to 10 dB the per-energy capacity ratio increases by value greater than the value resulted when the femtocell SIR increases from 10 dB to 30 dB.

- **The relation between the per-energy capacity ratio under fading conditions and path loss exponent:**

  The per-energy capacity ratio under fading conditions is directly proportional to the path loss exponent. However, the per-energy capacity ratio slopes or rate of increase under fading conditions with respect to the path loss exponent is almost constant. For instance, Fig. 4.4 in the downlink and Fig. 4.8 in the uplink depict the resultant per-energy capacity ratios under fading conditions versus the path loss exponent for some femtocell SIR values, as shown in these figures, only straight lines are resulted which means that the per-energy capacity ratio slope is certainly constant.

- **The degradation in the per-energy capacity ratio under fading conditions:**

  As shown in the figures above, the degradation in the per-energy capacity ratio due to fading is existing and clear. In addition, it is almost not dependent on

the path loss exponent or the femtocell SIR.

To explain more, in Fig. 4.3 in the downlink and Fig. 4.7 in the uplink, when the femtocell bandwidth = 0.1 the macrocell bandwidth (red color curves) and when femtocell SIR = -10 dB, the difference between the two curves in the two subfigures under fading condition or non fading condition is almost the same. The same observation is made when femtocell SIR = 10 dB and 30 dB. Moreover, for the femtocell bandwidth = 0.3 macrocell bandwidth (blue color lines) and if we concentrate on the difference in the per-energy capacity ratio between the path loss exponent = 4 line and the path loss exponent = 3 line we notice that the difference is almost equal under fading condition or non fading condition which means that in each subfigure the two lines was displaced due to fading by the same amount.

- **The relation between the per-energy capacity ratio performance in the uplink and the downlink:**

  As shown above, definitely the per-energy capacity ratio performance in the uplink outweighs the per-energy capacity ratio performance in the downlink. To emphasize this statement and by comparing Fig. 4.3 in the downlink to Fig. 4.7 in the uplink, it is clear that the per-energy capacity ratio performance in the uplink outweighs the per-energy capacity ratio performance in the downlink.

- **The relation between the per-energy capacity ratio performance and the bandwidth ratio between the femtocell and the macrocell:**

  As shown in the figures above, the per energy capacity ratio under fading conditions is directly proportional to the bandwidth ratio between the femtocell and macrocell since the per energy capacity ratio performance improves as more

bandwidth is given to the femtocell. However, the per-energy capacity ratio slope decreases as the bandwidth ratio between the femtocell and the macrocell increases.

To illustrate more, in Fig. 4.3 in the downlink and Fig. 4.7 in the uplink, when the path loss exponent = 4, it is clear that as the bandwidth ratio between the femtocell and the macrocell increases from 0.1 (red color lines) to 0.3 (blue color lines) the per energy capacity ratio performance improves by the greatest value and if the bandwidth ratio between the femtocell and the macrocell increases from 0.3 (blue color lines) to 0.5 (black color lines) the per energy capacity ratio performance also improves but by a value less than the value resulted earlier. The same remark and observation is noticed at the path loss exponent = 3 curves group and the path loss exponent = 2 curves group.

Thus, the per-energy capacity ratio slope is inversely proportional to the bandwidth ratio between the femtocell and the macrocell while the per-energy capacity ratio is directly proportional to the bandwidth ratio between the femtocell and the macrocell.

4.3.2 Macrocell Radius and Macrocell SIR

As shown in figures below, in this sample case, the per-energy capacity ratio performance under fading environment was investigated as a function of the two parameters: macrocell SIR and macrocell radius. The relation between the per-energy capacity ratio under fading environment and each parameter, in addition the resultant degradation in the per-energy capacity ratio under fading environment is illustrated in details in the following paragraphs.

- **Downlink channel:**

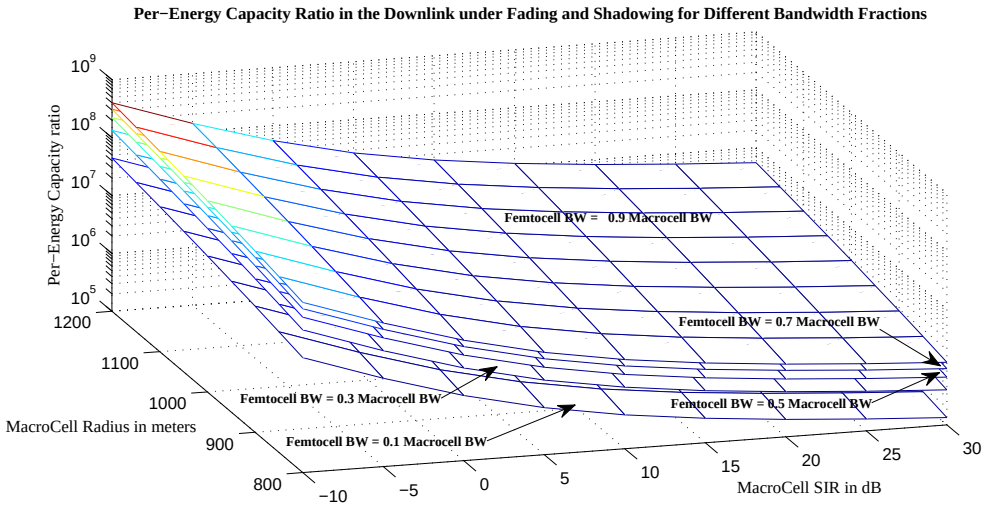

Figure 4 .9: Per-energy capacity ratios in the dedicated channel (downlink) under fading and shadowing (macrocell radius, macrocell SIR).

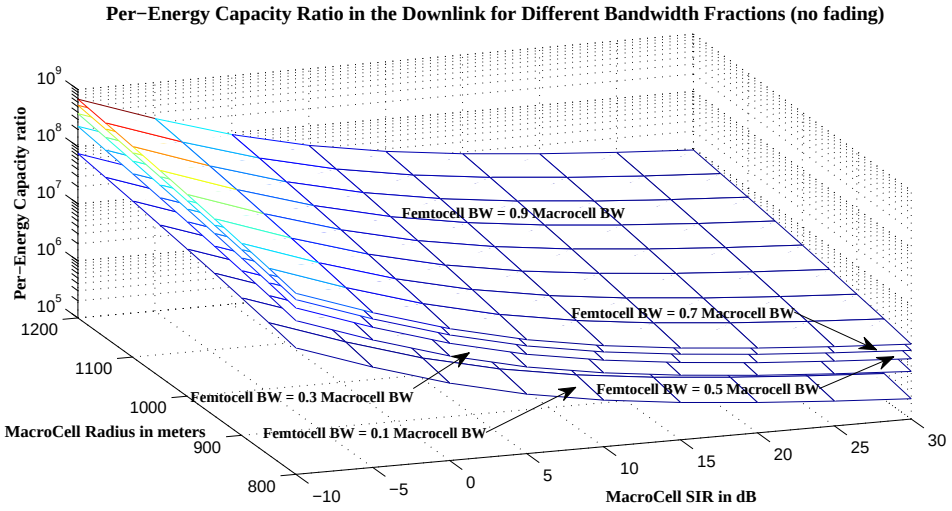

Figure 4 .10: Per-energy capacity ratios in the dedicated channel (downlink) without fading or shadowing (macrocell radius, macrocell SIR).

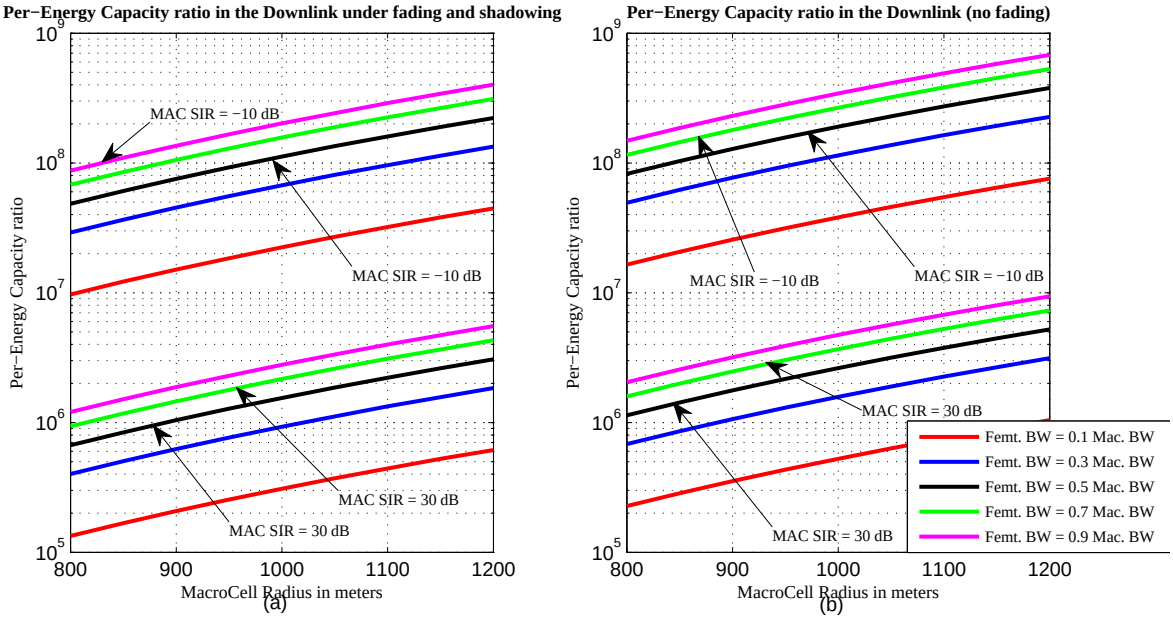

Figure 4 .11: Per-energy capacity ratios in the dedicated channel (downlink) as a function of macrocell radius for some macrocell SIR values (a) under fading condition (b) under non-fading condition.

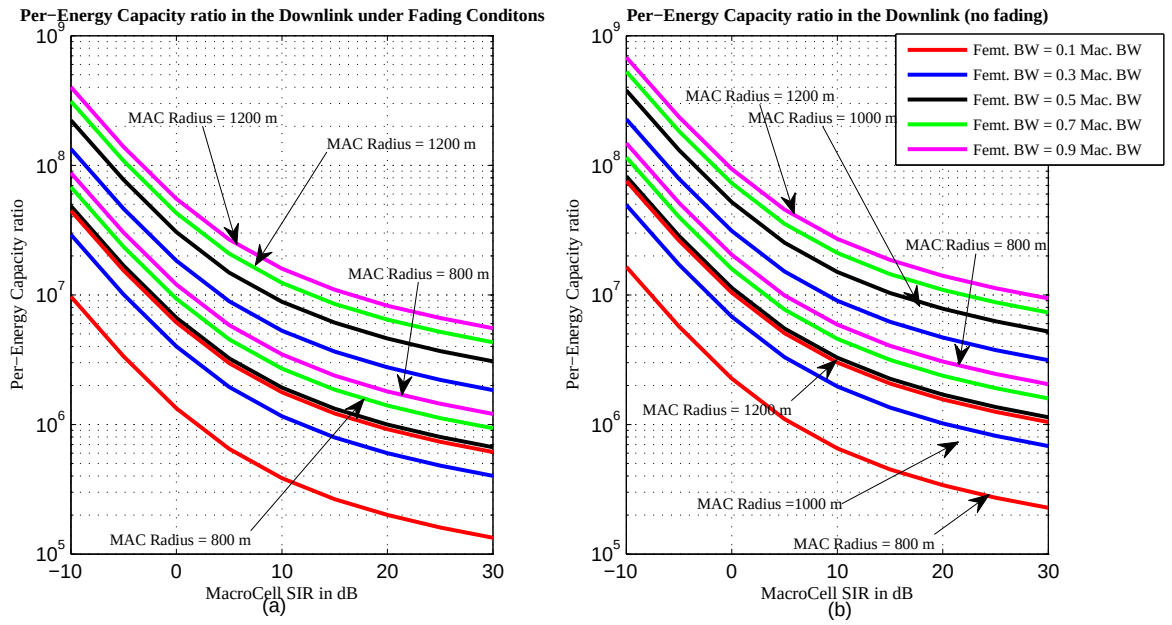

Figure 4 .12: Per-energy capacity ratios in the dedicated channel (downlink) as a function of macrocell SIR for some macrocell radius values (a) under fading condition (b) under non-fading condition.

- **Uplink channel:**

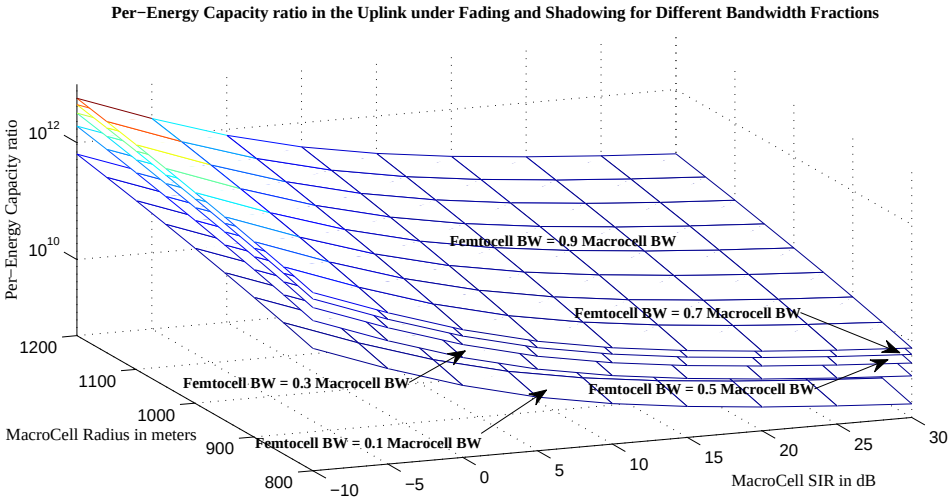

Figure 4 .13: Per-energy capacity ratios in the dedicated channel (uplink) under fading and shadowing (macrocell radius, macrocell SIR).

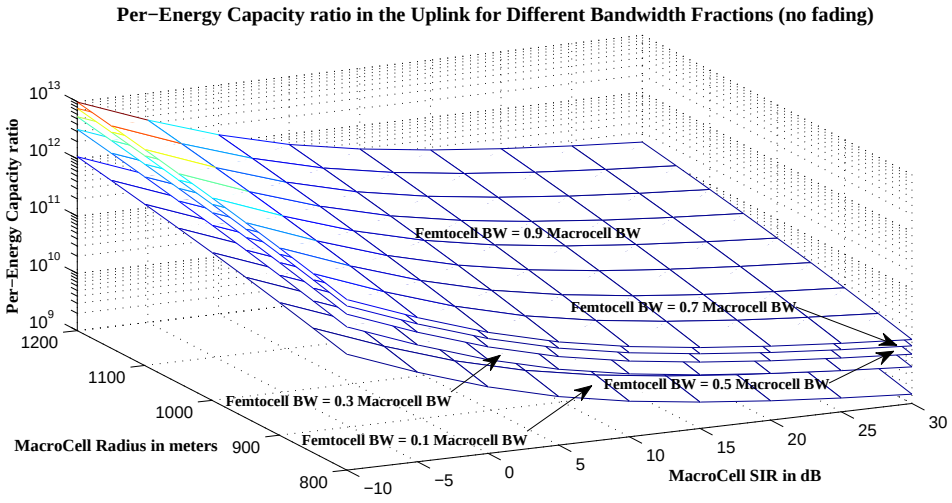

Figure 4 .14: Per-energy capacity ratios in the dedicated channel (uplink) without fading or shadowing (macrocell radius, macrocell SIR).

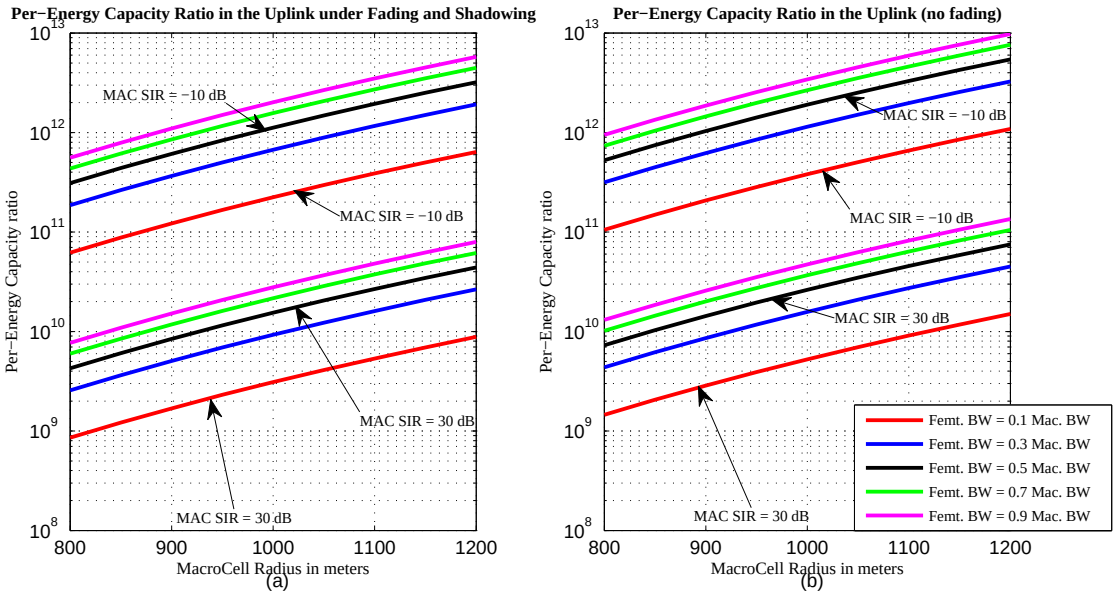

Figure 4 .15: Per-energy capacity ratios in the dedicated channel (uplink) as a function of macrocell radius for some macrocell SIR values (a) under fading condition (b) under non-fading condition.

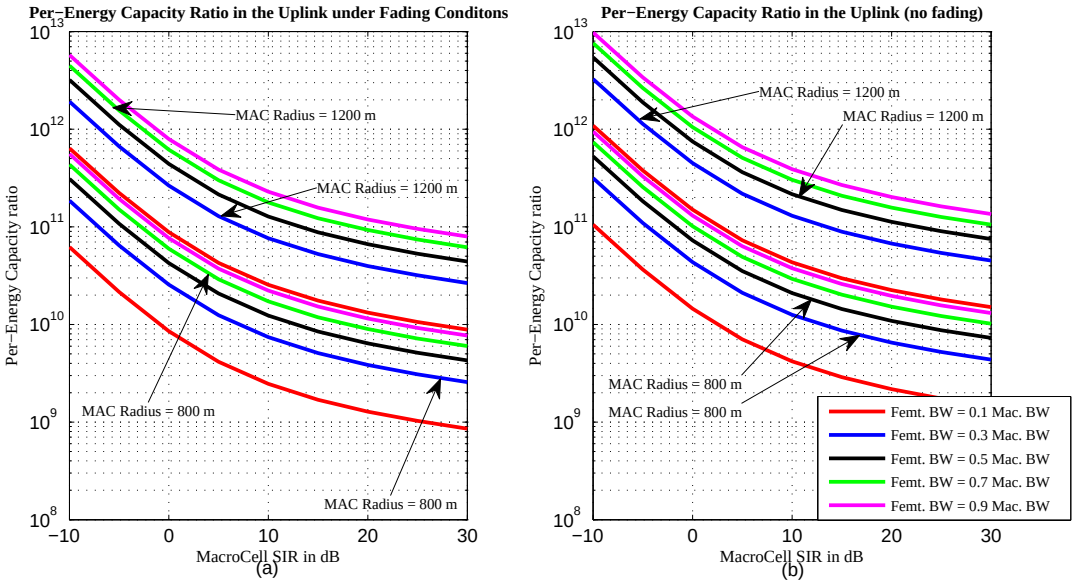

Figure 4 .16: Per-energy capacity ratios in the dedicated channel (uplink) as a function of macrocell SIR for some macrocell radius values (a) under fading condition (b) under non-fading condition.

- **The relation between the per-energy capacity ratio under fading conditions and the macrocell SIR:**

  The per-energy capacity ratio under fading conditions is inversely proportional to the macrocell SIR. For example in Fig. 4.12 in the downlink and Fig. 4.16 in the uplink, when the femtocell bandwidth = 0.1 the macrocell bandwidth (red color lines) and when the macrocell radius = 800 m, it is clear that the per-energy capacity ratio decreases as the macrocell SIR value increases. Another remark is, as the macrocell SIR value increases, the per-energy capacity ratio rate decreases with respect to the decreasing macrocell SIR. To explain more, in Fig. 4.11 in the downlink and Fig. 4.15 in the uplink, when the femtocell bandwidth = 0.5 the macrocell bandwidth (black color lines) and when the macrocell radius = 1000 m, as the macrocell SIR value increases from -10 dB to 10 dB, the per-energy capacity ratio decreases by value greater than the value resulted when the macrocell SIR increases from 10 dB to 30 dB.

- **The relation between the per-energy capacity ratio under fading conditions and macrocell radius:**

  The per energy capacity ratio under fading conditions is directly proportional to the macrocell radius. For example in Fig. 4.11 in the downlink and Fig. 4.15 in the uplink, when the femtocell bandwidth = 0.5 the macrocell bandwidth (black color lines) and when the macrocell SIR= 30 dB, it is clear that the per-energy capacity ratio increases as the macrocell radius value increases. In addition, the per energy capacity ratio slope under fading condition is constant with respect to the macrocell radius. For instance, Fig. 4.11 in the downlink and Fig. 4.15 in the uplink depict the resultant per-energy capacity ratios under fading environment versus the macrocell radius for some macrocell SIR values,

as shown in these figures the result is only straight lines which means that the per-energy capacity ratio slope or rate of increase is definitely constant.

- **The degradation in the per-energy capacity ratio under fading conditions:**

  As in the previous sample case, the degradation in the per-energy capacity ratio due to fading is obvious in both samples. In addition, it is almost independent and not related to either the macrocell radius or the macrocell SIR.

  Actually, if Fig. 4.11 in the downlink and Fig. 4.15 in the uplink are considered as examples, when the femtocell bandwidth = 0.5 the macrocell bandwidth (black color curves) and when macrocell SIR = -10 dB, the difference between the two curves in the two subfigures under fading conditions or non fading conditions is almost the same for all macrocell radius. The same remark is noticed at femtocell SIR = 10 dB and 30 dB. Moreover, in Fig. 4.12 in the downlink and Fig. 4.16 in the uplink, for the femtocell bandwidth = 0.1 macrocell bandwidth (red color lines), if we concentrate on the difference in the per-energy capacity ratio between the macrocell radius = 800 m line and the macrocell radius = 1000 m line it can be noticed that the difference is almost equal under fading conditions or non fading conditions which means that in each subfigure the two lines was displaced due to fading by the same amount.

- **The relation between the per-energy capacity ratio performance in the uplink and the downlink:**

  Like the previous sample case, the per-energy capacity ratio performance in the uplink is better than the per-energy capacity ratio performance in the downlink and by comparing Fig. 4.11 in the downlink to Fig. 4.15 in the uplink this

result is obviously noticed.

- **The relation between the per-energy capacity ratio performance and the bandwidth ratio between the femtocell and the macrocell:**

  As shown in the figures above, the per energy capacity ratio under fading conditions is directly proportional to the bandwidth ratio between the femtocell and the macrocell because the per energy capacity ratio performance improves when more bandwidth is given to the femtocell. However, the per-energy capacity ratio slope decreases as the bandwidth ratio between the femtocell and the macrocell increases. To illustrate more, in Fig. 4.9, Fig. 4.10 in the downlink and Fig. 4.13, Fig. 4.14 in the uplink, it is clear that as the bandwidth ratio between the femtocell and the macrocell increases, the per-energy capacity ratio planes becomes closer. As a result it is concluded that the per-energy capacity ratio slope is inversely proportional to the bandwidth ratio.

4.4 Fading analysis in the co-channel case

As in the dedicated channel case, in this part, the per-energy capacity ratio performance was evaluated under fading conditions as a function of the femtocell SIR, macrocell radius, macrocell SIR, and path loss exponent. However, in each case, three parameters were selected and the per-energy capacity ratio performance under fading environment as a function of that combination was investigated. For each case, eight figures were plotted: four figures represent the per-energy capacity ratio under fading environment in the downlink and the other four figures represent the per-energy capacity ratio under fading environment in the uplink. Consequently, several cases were investigated and results in the form of graphs were obtained. However, only sample

cases are shown in this part to avoid redundancy.

4.4.1 Femtocell SIR and macrocell radius

- **Downlink channel:**

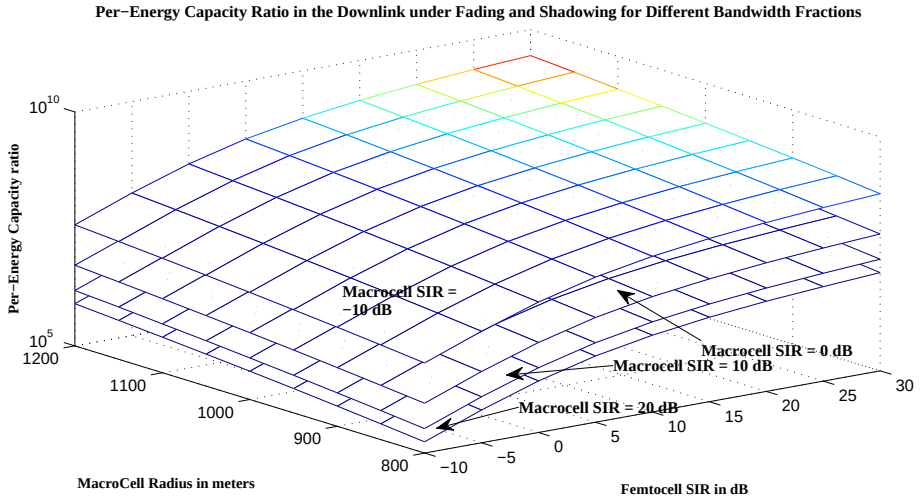

Figure 4 .17: Per-energy capacity ratios in the co-channel (downlink) under fading and shadowing (femtocell SIR, macrocell radius).

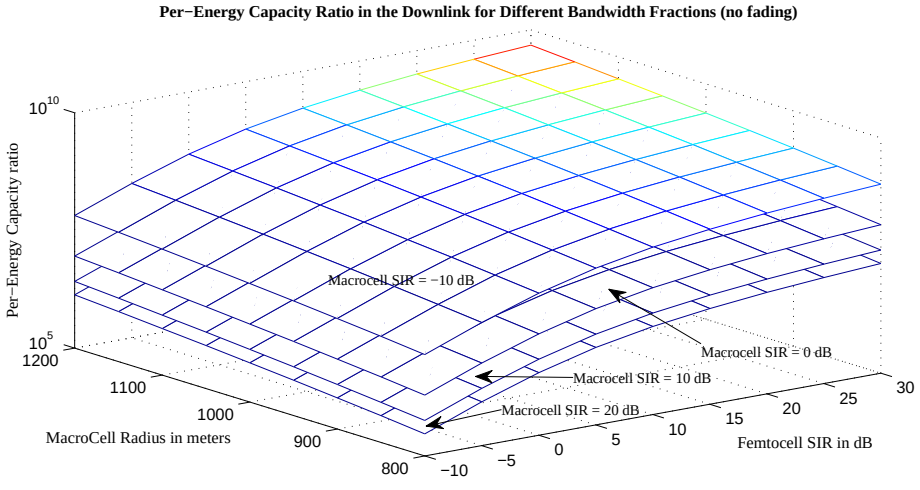

Figure 4 .18: Per-energy capacity ratios in the co-channel (downlink) without fading or shadowing (femtocell SIR, macrocell radius).

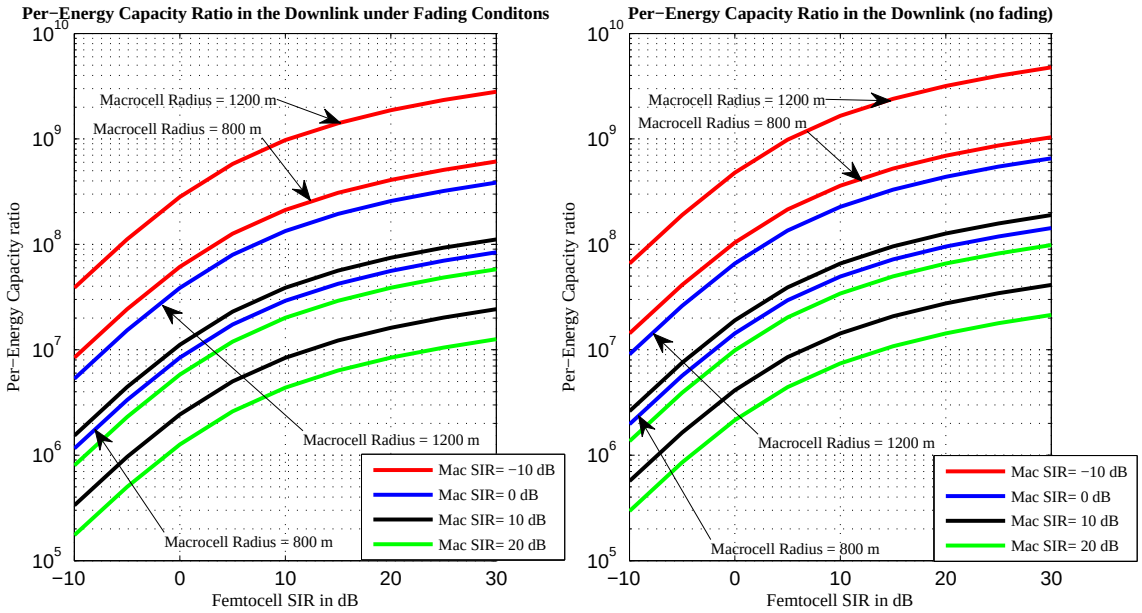

Figure 4 .19: Per-energy capacity ratios in the co-channel (downlink) as a function of femtocell SIR for some macrocell radius values (a) under fading condition (b) under non-fading condition.

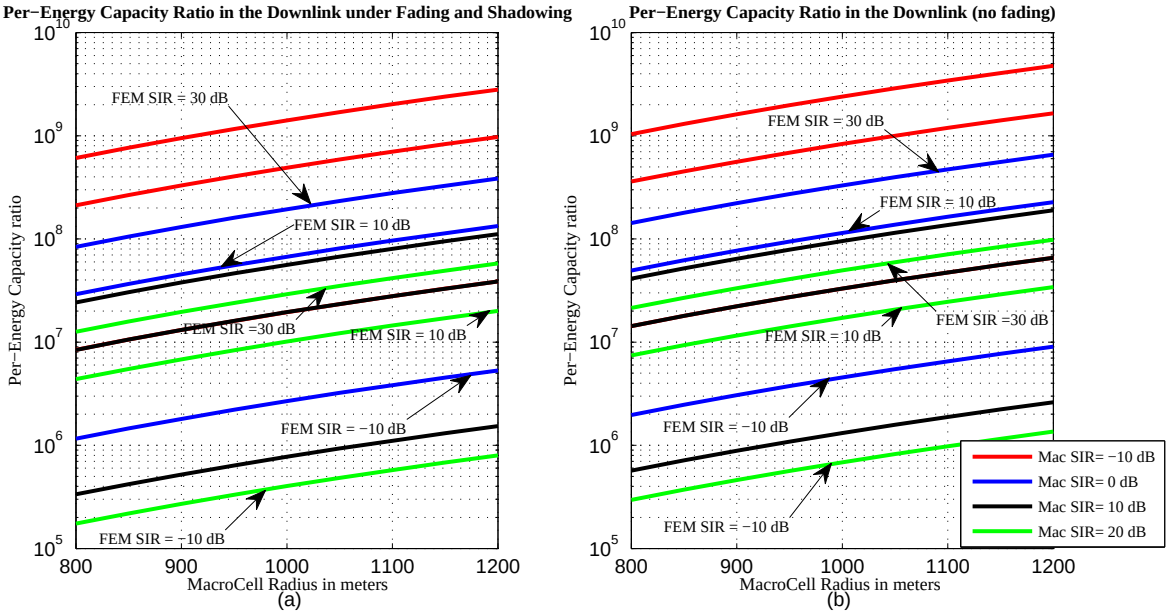

Figure 4 .20: Per-energy capacity ratios in the co-channel (downlink) as a function of macrocell radius for some femtocell SIR values (a) under fading condition (b) under non-fading condition.

- **Uplink channel:**

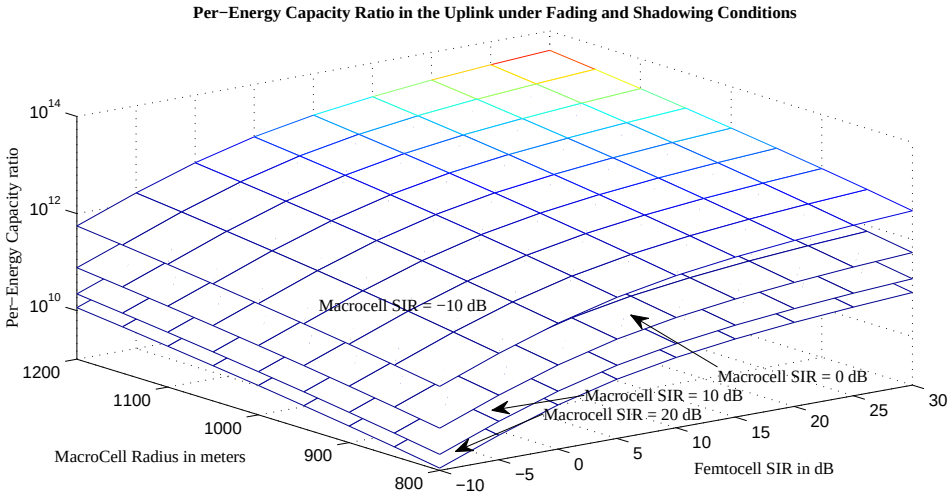

Figure 4 .21: Per-energy capacity ratios in the co-channel (uplink) under fading and shadowing (femtocell SIR, macrocell radius).

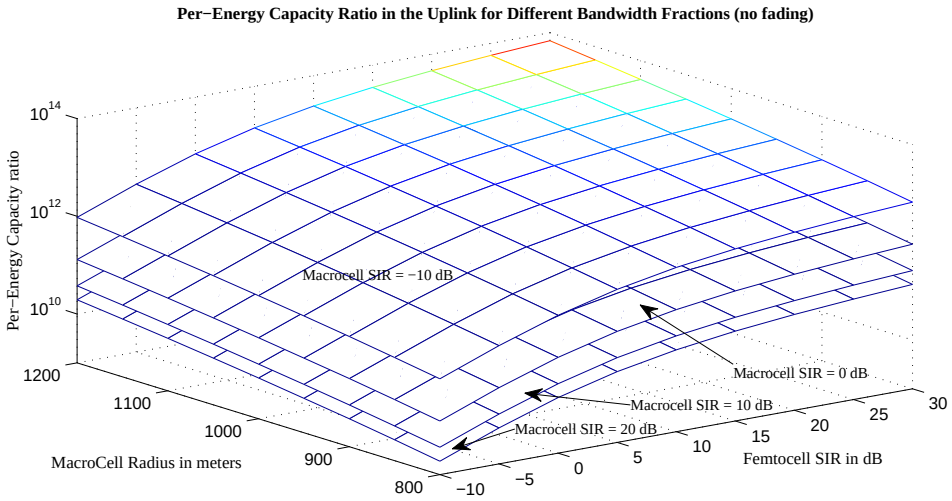

Figure 4 .22: Per-energy capacity ratios in the co-channel (uplink) without fading or shadowing (femtocell SIR, macrocell radius).

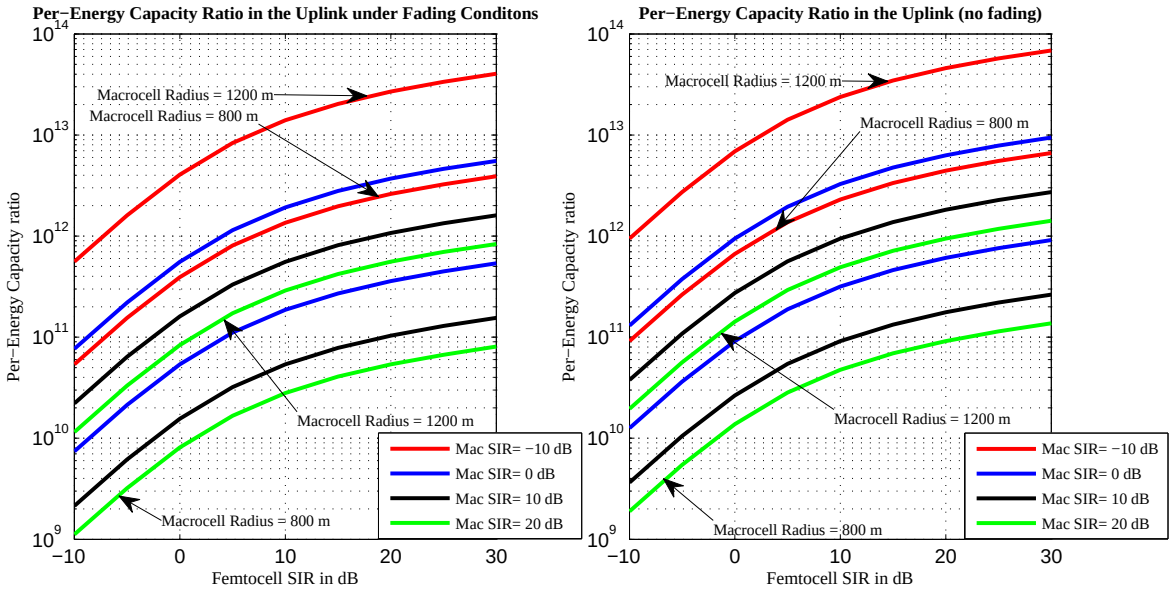

Figure 4 .23: Per-energy capacity ratios in the co-channel (uplink) as a function of femtocell SIR for some macrocell radius values (a) under fading condition (b) under non-fading condition.

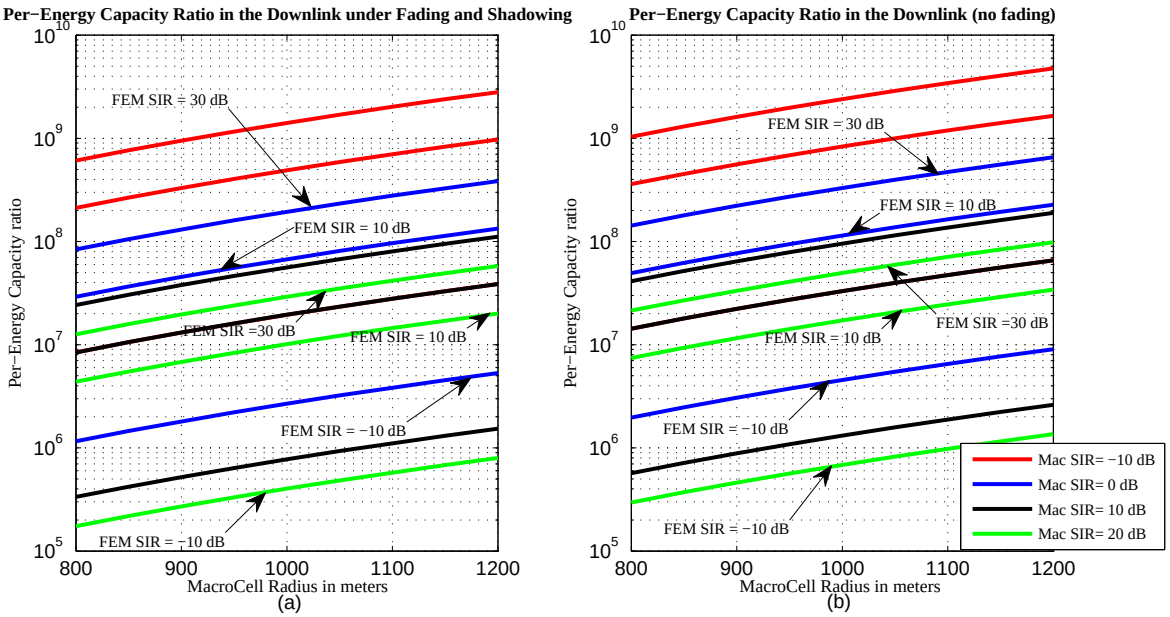

Figure 4 .24: Per-energy capacity ratios in the co-channel (uplink) as a function of macrocell radius for some femtocell SIR values (a) under fading condition (b) under non-fading condition.

As shown in the figures above, in this sample case, the per-energy capacity ratio performance under fading environment (co-channel case) was investigated as a function of the two parameters: femtocell SIR and macrocell radius. In each plot, the macrocell SIR was set to -10 dB, 0 dB, 10 dB, and 20 dB respectively. The relation between the per energy capacity ratio under fading environment and each parameter, and the resultant degradation in the per-energy capacity ratio under fading environment is illustrated in details in the following paragraphs.

- **The relation between the per-energy capacity ratio under fading conditions and the femtocell SIR:**

  The per-energy capacity ratio under fading environment is directly proportional to the femtocell SIR. Further, as the femtocell SIR value increases, the per energy capacity ratio rate of increase decreases with respect to the increasing femtocell SIR . For an example, in Fig. 4.20 in the downlink and Fig. 4.24 in the uplink, when the macrocell SIR = 0 dB (blue color lines) and when the macrocell radius = 1000 m, as the femtocell SIR value increases from -10 dB to 10 dB the per energy capacity ratio increases by value greater than the value resulted when the femtocell SIR increases from 10 dB to 30 dB.

- **The relation between the per-energy capacity ratio under fading conditions and the macrocell radius:**

  The per energy capacity ratio under fading environment is directly proportional to the macrocell radius. For example in 4.20 in the downlink and Fig. 4.24 in the uplink, when the macrocell SIR = 20 dB (green color lines) and when the femtocell SIR= -10 dB, it is clear that the per-energy capacity ratio increases as the macrocell radius value increases. In addition, the per energy capacity ratio slope under fading condition is constant with respect to the macrocell radius.

For instance, 4.20 and Fig. 4.24 depict the resultant per-energy capacity ratios under fading environment versus the macrocell radius for some macrocell SIR values, as shown in these figures the result is only straight lines which means that the per-energy capacity ratio slope or rate of increase is definitely constant.

- **The relation between the per-energy capacity ratio under fading conditions and the macrocell SIR:**

  As shown in figures above, the per-energy capacity ratio under fading environment is inversely proportional to the macrocell SIR. For example in 4.20 in the downlink, it is clear that the per-energy capacity ratio decreases as the macrocell SIR value increases and vice versa.

- **The degradation in the per-energy capacity ratio under fading conditions:**

  As shown in the figures above, in this sample case also, the degradation in the per-energy capacity ratio due to fading is apparent. In addition, it is almost not dependent on the femtocell SIR, the macrocell SIR, or the macrocell radius.

- **The relation between the per-energy capacity ratio performance in the uplink and the downlink:**

  In this sample case also, the per-energy capacity ratio performance in the uplink is better than the per-energy capacity ratio performance in the downlink and by comparing Fig. 4.19 in the downlink to Fig. 4.23 in the uplink this result is apparently noticed.

4.4.2 Macrocell Radius and Path loss exponent

- **Downlink channel:**

1. Macrocell SIR = 3 dB while femtocell SIR is variable

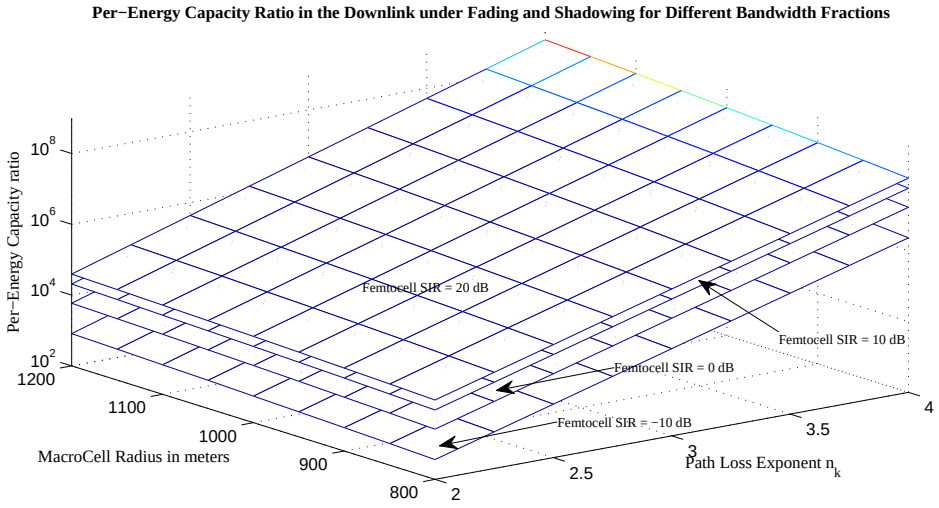

Figure 4 .25: Per-energy capacity ratios in the co-channel (downlink) under fading and shadowing (macrocell radius, path loss exponent).

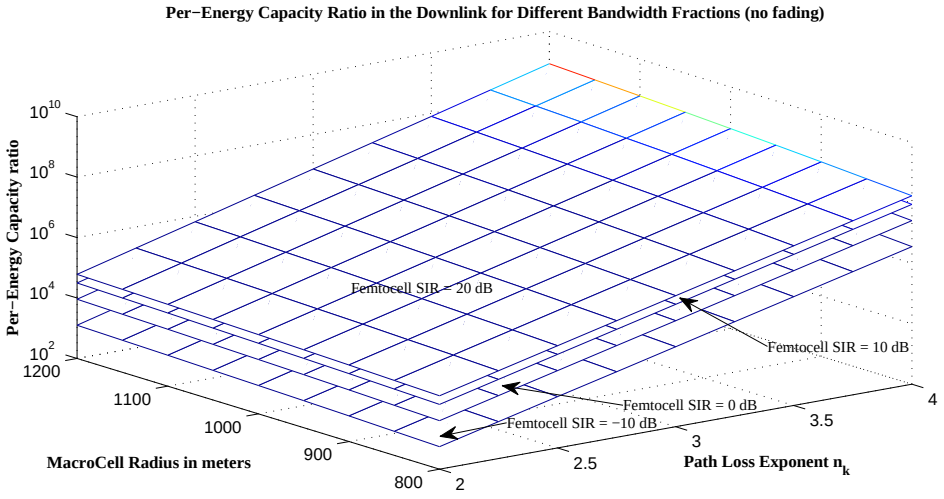

Figure 4 .26: Per-energy capacity ratios in the co-channel (downlink) without fading or shadowing (macrocell radius, path loss exponent).

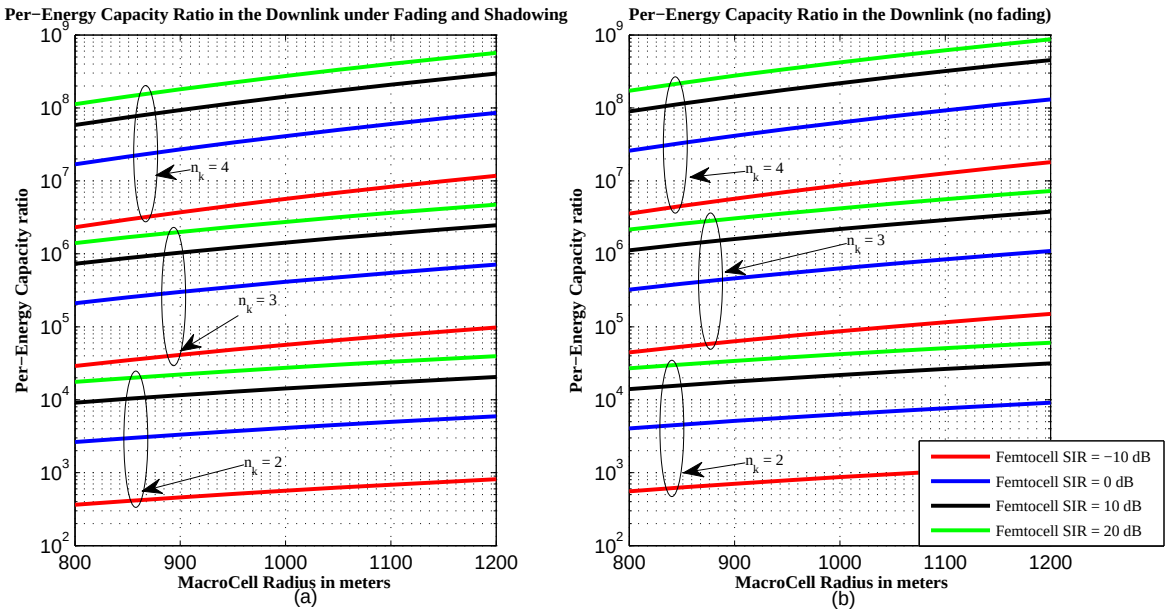

Figure 4 .27: Per-energy capacity ratios in the co-channel (downlink) as a function of macrocell radius for some path loss exponent values (a) under fading condition (b) under non-fading condition.

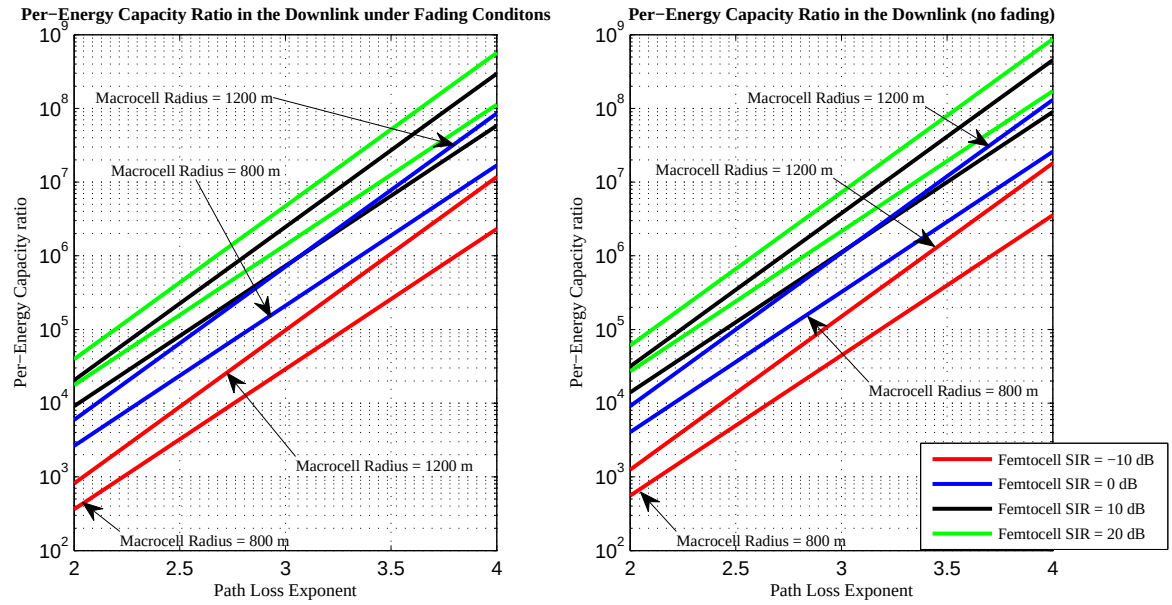

Figure 4 .28: Per-energy capacity ratios in the co-channel (downlink) as a function of path loss exponent for some macrocell radius values (a) under fading condition (b) under non-fading condition.

2. Femtocell SIR = 3 dB while macrocell SIR is variable:

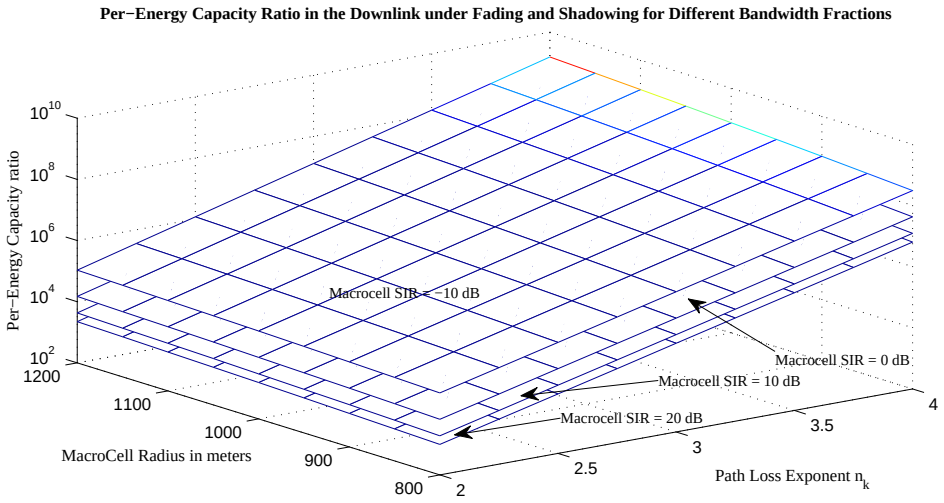

Figure 4 .29: Per-energy capacity ratios in the co-channel (downlink) under fading and shadowing (macrocell radius, path loss exponent).

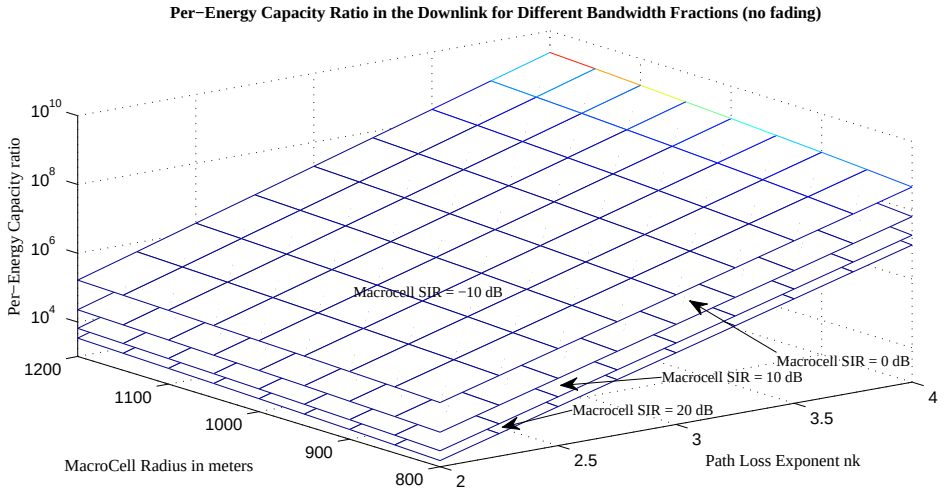

Figure 4 .30: Per-energy capacity ratios in the co-channel (downlink) without fading or shadowing (macrocell radius, path loss exponent).

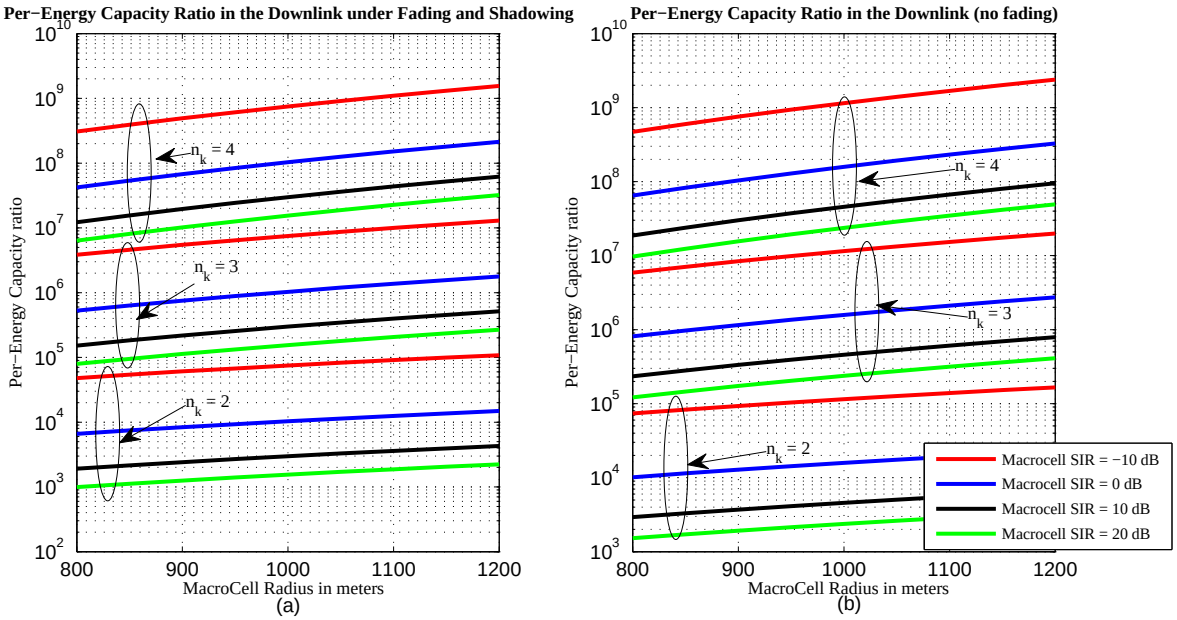

Figure 4 .31: Per-energy capacity ratios in the co-channel (downlink) as a function of macrocell radius for some path loss exponent values (a) under fading condition (b) under non-fading condition.

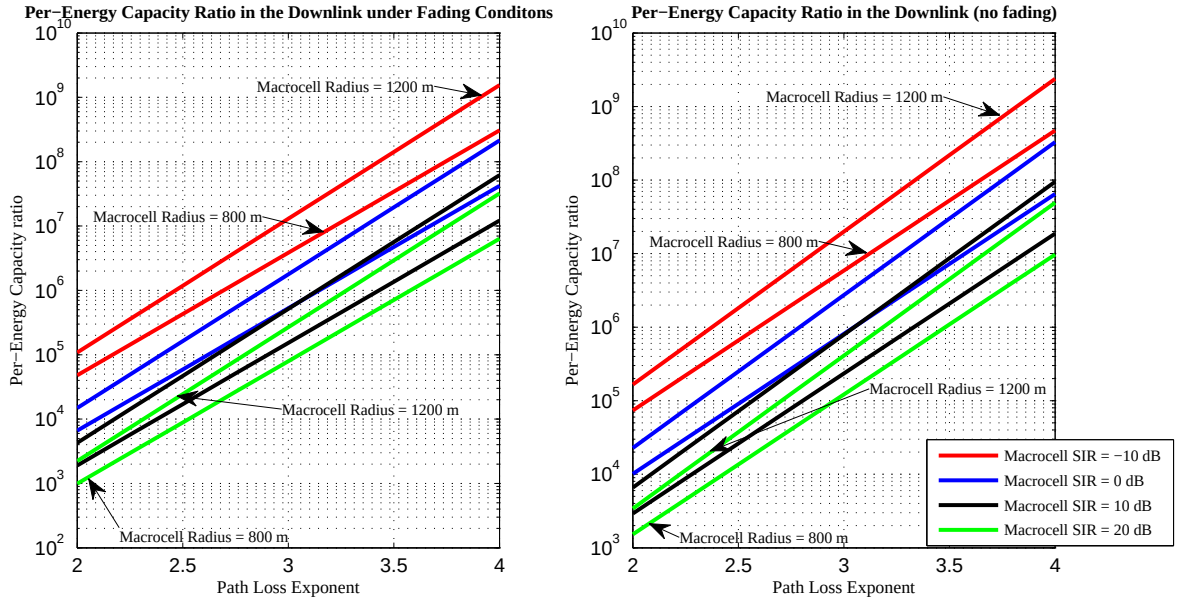

Figure 4 .32: Per-energy capacity ratios in the co-channel (downlink) as a function of path loss exponent for some macrocell radius values (a) under fading condition (b) under non-fading condition.

- **Uplink channel:**

  1. Macrocell SIR = 3 dB while femtocell SIR is variable:

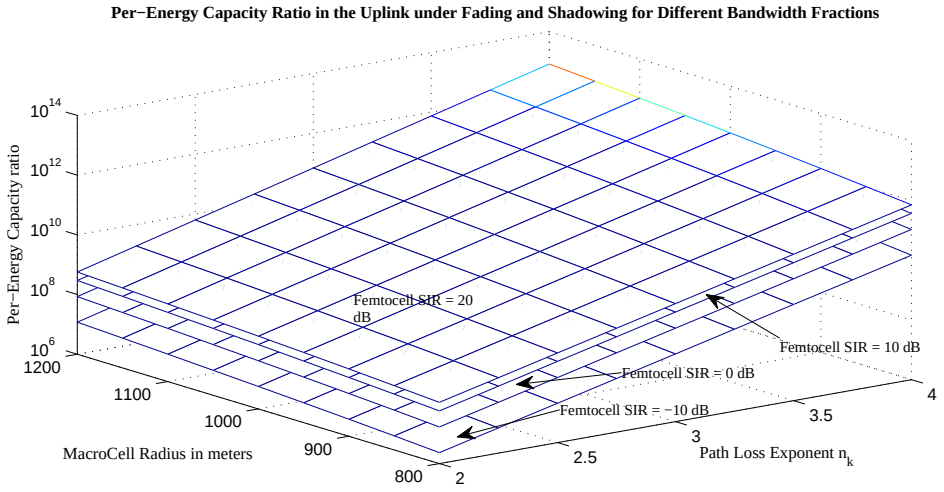

Figure 4 .33: Per-energy capacity ratios in the co-channel (uplink) under fading and shadowing (macrocell radius, path loss exponent).

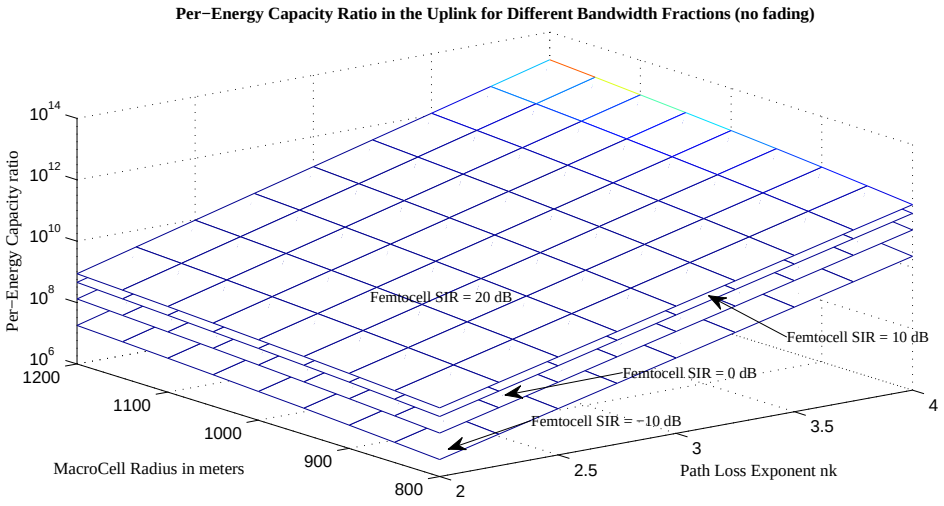

Figure 4 .34: Per-energy capacity ratios in the co-channel (uplink) without fading or shadowing (macrocell radius, path loss exponent).

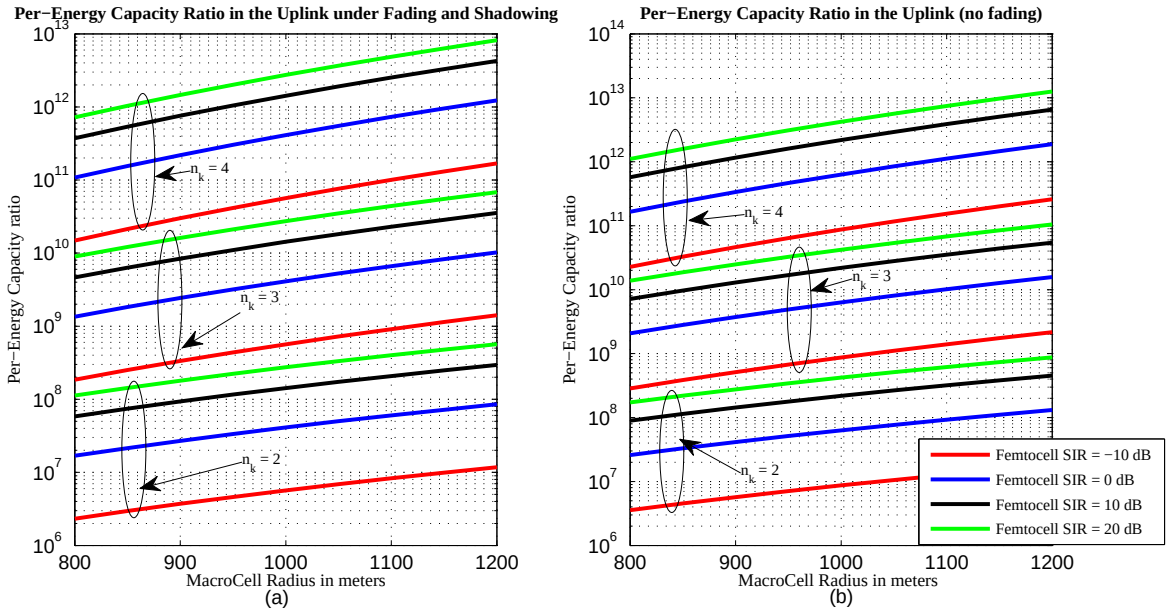

Figure 4 .35: Per-energy capacity ratios in the co-channel (uplink) as a function of macrocell radius for some path loss exponent values (a) under fading condition (b) under non-fading condition.

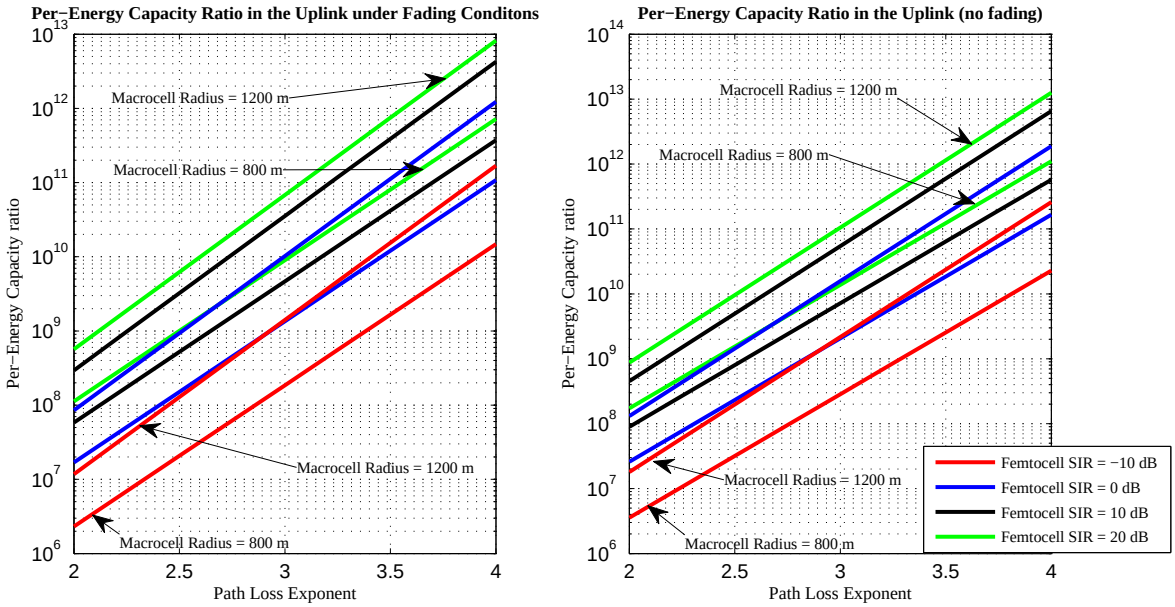

Figure 4 .36: Per-energy capacity ratios in the co-channel (uplink) as a function of path loss exponent for some macrocell radius values (a) under fading condition (b) under non-fading condition.

2. Femtocell SIR = 3 dB while macrocell SIR is variable:

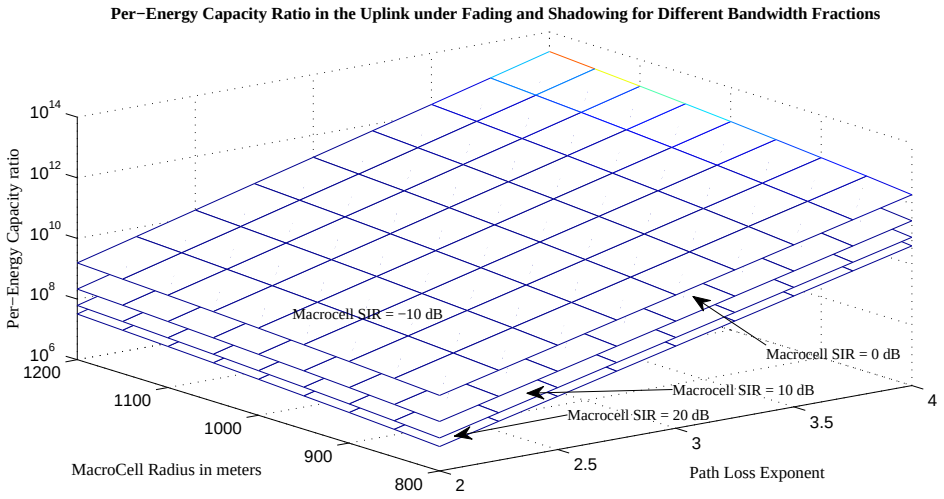

Figure 4 .37: Per-energy capacity ratios in the co-channel (uplink) under fading and shadowing (macrocell radius, path loss exponent).

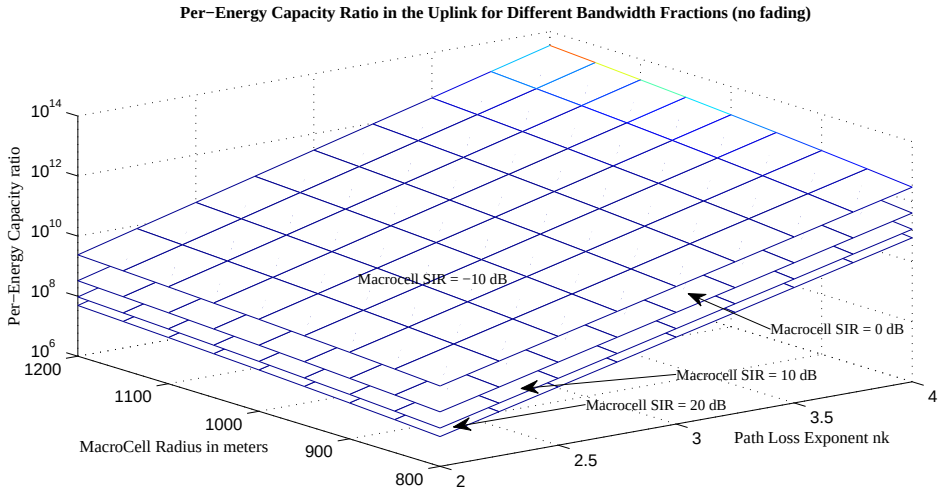

Figure 4 .38: Per-energy capacity ratios in the co-channel (uplink) without fading or shadowing (macrocell radius, path loss exponent).

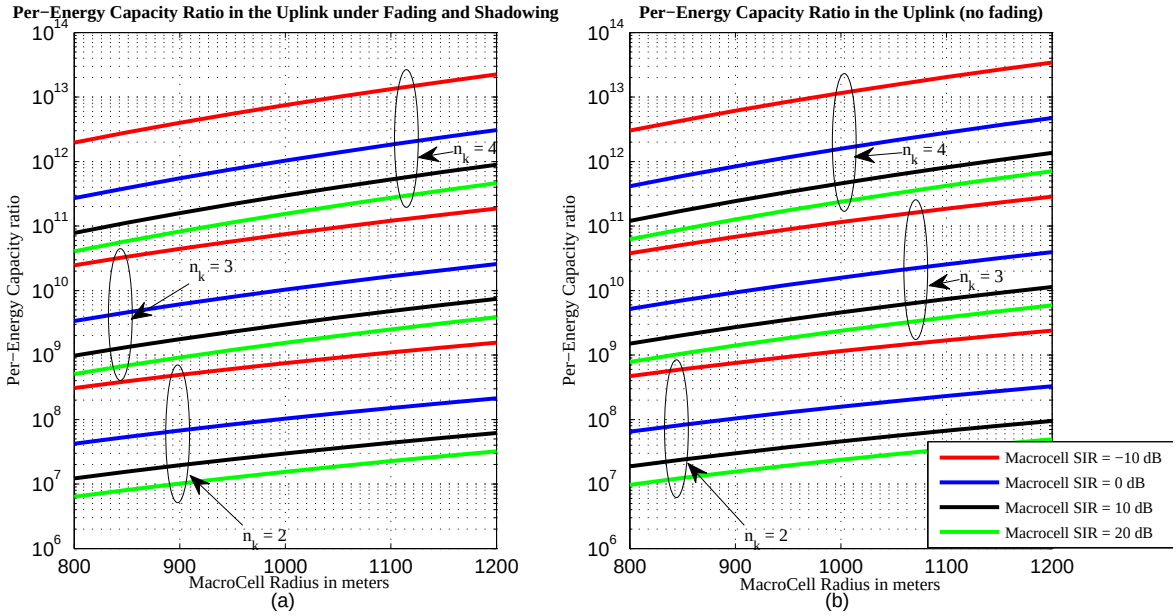

Figure 4 .39: Per-energy capacity ratios in the co-channel (uplink) as a function of macrocell radius for some path loss exponent values (a) under fading condition (b) under non-fading condition.

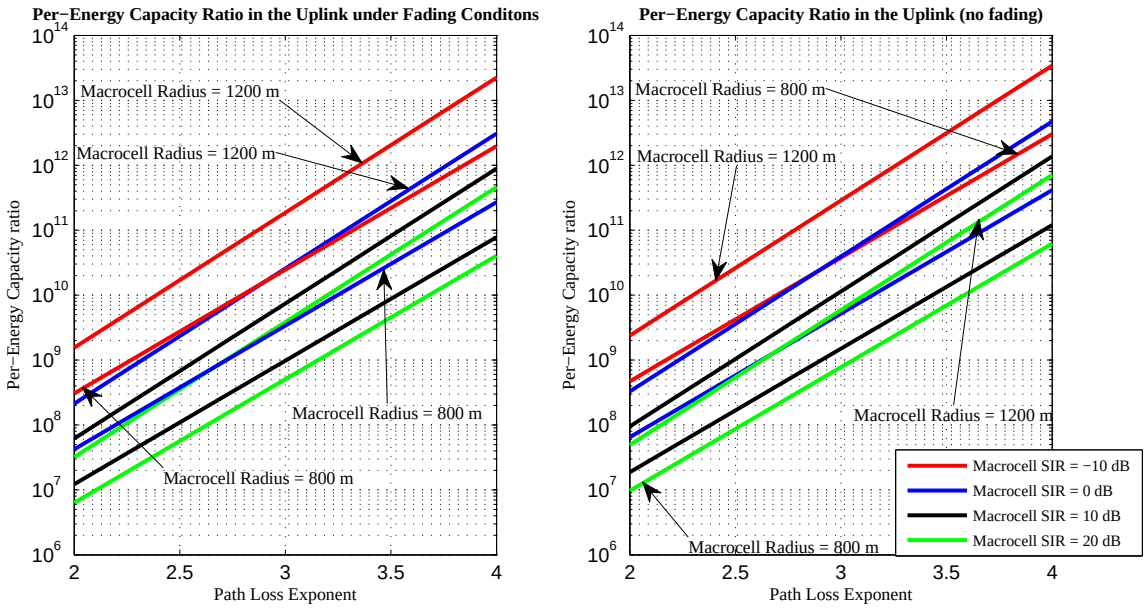

Figure 4 .40: Per-energy capacity ratios in the co-channel (uplink) as a function of path loss exponent for some macrocell radius values (a) under fading condition (b) under non-fading condition.

As shown in the figures above, in this part, the per-energy capacity ratio performance under fading environment (co-channel case) was investigated as a function of the two parameters: macrocell radius and path loss exponent. Furthermore, it was decided to include femtocell SIR or macrocell SIR in this simulation case besides he two parameters, and the used procedure was as follows: firstly the femtocell SIR was set to four cases -10 dB, 0 dB, 10 dB, and 20 dB while keeping the macrocell SIR constant equal to 3 dB then secondly the opposite was done where the macrocell SIR was set to four cases -10 dB, 0 dB, 10 dB, and 20 dB and the macrocell SIR was kept constant equal to 3 dB.

As a result as shown above, sixteen figures were plotted: eight figures represent the per-energy capacity ratio under fading environment in the downlink and the other eight figures represent the per-energy capacity ratio under fading environment in the uplink. The macrocell radius was investigated earlier in this part, thus only the path loss exponent is commented and discussed.

- **The relation between the per-energy capacity ratio under fading conditions and the path loss exponent:**

  As in the simulation in the dedicated case, in this simulation case, it is found that the per-energy capacity ratio under fading environment is directly proportional to the path loss exponent. Further, the per-energy capacity ratio slops under fading environment with respect to the path loss exponent is almost constant. For instance, Fig. 4.28 and Fig. 4.36 depict the resultant per-energy capacity ratios under fading environment versus the path loss exponent, as shown in these figures they result in only straight lines which means that the per-energy capacity ratio slope is certainly constant.

  In addition, in this sample case, it has been noticed that the value of the per-

energy capacity ratio slope under fading environment undergoes a slight change as the value of the macrocell SIR or the femtocell SIR changes. In the dedicated case, this happened when the bandwidth fraction given to the femtocell changes. Similarly in this sample case (co-channel case), this taken place as the value of the macrocell SIR or the femtocell SIR changes.

- **The degradation in the per-energy capacity ratio under fading conditions:**

  As shown in the figures above, similarly to the previous sample cases, the degradation in the per-energy capacity ratio due to fading is clear. In addition, it is almost not dependent on the femtocell SIR, the path loss exponent, the macrocell SIR, or the macrocell radius.

4.5 Summary

In this chapter, we have studied per-energy capacity ratio in the macro-femto environment under fading conditions. Only the femtocell-macrocell environment was considered because the per-energy capacity ratio performance is the best in this environment. In addition, the behavior of the per-energy capacity ratio under fading environment is studied with respect to femtocell SIR, macrocell SIR, path loss exponent, and macrocell radius in order to investigate the effect of these parameters on the per-energy capacity ratio performance. In the femtocell-macrocell environment, the per-energy capacity ratio under fading for the dedicated channel case and the co-channel case were evaluated. In addition, in each channel assignment both the downlink and uplink transmission channels were considered.

Another important task that was carried out in this chapter is, the derivation

of a new mathematical expression that was used in the investigation of the per-energy capacity ratio in macro-femto environment under fading conditions. Finally, the analysis of the per-energy capacity ratio degradation under fading conditions, which is one of the main objectives in this thesis, was carried out by investigating the difference in the per-energy capacity ratio performance under fading environment and non fading conditions. Thus, in all the simulation cases, the degradation in the per-energy capacity ratio due to fading was investigated and commented.

Chapter 5

Per-energy Capacity Ratio Degradation Due To Fading and Its Compensation

5.1 Introduction

In the previous chapter, the per-energy capacity ratio in the absence and presence of channel fading was investigated. In this chapter, two main tasks were in focus. The evaluation of the per-energy capacity ratio degradation percentage as a function of macrocell shadowing variance, femtocell shadowing variance, and distance (or time) was considered. The per-energy capacity ratio percentage degradation is used to compensate the per-energy capacity ratio degradation under fading conditions. This compensation for the per-energy capacity ratio degradation under fading conditions is considered as an inaccurate power control which brings back the per-energy capacity ratio near about its original value i.e. the value of the per-energy capacity ratio without fading.

5.2 Methodology

As shown above in (4 .10), the per-energy capacity ratio under fading conditions is a function of the fading ratio and hence of the channel type. This conclusion was inspiring to consider that there must be a mathematical background which could cause this result? Fortunately, a new result was derived. The degradation in the per-energy capacity ratio due to fading conditions is only a function of the fading ratio and hence it must be dependent on the fading parameters f_{mac} and f_{fem}. The fading ratio is defined as (f_{mac}/f_{fem}) where f_{mac} is the fading in the macrocell environment and f_{fem} is the fading in the femtocell environment. The degradation derivation is shown in the following section.

Beginning from the common percentage degradation rule:

$$Deg(\%) = \frac{\Gamma_u(k) - \Gamma_{u_{fad}}(k)}{\Gamma_u(k)} \times 100, \tag{5 .1}$$

where $\Gamma_u(k)$ and $\Gamma_{u_{fad}}(k)$ are the per-energy capacity under non-fading conditions and under fading conditions, respectively and substituting for $\Gamma_u(k)$ from (2.5) and $\Gamma_{u_{fad}}(k)$ from (4.9) in (5.1) the following equation results:

$$\begin{aligned} Deg(\%) &= \frac{\Gamma_c(k)\Gamma_s(k)^{-1} - \Gamma_c(k)\Gamma_{s_{fad}}(k)^{-1}}{\Gamma_c(k)\Gamma_s(k)^{-1}} \times 100, \\ &= \frac{\Gamma_c(k)}{\Gamma_c(k)}\Big[\frac{\Gamma_s(k)^{-1} - \Gamma_{s_{fad}}(k)^{-1}}{\Gamma_s(k)^{-1}}\Big] \times 100, \\ &= \frac{\Gamma_s(k)^{-1} - \Gamma_{s_{fad}}(k)^{-1}}{\Gamma_s(k)^{-1}} \times 100, \\ &= \Big[1 - \frac{\Gamma_{s_{fad}}(k)^{-1}}{\Gamma_s(k)^{-1}}\Big] \times 100, \\ &= \Big[1 - \frac{\Gamma_s(k)}{\Gamma_{s_{fad}}(k)}\Big] \times 100, \end{aligned} \tag{5 .2}$$

let us now substitute for the value of $\Gamma_{s_{fad}}$ from (4.8) in (5.2). As result we get:

$$\begin{aligned} Deg(\%) &= \Big[1 - \frac{\Gamma_s(k)}{\Gamma_{s_{fad}}(k)}\Big] \times 100, \\ &= \Big[1 - \frac{\Gamma_s(k)}{\frac{f_{mac}}{f_{fem}}\Gamma_s(k)}\Big] \times 100, \\ &= \Big[1 - \frac{1}{\frac{f_{mac}}{f_{fem}}}\Big] \times 100, \\ &= \Big[1 - \frac{1}{fadingratio}\Big] \times 100. \end{aligned} \tag{5 .3}$$

As shown above, (5.3) proves that the degradation percentile value in the per-energy capacity ratio is only a function of the fading ratio and hence it also shows that the per-energy capacity ratio degradation in the per-energy capacity ratio is only a function of the channel type. Thus, it is used to evaluate the degradation percentile value in the per-energy capacity ratio.

In simulation experiments, two different fading scenarios were considered: the macrocell environment where shadowing plus fast fading was present and the femtocell environment where only the shadowing is considered to be present. Therefore, it is important and motivating to analyze the effect of the macrocell shadowing variance, the femtocell shadowing variance, and the distance (or time) on the fading ratio and hence on per-energy capacity ratio degradation under fading conditions.

5.3 The per-energy capacity ratio percentage degradation

Consider below in Figs. 5.1 and 5.2, the two snapshots. The first snapshot is of the performance over 0.1 meter long tract while the second snapshot is over 0.3 meter long.

In each case, the per-energy capacity ratio degradation percentage is simulated as a function of the macrocell shadowing variance and the femtocell shadowing variance. The macrocell shadowing variance ranges from 4 dB to 16 dB while the femtocell shadowing variance ranges from 2 dB to 8 dB.

As shown below, the per-energy capacity ratio degradation percentage is directly proportional to both the macrocell shadowing variance and femtocell shadowing variance. Additionally, it is shown that the per-energy capacity ratio degradation percentage slope or rate of increase with respect to either the femtocell shadowing variance or the macrocell shadowing variance is not constant. Actually, the decrement in the per-energy capacity ratio percent degradation slope on either the femtocell shadowing variance or the macrocell shadowing variance increase is very small and not noticable. Nevertheless, if we concentrate on each subfigure we see that the lines in each subfigure don't go in parallel to each other as the variances increase but these lines tend to be closer to each other as the variances increase.

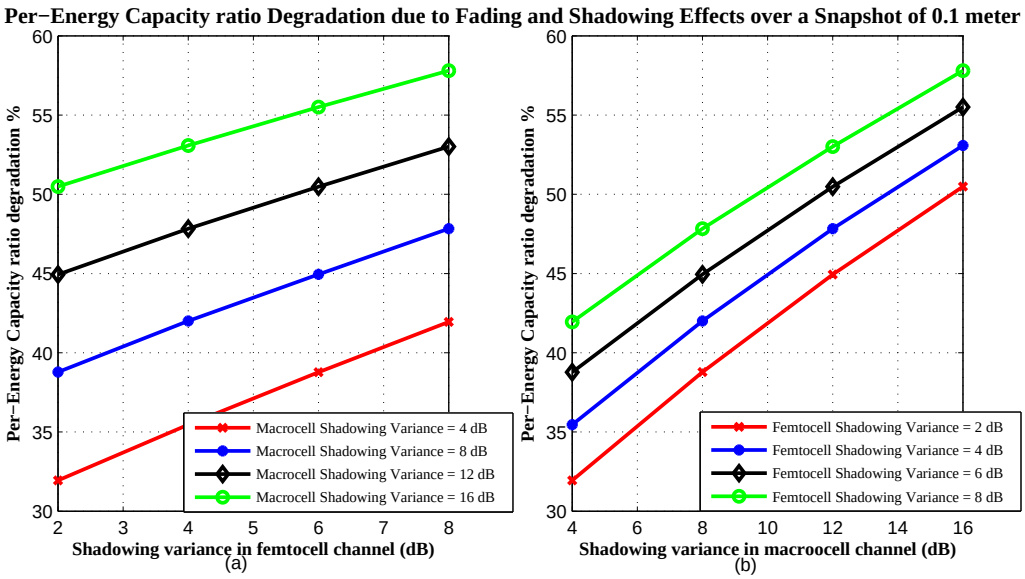

Figure 5 .1: Per-energy capacity ratio degradation percentages over a snapshot of 0.1 meter (a) as a function of shadowing variance in femtocell channel (b) as a function of shadowing variance in macrocell channel.

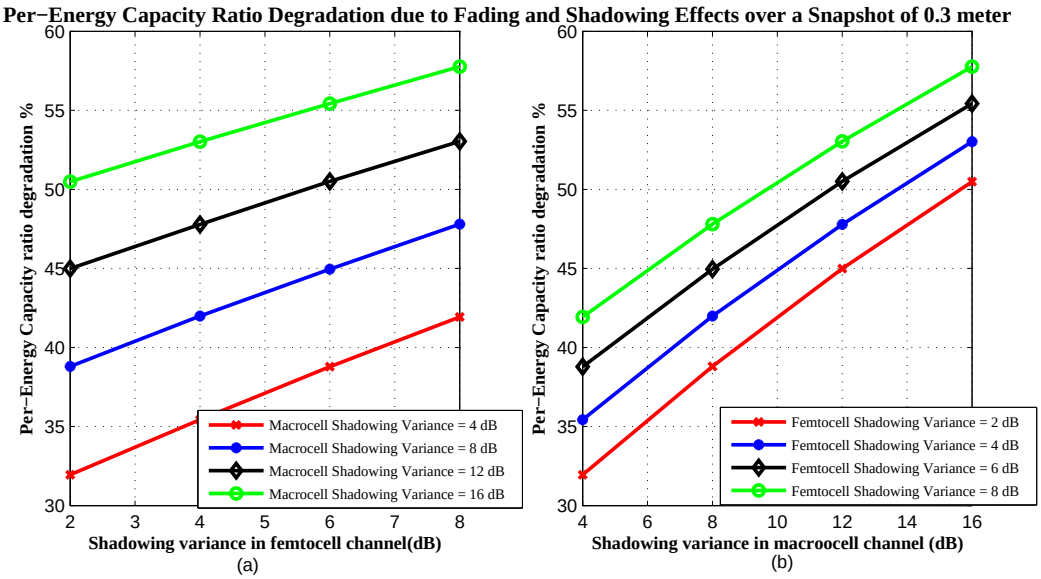

Figure 5 .2: Per-energy capacity ratio degradation percentages over a snapshot of 0.3 meter (a) as a function of shadowing variance in femtocell channel (b) as a function of shadowing variance in macrocell channel.

Another aspect is the relationship between the per-energy capacity ratio percentage degradation and the distance where it is found that the per-energy capacity ratio degradation percentage is not a function of distance (or time) because as the distance is increased from 0.1 m to 0.3 m it is found that the per-energy capacity ratio degradation percentages are almost similar in the two cases and no clear difference is noticed.

As a conclusion, many per-energy capacity ratio percentages degradation corresponding to the macrocell and femtocell shadowing variances were studied. In the simulation experiments for this thesis, the selected macrocell shadowing variances is 8 dB and the selected femtocell shadowing variances is 4 dB. Accordingly, the per-energy capacity ratio percentage degradation value in this case is 42 %. However, the two figures above are general and can be applied to any channel having a fading behavior similar to the channel considered here.

5.4 The per-energy capacity ratio degradation compensation

In this section, the resultant per-energy capacity ratio degradation percentage (42 %) is used to compensate for the degradation that had taken place in the per-energy capacity ratio due to fading. The difference between the per-energy capacity ratio without fading and the per-energy capacity ratio after the degradation compensation is studied in the cases of dedicated channel assignment as well as the co-channel assignment. In addition, both the downlink and uplink channels are considered. This difference is taken as an error due to inaccurate power control.

To illustrate how the compensation for degradation works under fading conditions, four sample cases are considered. In the case of dedicated channel for both downlink and uplink, the difference between the per-energy capacity ratio under non-fading conditions and the per-energy capacity ratio after the degradation compensation as a function of the femtocell SIR and the macrocell radius is investigated. Whereas in the co-channel case, for both downlink and uplink, the difference between the per-energy capacity ratio under non-fading conditions and the per-energy capacity ratio after the degradation compensation as a function of the femtocell SIR and the path loss is investigated.

As shown below, the difference between the per-energy capacity ratio under non-fading conditions and the per-energy capacity ratio after the degradation compensation is almost negligible. In addition, the error due to inaccurate power control is less than 1.5% which is really remarkable results.

For an example (shwon in Fig. 5.4), when the femtocell bandwidth = 0.9 the macrocell bandwidth (magenta color lines) and when the macrocell radius = 1200 m, the difference (degradation) between the per-energy capacity ratio under fading

conditions and non fading conditions is clear. However after the degradation compensation, the new difference (error) between the per-energy capacity ratio after the degradation compensation and the per-energy capacity ratio under non fading conditions is almost insignificant. In addition Fig. 5.5 depicts that when the femtocell bandwidth = 0.9 the macrocell bandwidth (magenta color lines) and when the macrocell radius = 1200 m, the error due to inaccurate power control is less than 1%. The results for each case are shown below:

1. **Femtocell SIR and macrocell radius**

   (a) **Dedicated channel-Downlink**

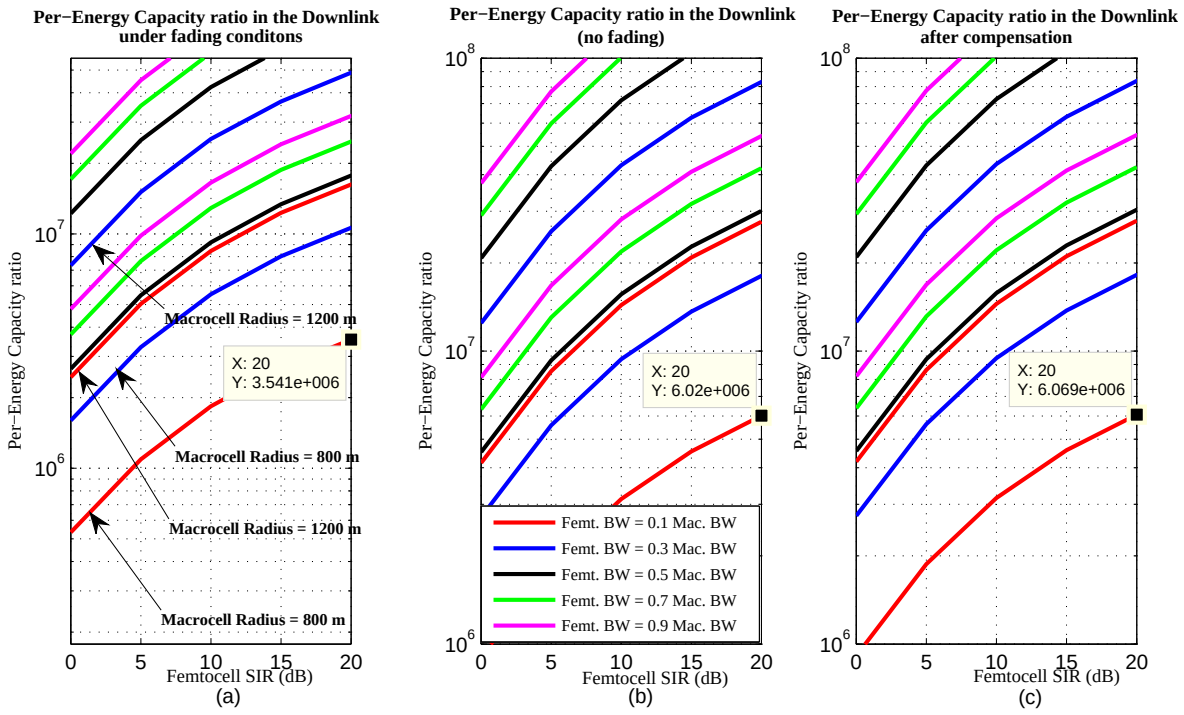

Figure 5 .3: Per-energy capacity ratio (dedicated channel-downlink) as a function of the femtocell SIR (a) under fading conditions (b) under non-fading conditions (c) after the degradation compensation.

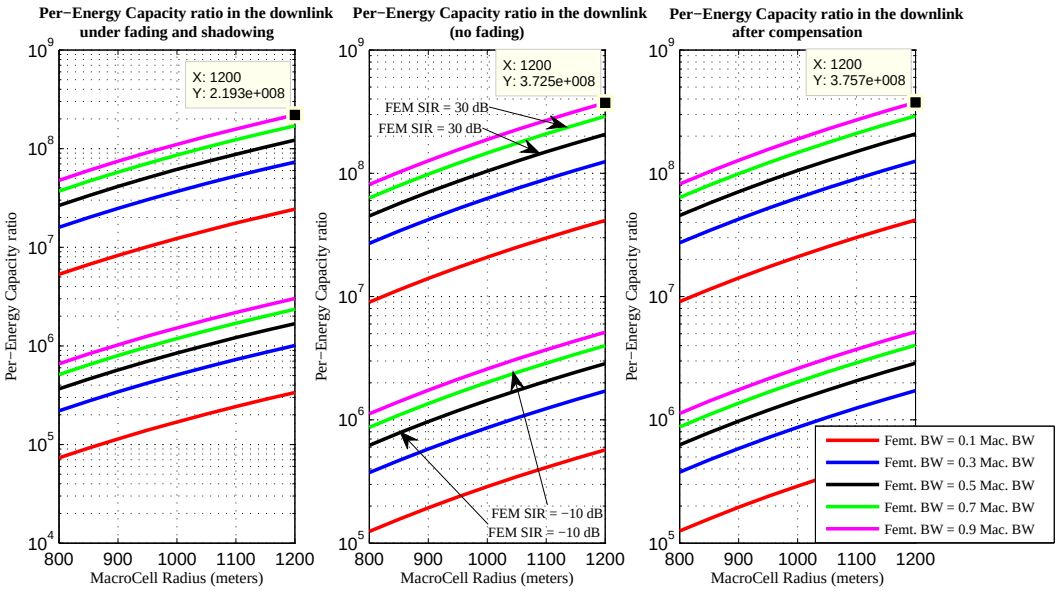

Figure 5 .4: Per-energy capacity ratio (dedicated channel-downlink) as a function of the macrocell radius (a) under fading conditions (b) under non-fading conditions (c) after the degradation compensation.

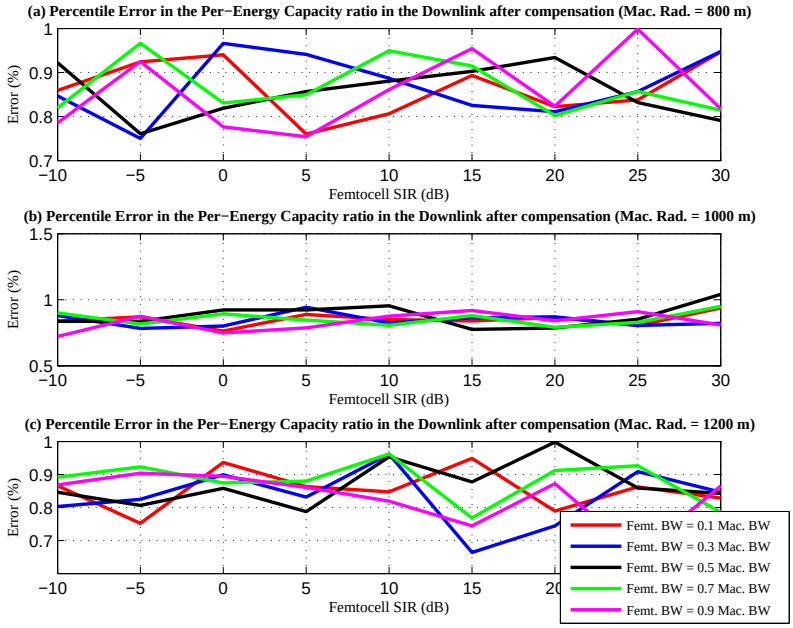

Figure 5 .5: Error in the inaccurate power control as a function of the femtocell SIR (dedicated channel-downlink) (a) macrocell radius = 800 m (b) macrocell radius = 1000 m (c) macrocell radius = 1200 m.

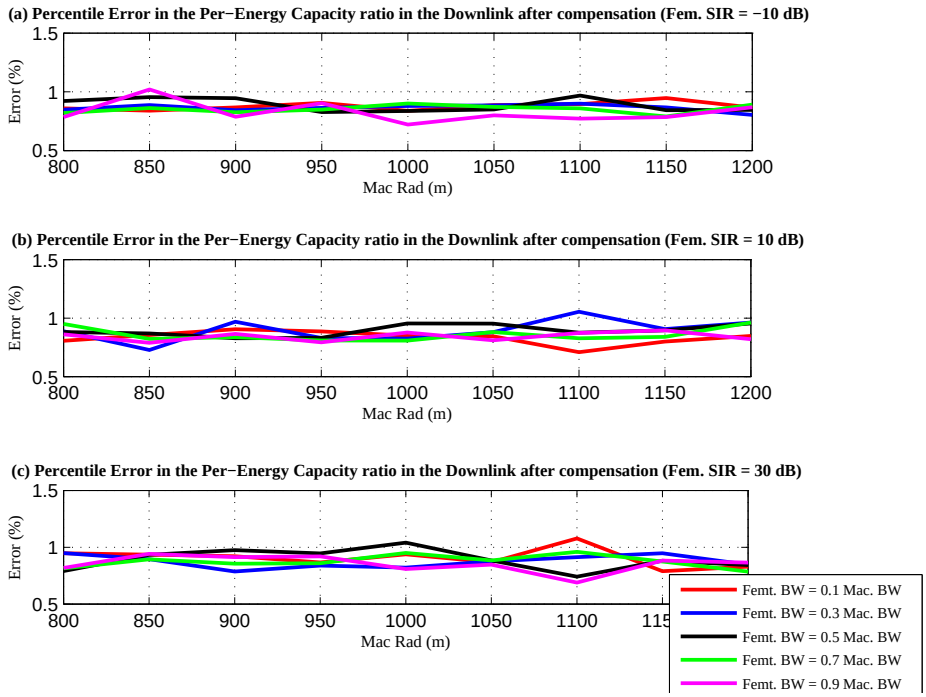

Figure 5 .6: Error in the inaccurate power control as a function of the macrocell radius (dedicated channel-downlink) (a) femtocell SIR = -10 dB (b) femtocell SIR = 10 dB (c) femtocell SIR = 30 dB.

(b) **Dedicated channel-Uplink**

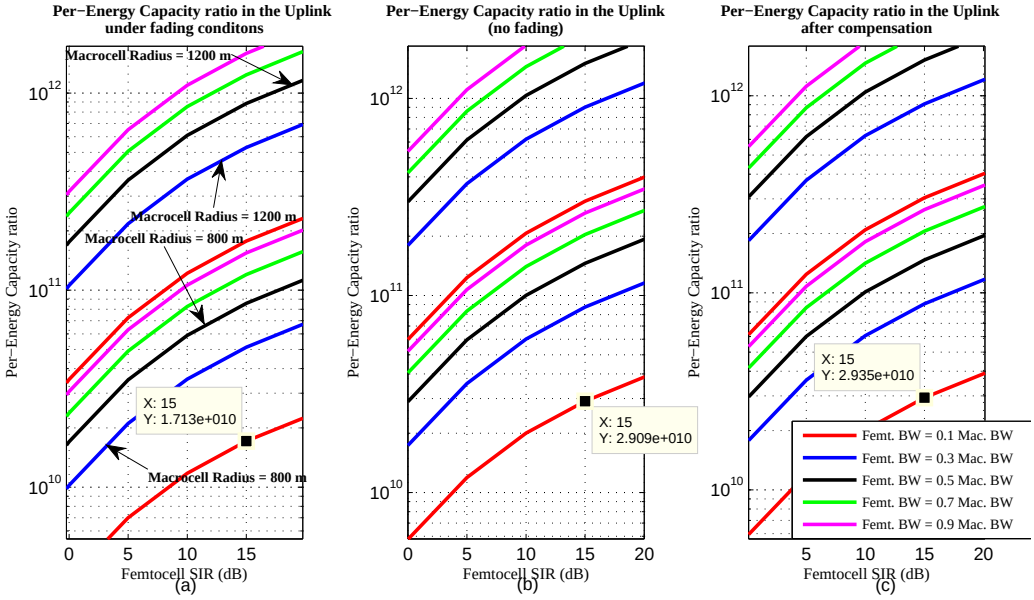

Figure 5 .7: Per-energy capacity ratio (dedicated channel -uplink) as a function of the femtocell SIR (a) under fading conditions (b) under non-fading conditions (c) after the degradation compensation.

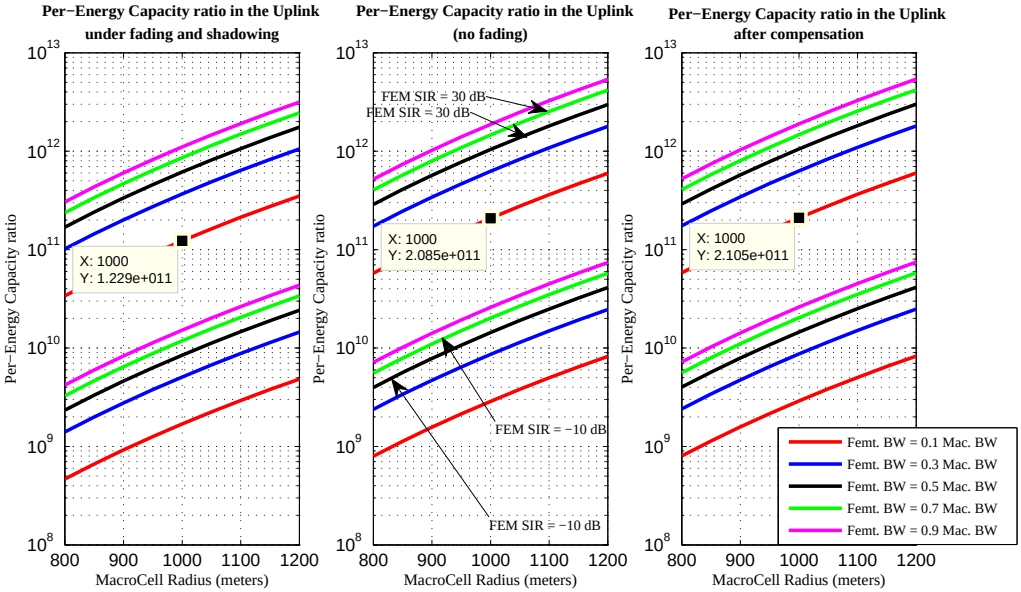

Figure 5 .8: Per-energy capacity ratio (dedicated channel -uplink) as a function of the macrocell radius (a) under fading conditions (b) under non-fading conditions (c) after the degradation compensation.

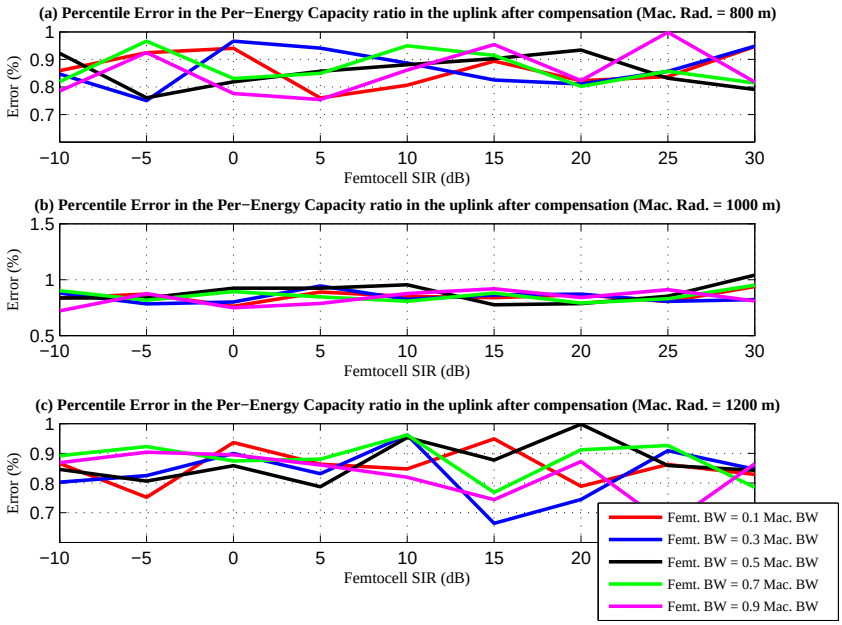

Figure 5 .9: Error in the inaccurate power control as a function of the femtocell SIR (dedicated channel -uplink) (a) macrocell radius = 800 m (b) macrocell radius = 1000 m (c) macrocell radius = 1200 m.

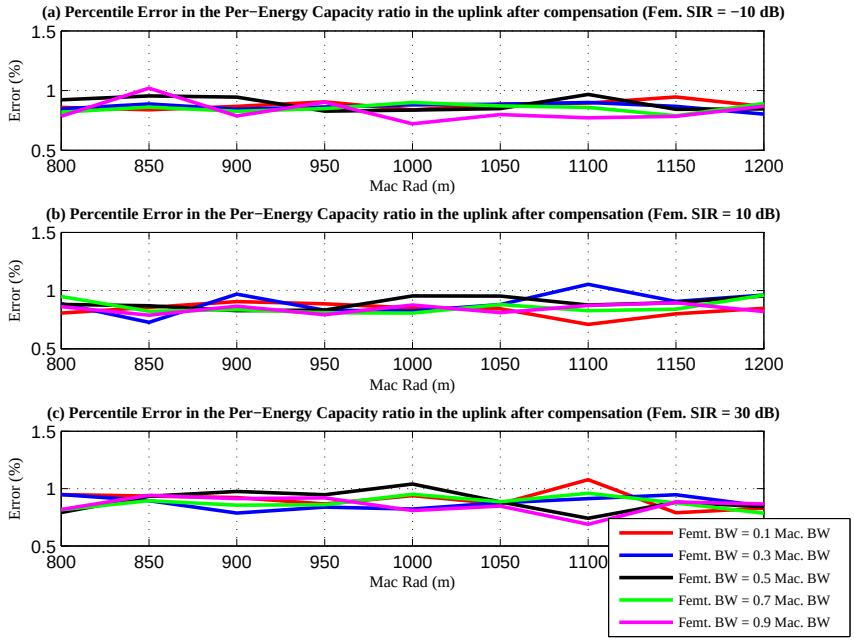

Figure 5 .10: Error in the inaccurate power control as a function of the macrocell radius (dedicated channel -uplink) (a) femtocell SIR = -10 dB (b) femtocell SIR = 10 dB (c) femtocell SIR = 30 dB.

2. **Femtocell SIR and path loss exponent**

(a) **Co-channel-Downlink**

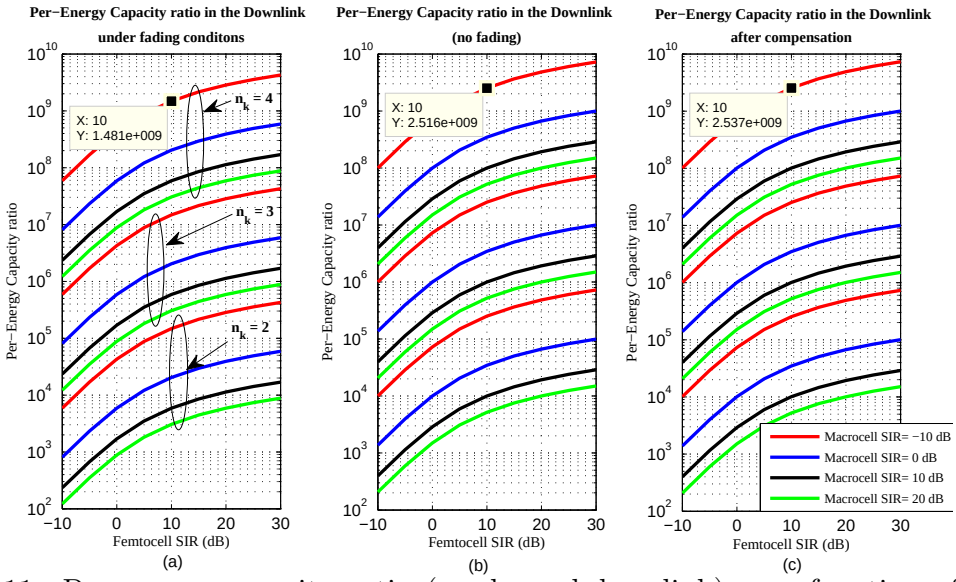

Figure 5 .11: Per-energy capacity ratio (co-channel-downlink) as a function of the femtocell SIR (a) under fading conditions (b) under non-fading conditions (c) after the degradation compensation.

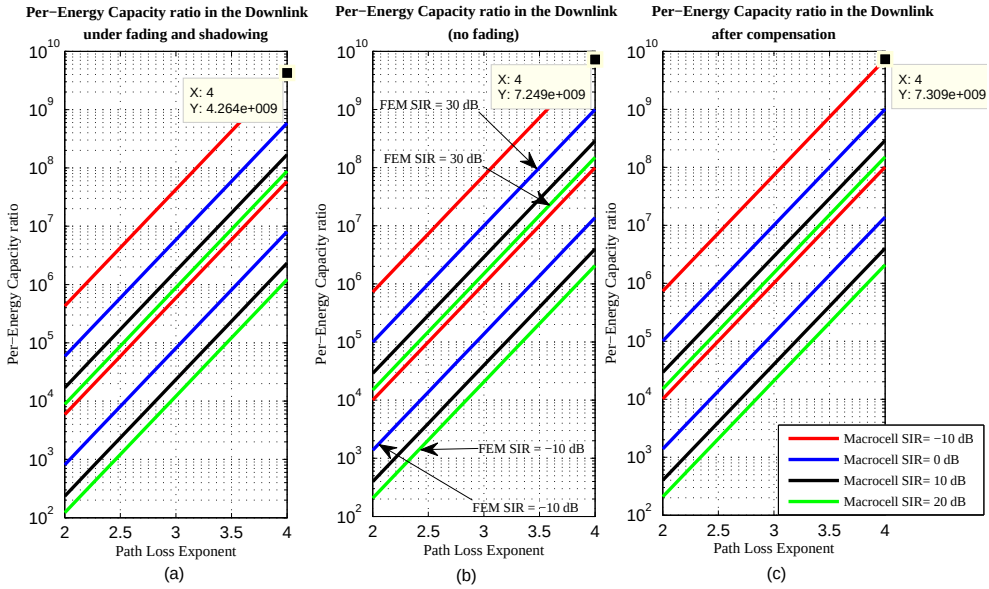

Figure 5 .12: Per-energy capacity ratio (co-channel-downlink) as a function of the path loss exponent (a) under fading conditions (b) under non-fading conditions (c) after the degradation compensation.

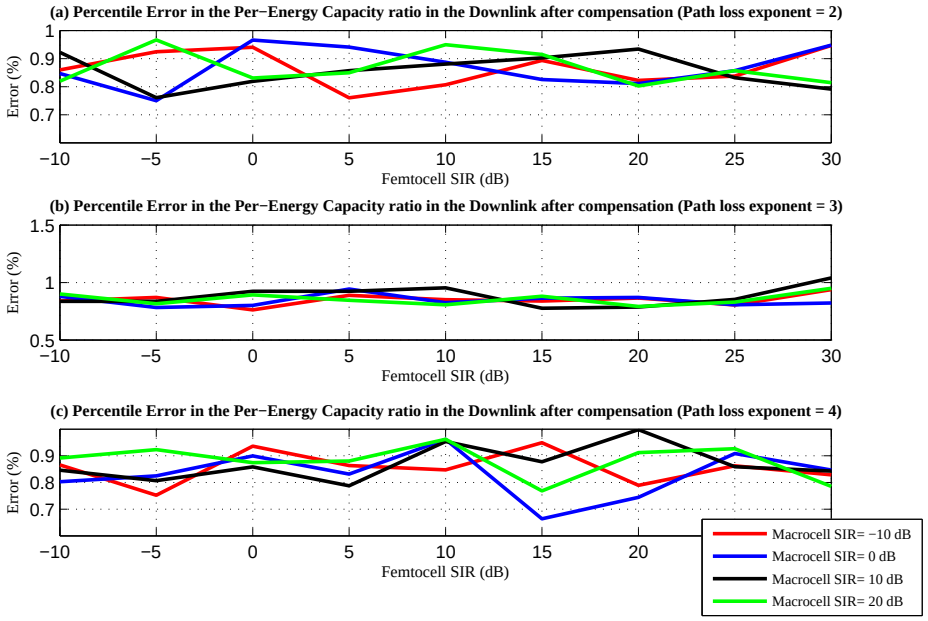

Figure 5 .13: Error in the inaccurate power control as a function of the femtocell SIR (co-channel-downlink) (a) path loss exponent = 2 (b) path loss exponent = 3 (c) path loss exponent = 4.

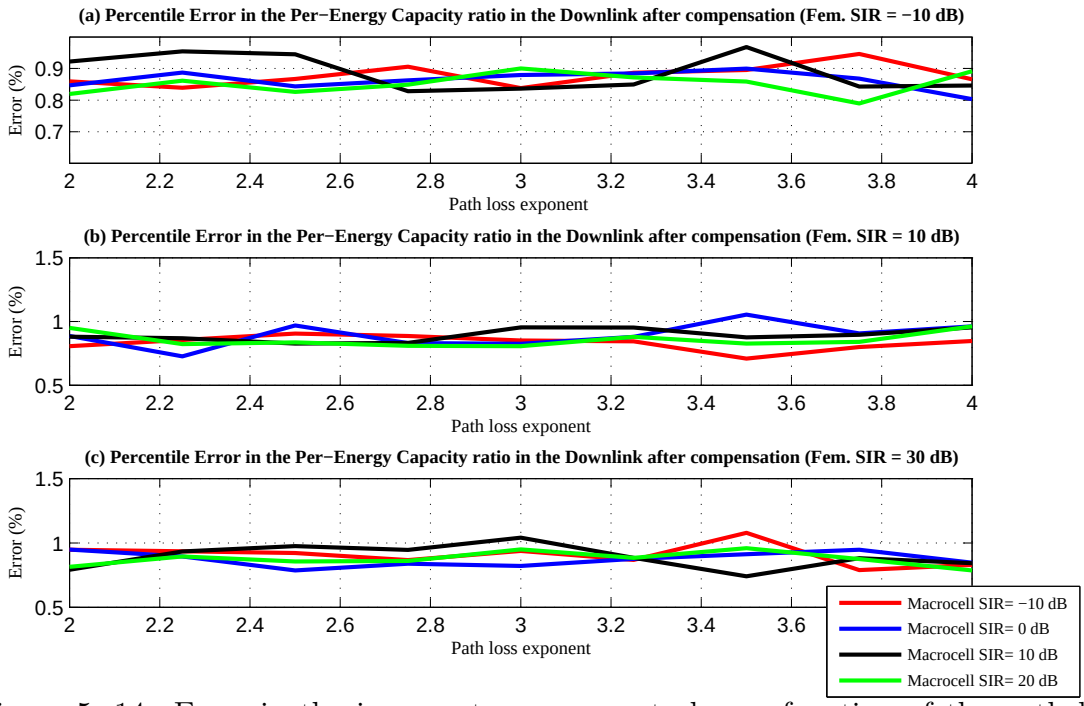

Figure 5 .14: Error in the inaccurate power control as a function of the path loss exponent (co-channel-downlink) (a) femtocell SIR = -10 dB (b) femtocell SIR = 10 dB (c) femtocell SIR = 30 dB.

(b) **Co-channel-Uplink**

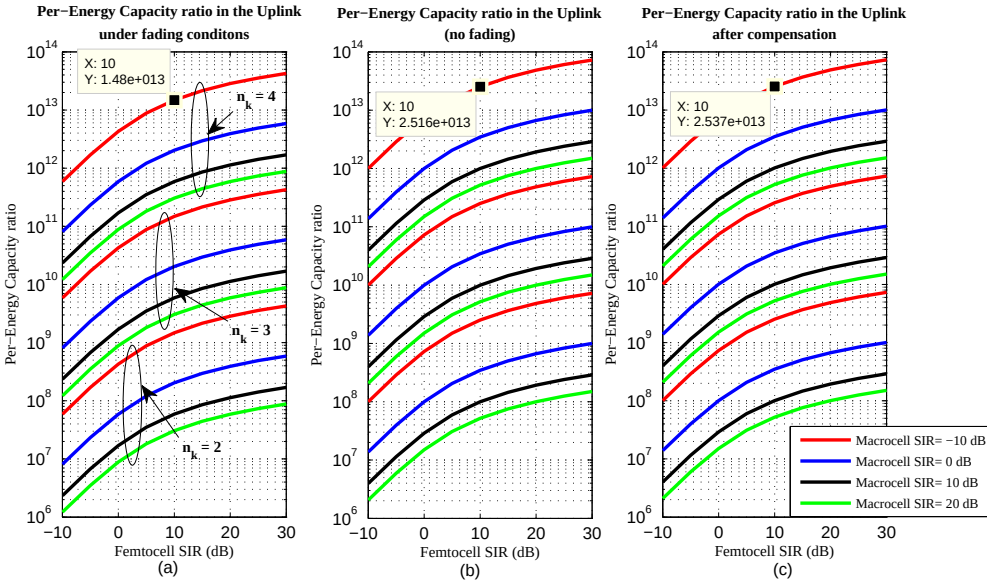

Figure 5 .15: Per-energy capacity ratio (co-channel-uplink) as a function of the femtocell SIR (a) under fading conditions (b) under non-fading conditions (c) after the degradation compensation.

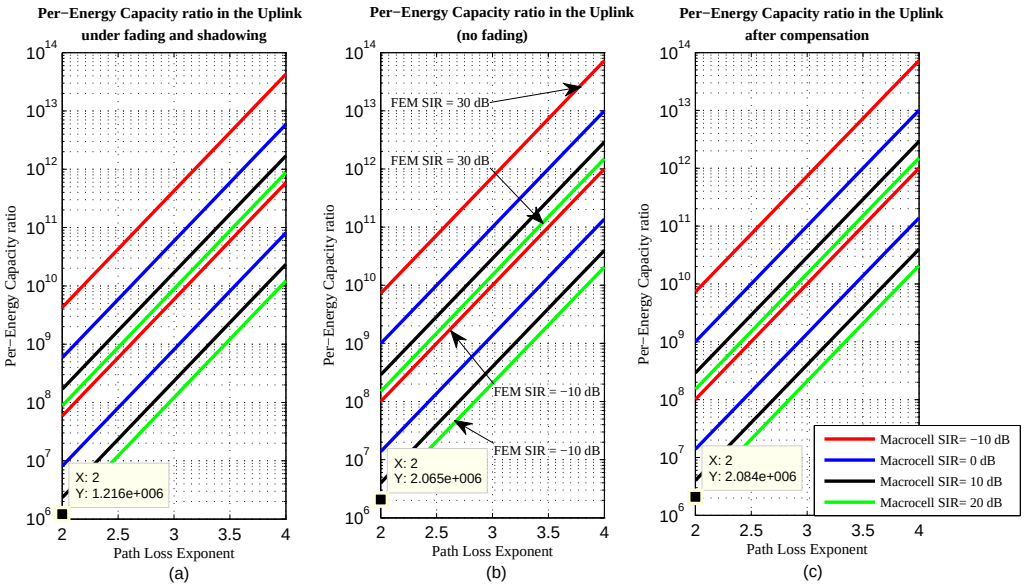

Figure 5 .16: Per-energy capacity ratio(co-channel-uplink) as a function of the path loss exponent (a) under fading conditions (b) under non-fading conditions (c) after the degradation compensation.

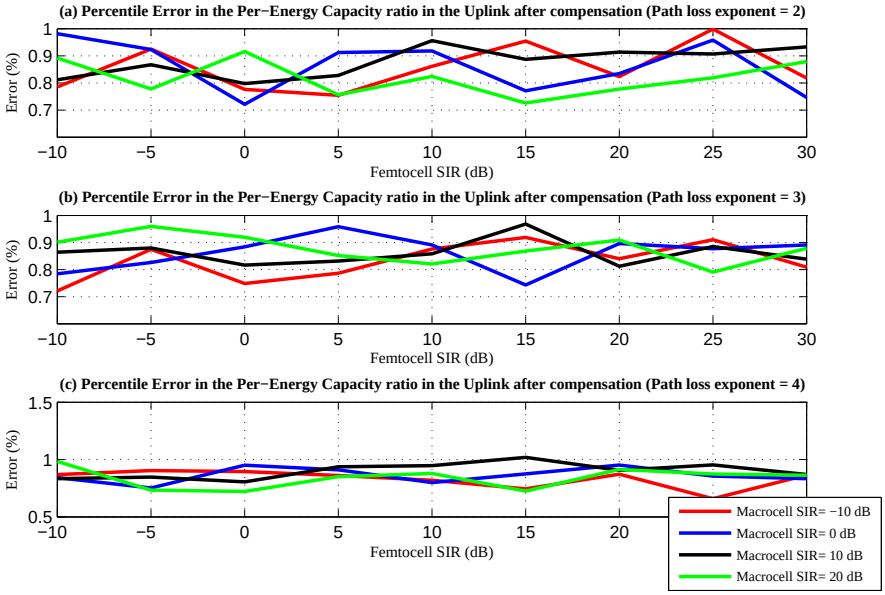

Figure 5 .17: Error in the inaccurate power control as a function of the femtocell SIR (co-channel-uplink) (a) path loss exponent = 2 (b) path loss exponent = 3 (c) path loss exponent = 4.

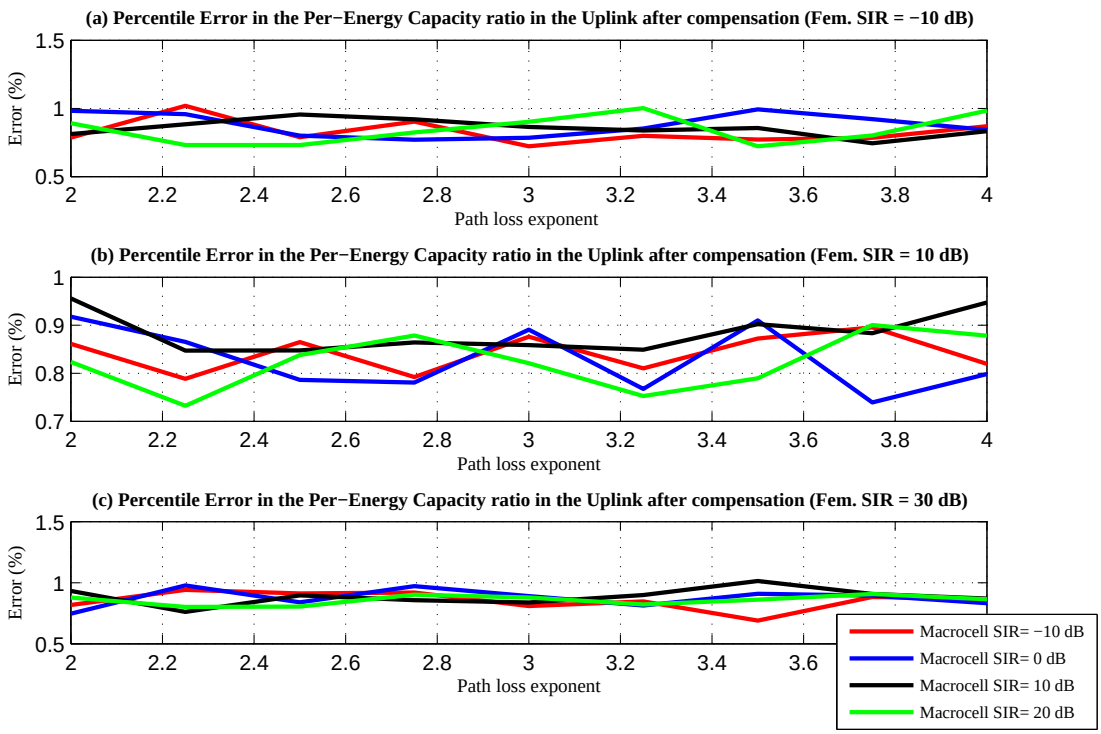

Figure 5 .18: Error in the inaccurate power control as a function of the path loss exponent (co-channel-uplink) (a) femtocell SIR = -10 dB (b) femtocell SIR = 10 dB (c) femtocell SIR = 30 dB.

As shown above, the results support the mathematical derivation which showed that the degradation in the per-energy capacity ratio under fading condition is a function of the channel type only.

5.5 The instantaneous error in the per-energy capacity ratio under inaccurate power control

Power control is never perfect as it is very difficult to implement it. The practical power control is usually approximate and therefore always results in some error. However, implementation of power control results in energy saving even if it is not exact.

In this regards, the instantaneous error under inaccurate power control of the per-energy capacity ratio and the per-energy capacity under perfect power control, the

case when there is no fading, have been plotted versus the number of samples. The fluctuation around the mean value (no fading value) is considered to follow a uniform distribution with maximum error of 1% and 3%, respectively. In each snapshot six different values for the path loss exponent were considered. The path loss exponent has been considered as a sample case parameter to show how the instantaneous error under inaccurate power control of the per-energy capacity ratio and the per-energy capacity under perfect power control is behaved.

Actually, it is considered that the desired perfect power control of the per-energy capacity ratio is achieved, therefore it remains to show what will be the result if an inaccurate power control is applied to the per-energy capacity ratio with an approximated maximum error of 1% or 3%. The response in the two sample cases is illustrated below in Fig. 5.19, Fig. 5.20, Fig. 5.21, and Fig. 5.22.

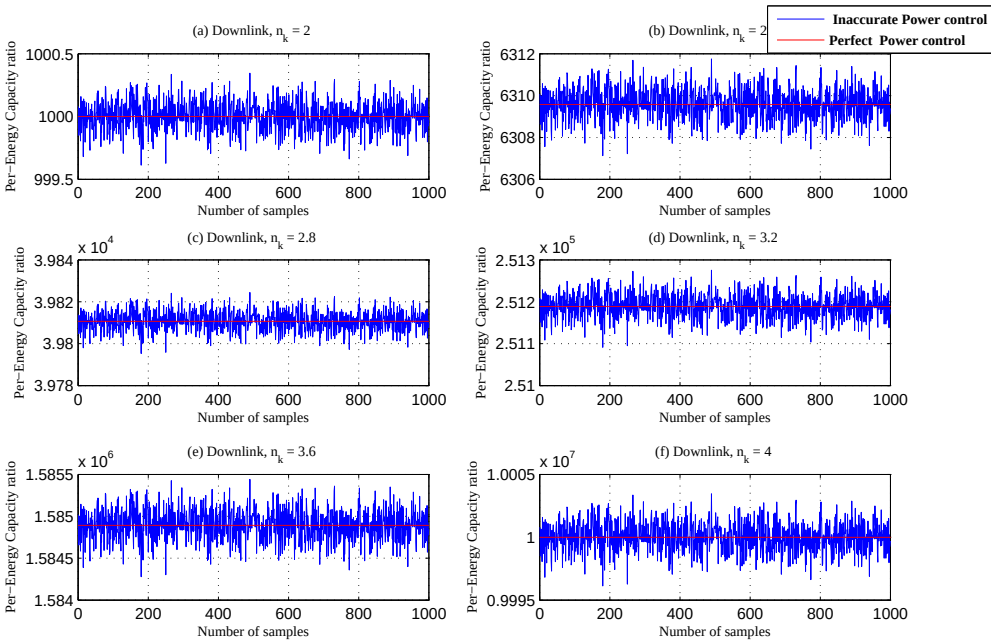

Figure 5 .19: Inaccurate power control of the per-energy capacity ratio (downlink) with 3% max. error for six different path loss exponent values.

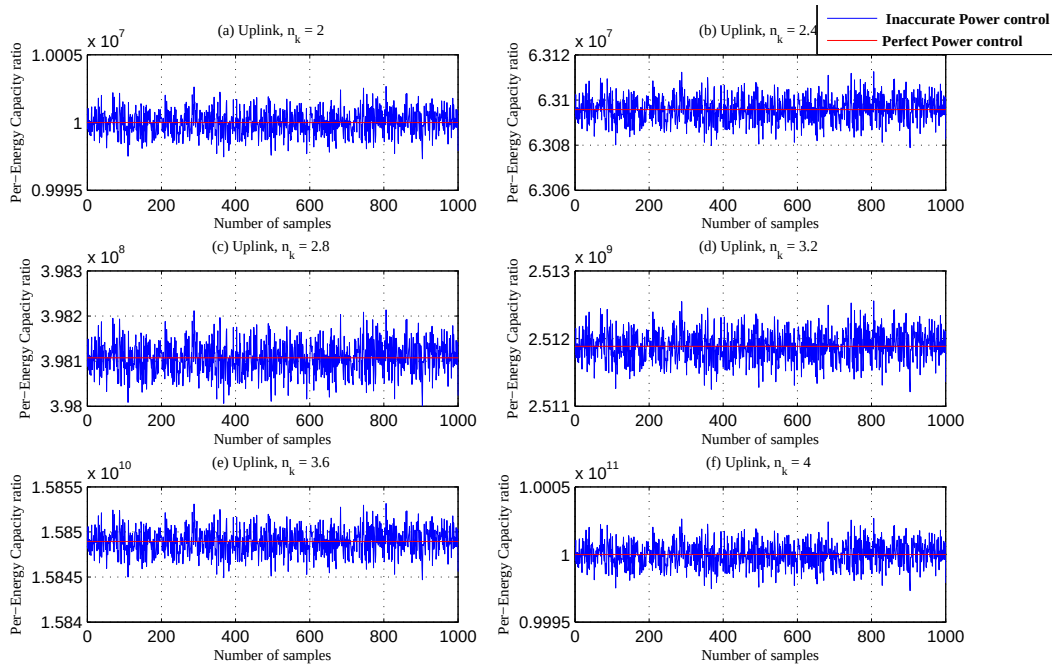

Figure 5 .20: Inaccurate power control of the per-energy capacity ratio (uplink) with 3% max. error for six different path loss exponent values.

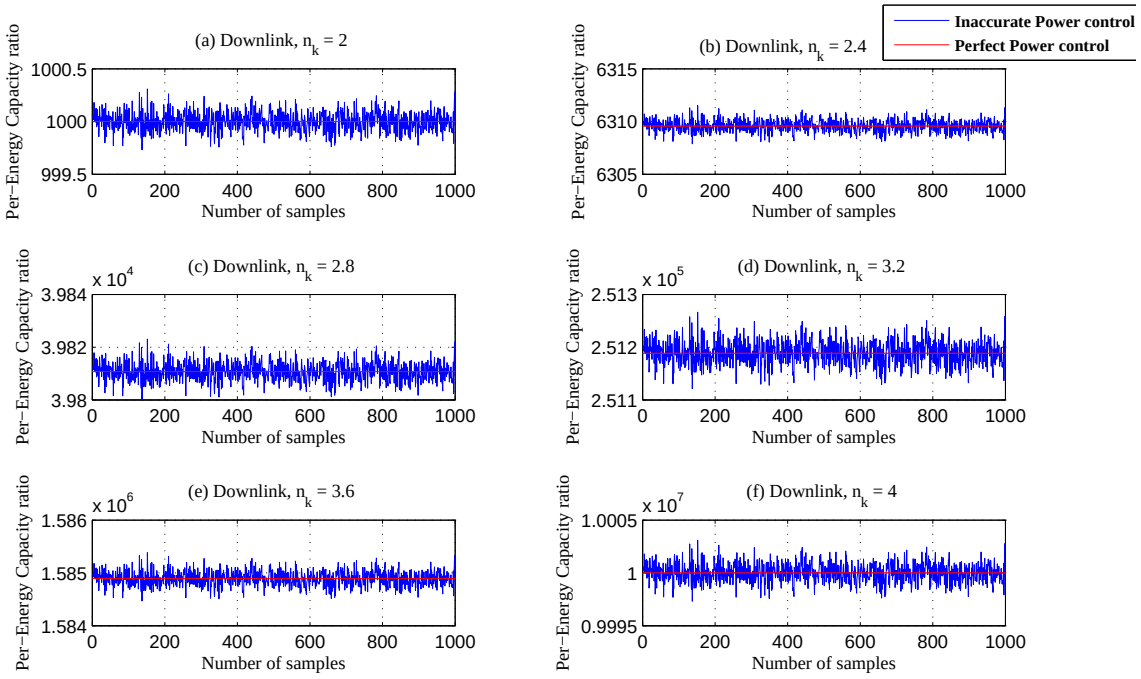

Figure 5 .21: Inaccurate power control of the per-energy capacity ratio (downlink) with 1% max. error for six different path loss exponent values.

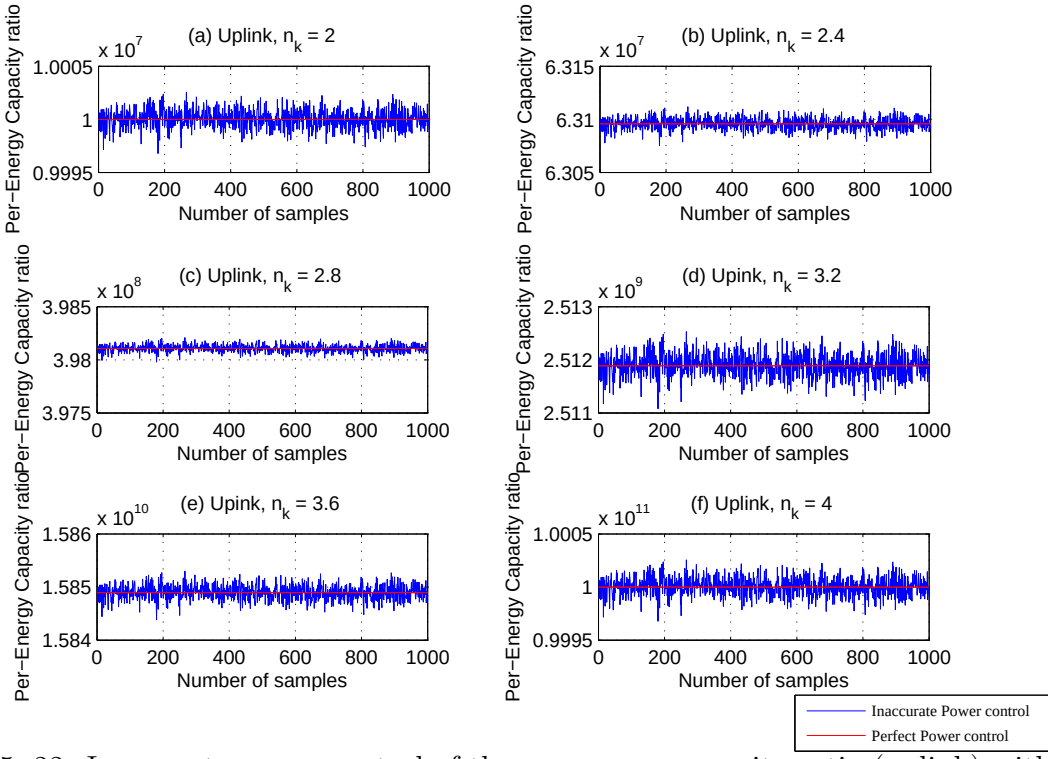

Figure 5 .22: Inaccurate power control of the per-energy capacity ratio (uplink) with 1% max. error for six different path loss exponent values.

5.6 Summary

In this chapter, the percentile degradation in the per-energy capacity ratio due to fading is evaluated as a function of macrocell shadowing variance, femtocell shadowing variance, and distance (or time). In addition, a new mathematical expression that is used in the determination of the percentile degradation in the per-energy capacity ratio due to fading has been derived. In the new mathematical expression, it was proven that the percentile degradation in the per-energy capacity ratio due to fading is only a function of the fading ratio and hence it is a function of the fading parameters f_{mac} and f_{fem}.

Using the derived expression we have estimated the degradation compensation value that should be used to bring back the per-energy capacity ratio to its original value. The degradation compensation for the per-energy capacity ratio degradation

under fading conditions was considered as an inaccurate power control. Finally, the expected instantaneous per-energy capacity ratio under the inaccurate power control has been studied.

Chapter 6

Conclusion and Future Work

In wireless communications, huge improvement and rapid expansion has taken place in all aspects technologies, devices, services, data traffic, ... etc. One of the main consequences of that advance is the increased energy consumption in wireless communication network. As result, energy efficiency and its metrics have emerged as important research directions of designing future networks not only from performance and cost efficiency point of view but also from energy efficiency point of view.

Femtocells are low-power radio access points that provide wireless voice and broadband services to home and small business customers. Introducing femtocell to act as underlay or overlay layer can significantly improve the performance and the energy efficiency of the wireless communication network.

Fading is an important characteristic in wireless communication - reason why it was decided to investigate the per-energy capacity ratio in macro-femto environment under fading conditions. It is caused by interference between two or more versions of the transmitted signal which arrive at the receiver at slightly different times.

This thesis has studied all the above mentioned issues from different prospectives providing good conclusions via the study of the per-energy capacity ratio in macro-

femto environment under fading conditions and in accurate power control. We have derived two new mathematical expressions that are used in the investigation of the per-energy capacity ratio in macro-femto environment under fading conditions and in the determination of the percentile degradation in the per-energy capacity ratio due to fading. In addition, parameters like femtocell SIR, macrocell radius, macrocell SIR, and path loss exponent were included in the simulation experiments in order to investigate the relation between the per-energy capacity ratio in macro-femto environment under fading conditions and these parameters. Additionally, both downlink and uplink transmission were considered in all part of the study. Furthermore, using the dedicated channel bandwidth allocation strategy, different bandwidth fractions were given to the femtocell in comparison to the macrocell to investigate the relation between the per-energy capacity ratio in macro-femto environment under fading conditions and the femtocell-macrocell bandwidth ratio. Finally, in addition to the dedicated channel bandwidth allocation strategy the co-channel bandwidth allocation strategy is included in the simulation experiments.

6.1 Conclusions

As a result of the tasks accomplished, we have concluded the following. Firstly, the deployment of femtocells besides the macrocell is energy efficient in the presence and in the absence of fading. Secondly, the percentile degradation in the per-energy capacity ratio due to fading is a function of the fading ratio and hence is a function of the fading behavior of the communication channel. Moreover, the per-energy capacity ratio in macro-femto environment is directly proportional to femtocell SIR, macrocell radius, and path loss exponent. However, it is inversely proportional to macrocell SIR. In addition, as the bandwidth fraction given to the femtocell in comparison to

the macrocell increases the performance of the per-energy capacity ratio in macro-femto environment improves. Finally, the per-energy capacity ratio performance, under fading and non-fading conditions, in the uplink is better than the per-energy capacity ratio performance in the downlink. Similarly, the per-energy capacity ratio performance, under fading and non-fading conditions, in the co-channel operation is better than the per-energy capacity ratio performance in the dedicated channel operation.

6.2 Suggestions for Future Work

The reasons behind the change in the per-energy capacity ratio slope with respect to the some parameters, like femtocell SIR and macrocell SIR, or the bandwidth ratio between the femtocell and the macrocell was not focused in this thesis. Thus, the investigation of these reasons should be considered as future work.

In addition, it is felt that a different strategy should be adopted to design the wireless communication networks. It is proposed that the femtocells should act as the main layer in the wireless network and other network components like the macrocells should be used to enhance the quality of service (QoS). In this regards, a new call handling algorithm will be required to creatively arrange the call handling in a network at which the priority of receiving calls is given to the femtocell rather than the macrocell.

Bibliography

[1] D. Feng, C. Jiang, G. Lim, L. Cimini Jr, G. Feng, and G. Li, "A survey of energy-efficient wireless communications," 2012.

[2] J. Zhang, G. De la Roche, *et al.*, *Femtocells: technologies and deployment*. Wiley Online Library, 2010.

[3] C. Han, T. Harrold, S. Armour, I. Krikidis, S. Videv, P. M. Grant, H. Haas, J. Thompson, I. Ku, C.-X. Wang, T. A. Le, M. Nakhai, J. Zhang, and L. Hanzo, "Green radio: radio techniques to enable energy-efficient wireless networks," *Communications Magazine, IEEE*, vol. 49, pp. 46–54, June 2011.

[4] H. Leem, S. Y. Baek, and D. K. Sung, "The effects of cell size on energy saving, system capacity, and per-energy capacity," in *Wireless Communications and Networking Conference (WCNC), 2010 IEEE*, pp. 1–6, IEEE, 2010.

[5] J. P. León, F. Bader, and M.-S. Alouini, "Per-energy capacity and handoff strategies in macro-femto cells environment," in *Wireless Communications and Networking Conference Workshops (WCNCW), 2012 IEEE*, pp. 1–6, IEEE, 2012.

[6] B. Gammage, D. C. Plummer, E. Thompson, L. Fiering, H. LeHong, F. Karamouzis, C. Rold, K. Collins, W. Clark, N. Jones, *et al.*, "Gartners top

predictions for it organizations and users, 2010 and beyond: A new balance," *Gartner Report*, 2009.

[7] R. Tafazolli and J. Saarnio, "emobility mobile and wireless communications technology platform: Strategic research agenda," *Version 7, 2008, Available at http://www. emobility. eu. org, last checked: May 2010*, 2005.

[8] T. Chen, H. Kim, and Y. Yang, "Energy efficiency metrics for green wireless communications," in *Wireless Communications and Signal Processing (WCSP), 2010 International Conference on*, pp. 1–6, IEEE, 2010.

[9] T. Chen, Y. Yang, H. Zhang, H. Kim, and K. Horneman, "Network energy saving technologies for green wireless access networks," *Wireless Communications, IEEE*, vol. 18, no. 5, pp. 30–38, 2011.

[10] E. C. Strinati and L. Hérault, "Holistic approach for future energy efficient cellular networks," *e & i Elektrotechnik und Informationstechnik*, vol. 127, no. 11, pp. 314–320, 2010.

[11] P. Grant, "Green radio -the case for more efficient cellular basestations," *MCVE Core 5 Programme, presented at the Globecom*, 10, 2010.

[12] M. Gruber, O. Blume, D. Ferling, D. Zeller, M. A. Imran, and E. C. Strinati, "Earthenergy aware radio and network technologies," in *Personal, Indoor and Mobile Radio Communications, 2009 IEEE 20th International Symposium on*, pp. 1–5, IEEE, 2009.

[13] I. Godor *et al.*, "Most promising tracks of green network technologies," *EARTH D3*, vol. 1.

[14] R. Esnault, "Optimising power efficiency in mobile radio networks (opera-net) project presentation," 2008.

[15] "Optimising power efficiency in mobile radio networks," *OPERA-Net PROJECT STAND # 42, 2010 NEM Summit Towards Future Media Internet, Barcelona, Spain, Oct 2010.*

[16] Wireless@KTH, "ewin: Energy-efficient wireless networking," *http://wireless.kth.se/blog/projects/ewin/.*

[17] "Energy efficiency enhancements in radio access networks," *Wireless@KTH Research Strategy Document 2008-2010, Wireless@KTH, 2008, http://www.wireless.kth.se/images/stories/Strategy/Research plan08.pdf.*

[18] J. Cullen, *Radio frame presentation.* in Femtocell Europe 2008, London, UK, June 2008.

[19] Femto-Forum, "http://www.femtoforum.org,"

[20] Infonetics, "4q12 femtocell equipment market highlights," August 2007, White paper.

[21] D. Duffy, "Femtocell market set for strong growth in 2011," *Informa Telecoms & Media*, 2010.

[22] A. Golaup, M. Mustapha, and L. B. Patanapongpibul, "Femtocell access control strategy in umts and lte," *Communications Magazine, IEEE*, vol. 47, no. 9, pp. 117–123, 2009.

[23] C. Han, T. Harrold, S. Armour, I. Krikidis, S. Videv, P. M. Grant, H. Haas, J. S. Thompson, I. Ku, C.-X. Wang, *et al.*, "Green radio: radio techniques to enable

energy-efficient wireless networks," *Communications Magazine, IEEE*, vol. 49, no. 6, pp. 46–54, 2011.

[24] "2010 wireless smart phone customer satisfaction study, j.d. power and associates," *2010, http://www.jdpower.com/Electronics/ratings/ Wireless-Smartphone-Ratings-(Volume-1).*

[25] G. B. Creus and M. Kuulusa, "Optimizing mobile software with built-in power profiling," in *Mobile Phone Programming*, pp. 449–462, Springer, 2007.

[26] "The energy star computer specification version 6.0," *https://energystar.gov/products/specs/node/143 last checked: Nov 2012.*

[27] E.-S. Jung and N. H. Vaidya, "An energy efficient mac protocol for wireless lans," in *INFOCOM 2002. Twenty-First Annual Joint Conference of the IEEE Computer and Communications Societies. Proceedings. IEEE*, vol. 3, pp. 1756–1764, IEEE, 2002.

[28] C. E. Jones, K. M. Sivalingam, P. Agrawal, and J. C. Chen, "A survey of energy efficient network protocols for wireless networks," *wireless networks*, vol. 7, no. 4, pp. 343–358, 2001.

[29] Y. Chen, S. Zhang, S. Xu, and G. Y. Li, "Fundamental trade-offs on green wireless networks," *Communications Magazine, IEEE*, vol. 49, no. 6, pp. 30–37, 2011.

[30] H. Kwon and T. Birdsall, "Channel capacity in bits per joule," *Oceanic Engineering, IEEE Journal of*, vol. 11, no. 1, pp. 97–99, 1986.

[31] S. Verdú, "Spectral efficiency in the wideband regime," *Information Theory, IEEE Transactions on*, vol. 48, no. 6, pp. 1319–1343, 2002.

[32] V. Rodoplu and T. H. Meng, "Bits-per-joule capacity of energy-limited wireless networks," *Wireless Communications, IEEE Transactions on*, vol. 6, no. 3, pp. 857–865, 2007.

[33] F. Meshkati, H. V. Poor, S. C. Schwartz, and N. B. Mandayam, "An energy-efficient approach to power control and receiver design in wireless data networks," *Communications, IEEE Transactions on*, vol. 53, no. 11, pp. 1885–1894, 2005.

[34] F. Meshkati, H. V. Poor, S. C. Schwartz, and R. V. Balan, "Energy-efficient resource allocation in wireless networks with quality-of-service constraints," *Communications, IEEE Transactions on*, vol. 57, no. 11, pp. 3406–3414, 2009.

[35] G. Miao, N. Himayat, and G. Y. Li, "Energy-efficient link adaptation in frequency-selective channels," *Communications, IEEE Transactions on*, vol. 58, no. 2, pp. 545–554, 2010.

[36] J. B. Andersen, T. S. Rappaport, and S. Yoshida, "Propagation measurements and models for wireless communications channels," *Communications Magazine, IEEE*, vol. 33, no. 1, pp. 42–49, 1995.

[37] "Physical layer aspects for evolved universal terrestrial radio access (e-utra)," *3GPP TR 25.814 V.7.1.0*, Sept. 2006.

[38] B. G. Lee, D. Park, and H. Seo, *Wireless communications resource management*. Wiley. com, 2009.

Vitae

Name: Mohammed Abobaker Mohammed Khalifa.

Email: g200902970@kfupm.edu.sa or Khalifa1976@yahoo.com

Nationality: Yemeni.

Date of birth: February 24, 1976.

Temporary address	**Permanent Address**
31261- Dhahran, Saudi Arabia	Yemen, Aden, Khormakser,
KFUPM, P. O. Box (8625)	October zone, Mayoon street,
Mobile: 00966-530648084	House No. 20.
	Mobile: 00967-777541153

EDUCATION:

Expected defense in May 2014	Master candidate, Telecommunication Engineering, King Fahd University for Petroleum and Minerals, Saudi Arabia.	
	Thesis Title:	Per-Energy Capacity in Macro-Femto Environment under Fading Condition and Inaccurate Power Control
	Thesis Advisor:	Prof. Azzedine Zerguine.
	Thesis Co-Advisor:	Chair Prof. Asrar U.H. Sheikh.
September 2001	Bachelor in Electrical and Electronic Engineering, Aden University, Yemen. Final Grade: (V. Good) 4.39 out of 5.	

TEACHING & PROFESSIONAL EXPERIENCE:

Dec 2001 to July 2009
- Graduate assistant at Aden Community College (ACC) - Yemen.

May 2002 to Oct 2007
- Chair, Computer Department, at Aden Community College (ACC) – Yemen, from May 2002 to Dec 2003.
- Chair, Computer engineering and software Department, at Aden Community College (ACC) – Yemen, from Jan 2003 to Aug 2004.
- Chair, Computer and communication engineering Department, at Aden Community College (ACC) – Yemen, from Sep 2004 to Oct 2006.